

Biennial report for Permanent Supersite/Natural Laboratory

Virunga Volcanoes Supersite: 2020- 2021

History	http://geo-gsnl.org/supersites/permanent-supersites/virunga-supersite/
Supersite Coordinator	<i>Charles Balagizi</i> <i>Goma Volcano Observatory</i> <i>142, Avenue du Rond-Point,</i> <i>Quartier des Volcans,</i> <i>Goma City, Democratic Republic of the Congo</i> <i>Email: balagizi.charles@gmail.com</i> <i>Cell : +243 975803568</i>

1. Abstract

The Virunga was established in November 2017 as a permanent Supersite with the aim of improving the geophysical scientific research and Geohazards assessment in support of Disaster Risk Reduction (DDR) in the Virunga Volcanic Province and the Lake Kivu basin. The CEOS guarantees a free access to Earth Observatory (EO) data, while the pool of collaboration built around the Supersite potentially supports the access to equipment for ground-based data collection and processing. From November 2017 to November 2019, in addition to implementing the Supersite; collaboration was built between the GVO and the world leading observatories and agencies, the free access to EO data with first steps towards collecting some ground-based data, training of some local scientists, and the adherence to the Virunga Supersite of world top-level geoscientists in the field of active volcano monitoring and hazards assessment. The later allowed the assessment of volcanic hazards around Nyiragongo and Nyamulagira, which included the production of hazards maps for future volcanic eruptions management, the collection of ground-based data to produce Risk and Recovery mapping. On the evening of May 22nd 2021, Nyiragongo volcano suddenly erupted from three vents that opened along a system of fractures on the southern flanks of the volcano. Two major lava flows were produced with one having its direction toward Goma city. Fortunately, these lava flows stopped their run before reaching the densely populated areas, with one being only at ~1 km from the Goma international Airport. Still, the lava flows had already destroyed about 3,600 houses while another 1,000 were severely damaged causing at least 30,000 persons to be in the need of shelter and other humanitarian assistance. The volcanic eruption further caused the death of 38 persons, disrupted the water supply infrastructures in Goma and the surrounding: estimated 550,000 persons lost access to water. An intense seismic activity followed the eruption and persisted for ~2 weeks, and caused sever damages to houses and infrastructures such as roads, water and electricity networks. Furthermore, the earthquakes caused important ground deformation in Goma and Gisenyi cities, which brought the fear of magma rising and accumulating beneath Goma and Lake Kivu. This raised a scenario of a new eruption with active vents inside Goma city or Lake Kivu, and led local authorities to evacuate estimated 400,000 people. Virunga Supersite scientific team supported the response to the Nyiragongo 2021 volcanic crisis through data processing, which yielded the production of key information that was delivered to local authorities and supported the management of the volcanic and humanitarian crises.

In September 2021 a new effusive activity began inside Nyiragongo main crater, along with a sustained seismic activity and ground deformation to the southern flank of the volcano. The fast renew of the activity denotes the strong and urgent need to starting prepare for the next Nyiragongo volcanic eruption; and the Virunga Supersite is willing to be part of this goal. This preparation strongly need an enhanced monitoring infrastructure that would permit follow up



www.geo-gsnl.org



the complex Nyiragongo-Nyamulagira rift-zone volcanism, forecast the spatiotemporal extent of the next eruption which will reduce its impacts. Furthermore, a proper training of local scientists is part of the well properness to the next Nyiragongo crisis, which the Supersite has already started.

2. Scientists/science teams

Charles M. Balagizi	<i>Geochemistry and Environmental Department, Goma Volcano Observatory. 142, Avenue du Rond-Point, Quartier des Volcans, Goma City, Democratic Republic of the Congo</i> <i>balagizi.charles@gmail.com</i> https://www.researchgate.net/profile/Charles_Balagizi
Georges Mavonga	<i>Department of Seismology, Goma Volcano Observatory 142, Avenue du Rond-Point, Quartier des Volcans, Goma City, Democratic Republic of the Congo</i> <i>mavotulu@gmail.com</i>
Albert Kyambikwa	<i>Department of Seismology, Goma Volcano Observatory 142, Avenue du Rond-Point, Quartier des Volcans, Goma City, Democratic Republic of the Congo</i> <i>albertuskabi@gmail.com</i>
Arsène T. Sadiki	<i>Department of Seismology, Goma Volcano Observatory 142, Avenue du Rond-Point, Quartier des Volcans, Goma City, Democratic Republic of the Congo</i> <i>sadikiarsenetb@gmail.com</i>
Honoré Ciraba	<i>Department of Geodesy, Goma Volcano Observatory 142, Avenue du Rond-Point, Quartier des Volcans, Goma City, Democratic Republic of the Congo</i> <i>honoreciraba@yahoo.fr</i>
King Iragi	<i>Department of Geodesy, Goma Volcano Observatory 142, Avenue du Rond-Point, Quartier des Volcans, Goma City, Democratic Republic of the Congo</i> <i>honoreciraba@yahoo.fr</i>
Jonathan Kavuke	<i>Department of Geodesy, Goma Volcano Observatory 142, Avenue du Rond-Point, Quartier des Volcans, Goma City, Democratic Republic of the Congo</i> <i>jkavuke@gmail.com</i>
Sandra Nzamu	<i>Department of Geodesy, Goma Volcano Observatory 142, Avenue du Rond-Point, Quartier des Volcans, Goma City, Democratic Republic of the Congo</i> <i>iragiking7@gmail.com</i>
Bonheur Ngangu	<i>Department of Geodesy, Goma Volcano Observatory 142, Avenue du Rond-Point, Quartier des Volcans, Goma City, Democratic Republic of the Congo</i> <i>bonheurrugain@gmail.com</i>
Niche Mashagiro	<i>Department of Technics, Goma Volcano Observatory 142, Avenue du Rond-Point, Quartier des Volcans, Goma City, Democratic Republic of the Congo</i> <i>bonheurrugain@gmail.com</i>
Marcellin Kasereka	<i>Geochemistry and Environmental Department, Goma Volcano Observatory. 142, Avenue du Rond-Point, Quartier des Volcans, Goma City, Democratic Republic of the Congo</i> <i>marcellinkasereka16@gmail.com</i>
Faustin Safari	<i>Geochemistry and Environmental Department, Goma Volcano Observatory. 142, Avenue du Rond-Point, Quartier des Volcans, Goma City, Democratic Republic of the Congo</i> <i>safarifaustin3@gmail.com</i>

Marcel Bahati Rusimbuka	<i>Geochemistry and Environmental Department, Goma Volcano Observatory. 142, Avenue du Rond-Point, Quartier des Volcans, Goma City, Democratic Republic of the Congo</i> rusimbuka3@gmail.com
Titus Habiyakare	<i>Rwanda Mines, Petroleum and Gas Board(RMB), Seismology Section Kigali, Rwanda</i> titus.habiyakare@rmb.gov.rw
Tite Niyitegeka	<i>Rwanda Mines, Petroleum and Gas Board(RMB), Seismology Section Kigali, Rwanda</i> tite.niyitegeka@rmb.gov.rw
Bo Galle	<i>Chalmers University of Technologie, Hörsalsvägen 11, Floor 4</i> bo.galle@chalmers.se http://www.chalmers.se/en/Pages/default.aspx
Michael Poland	<i>U.S. Geological Survey, Cascades Volcano Observatory 1300 SE Cardinal Court, Suite 100 Vancouver, WA 98683</i> mpoland@usgs.gov https://www.usgs.gov/staff-profiles/michael-poland
Marcello Liotta	<i>Istituto Nazionale di Geofisica e Vulcanologia Via Ugo La Malfa, 153 90146 - Palermo (Italy)</i> marcello.liotta@ingv.it https://sites.google.com/ingv.it/marcello-liotta/
Yosuke Aoki	<i>Earthquake Research Institute, University of Tokyo 1-1 Yayoi 1, Bunkyo-ku- Tokyo 113-0032, Japan</i> yaoki@eri.u-tokyo.ac.jp http://www.eri.u-tokyo.ac.jp
Adriano Nobile	<i>KAUST – King Abdullah University of Science and Technology Earth Science and Engineering - Crustal Deformation and InSAR group</i> adriano.nobile@kaust.edu.sa
Gaetana Ganci	<i>Istituto Nazionale di Geofisica e Vulcanologia Piazza Roma, 2 - 95125 Catania</i> gaetana.ganci@ingv.it
Annalisa Cappello	<i>Istituto Nazionale di Geofisica e Vulcanologia Piazza Roma, 2 - 95125 Catania</i> annalisa.cappello@ingv.it
Cristina Proietti	<i>Istituto Nazionale di Geofisica e Vulcanologia Piazza Roma, 2 - 95125 Catania</i> cristina.proietti@ingv.it
Stephan Kolzenburg	<i>Department of Geology - University at Buffalo 126 Cooke Hall, Buffalo, NY 14260</i> stephank@buffalo.edu
Sven Borgstrom	<i>Istituto Nazionale di Geofisica e Vulcanologia, Vesuviano Observatoy, Italia</i> sven.borgstrom@ingv.it
Mario Mattia	<i>Istituto Nazionale di Geofisica e Vulcanologia Piazza Roma, 2 - 95125 Catania-Italia</i> mario.mattia@ingv.it
Eugenio Privitera	<i>Istituto Nazionale di Geofisica e Vulcanologia Piazza Roma, 2 - 95125 Catania-Italia</i> eugenio.privitera@ingv.it

Mauro Coltelli	<i>Istituto Nazionale di Geofisica e Vulcanologia Piazza Roma, 2 - 95125 Catania mauro.coltelli@ingv.it</i>
Sebastien Valade	<i>Universidad Nacional Autónoma de México Instituto de Geofísica valade@igeofisica.unam.mx</i>
Diego Coppola	<i>Dipartimento di Scienze della Terra, Università degli Studi di Torino TORINO, Italia diego.coppola@unito.it</i>
Peter Kelly	<i>Volcano Disaster Assistance Program, USGS Cascades Volcano Observatory 1300 SE Cardinal Court; Vancouver, WA 98683-USA pkelly@usgs.gov</i>
Julia P Griswold	<i>Volcano Disaster Assistance Program, USGS Cascades Volcano Observatory 1300 SE Cardinal Court; Vancouver, WA 98683-USA pkelly@usgs.gov</i>
Cristiano Tolomei	<i>Istituto Nazionale di Geofisica e Vulcanologia Osservatorio Nazionale Terremoti Via di Vigna Murata 605, 00143 Rome, Italy cristiano.tolomei@ingv.it</i>
Lisa Beccaro	<i>Istituto Nazionale di Geofisica e Vulcanologia Osservatorio Nazionale Terremoti Via di Vigna Murata 605, 00143 Rome, Italy lisa.beccaro@ingv.it</i>
Elisa Trasatti	<i>Istituto Nazionale di Geofisica e Vulcanologia Osservatorio Nazionale Terremoti Via di Vigna Murata 605, 00143 Rome, Italy elisa.trasatti@ingv.it</i>

Scientists/science teams issues

Local scientists are still less involved in the processing and interpretation of data, particularly the EO data. We hope that this issue will be solved with the training of local scientists (some have gained scholarships to attend masters and dedicated training, in collaboration with international scientists). Another solution, and more inclusive is to organize an onsite/online training(s) that may allow the participation of a large number of local scientists, and provide them with skills on how to process and interoperate the data, particularly the EO data obtained under the Virunga Supersite umbrella.

3. In situ data

Type of data	Data provider	How to access	Type of access
Seismic	Goma Volcano Observatory (GVO)	Published papers* Contact GVO**	Unregistered Public
GPS	GVO	Contact GVO**	GSNL scientists
Gas measurements	GVO	Published papers* Contact GVO**	Unregistered Public GSNL scientists
Surface waters chemistry including Lake kivu	GVO	Published papers* Contact GVO**	Unregistered Public GSNL scientists
Rainwater chemistry	GVO	Published papers* Contact GVO**	Unregistered Public GSNL scientists

**Published data are freely accessible; the Goma Volcano Observatory may be contacted for guidance in case of issues*

***Archived unpublished data or recently collected data are available on request, and based on the data policy for data sharing and management among the Virunga Supersite scientific community.*

In situ data issues

Some in situ data that is collected in partnership with international collaborators is still not accessible to other scientists, despite the Data Policy that was proposed by the Supersite and approved by the GVO's staff, after they have amended it (the data policy is available here, http://geo-gsnl.org/wp-content/Documents/Supersites/Virunga/History/Virunga%20Supersite_Data%20Policy.pdf). In this data policy, it is stipulated that the "ground based data and results should be made available for full and open access after publication or in any case within 2 years ("embargo period") since their collection/generation". However, the ground-based data that was collected even more than two years ago is still not available to other scientists.

4. Satellite data

<In the table below please list all satellite data types available for the Supersite>

Type of data	Data provider	How to access	Type of access
COSMO-SkyMed	ASI	POC requests access from ASI for GSNL scientists individual users, data then accessible via UNAVCO	GSNL scientists
Pleiades	CNES	POC requests access from CNES for individual users	GSNL scientists
Sentinel-1 a/b	ESA	https://scihub.copernicus.eu/	Registered public
ASTER EO-1 (Hyperion) MODIS	NASA	https://terra.nasa.gov/about/terra-instruments/modis https://modis.gsfc.nasa.gov/	Registered public
Landsat	USGS	https://www.usgs.gov/land-resources/nli/landsat/landsat-data-access?qt-science_support_page_related_con=0#qt-science_support_page_related_con	Registered public
AVHRR	NOAA	https://earth.esa.int/web/guest/missions/3rd-party-missions/current-missions/noaa-avhrr	Registered public

Satellite data issues

❖ Problems with Pleiades images

Concerning the Pleiades images in the Virunga region, one of the biggest issues is the possibility to find acquisitions with a minimum percentage of clouds. The acquisition plan started in December 2018 and, in spite of this, the two volcanic areas Nyiragongo and Nyamuragira, are still covered by clouds. The redundancy of acquisitions in the same region is the only means to obtain the complete coverage. The programming period was extended until August 31st 2022, so we hope to cover the missing areas in the next few months.

Another problem raised during 2021 since the acquisition parameters were changed in order to increase the chance of acquisition. We indeed change the maximum value of B/H ratio from 0.3 to 0.4 and the incidence angle from 20° to 15°. This probably, together with a higher cloud coverage, impacted the quality of the DSM produced from the acquisition of 12 November 2021.

From the technical point of view, many Pleiades scenes are split into smaller tiles for size management while a unique Rational Polynomial Coefficient (RPC) file is provided for the scene. This is not easily handled by the MicMac software. Indeed MicMac requires an RPC file for each image. In order to deal with this aspect, we merged the tiles into a single file and then processed it with MicMac. In this way we solved the problem, but the processing is very time consuming.

5. Research results

5.1. In situ Data

5.1.1. Seismic activity associated with the Nyiragongo May 2021 volcanic eruption

We summarize the seismo-volcanic activity observed in the Virunga volcanic province, western branch of the East African Rift System for the period from January 1 to December 31, 2021. The seismic data was recorded by the Goma Volcano Observatory seismic network installed around the Nyiragongo and Nyamulagira volcanoes and on the western side of Lake Kivu. The analysis focused mainly on the location of volcanic and tectonic earthquakes in the region, as well as the assessment of the level of volcanic tremors (RSAM, Real-time Seismic Amplitude Measurement) on the two volcanoes.

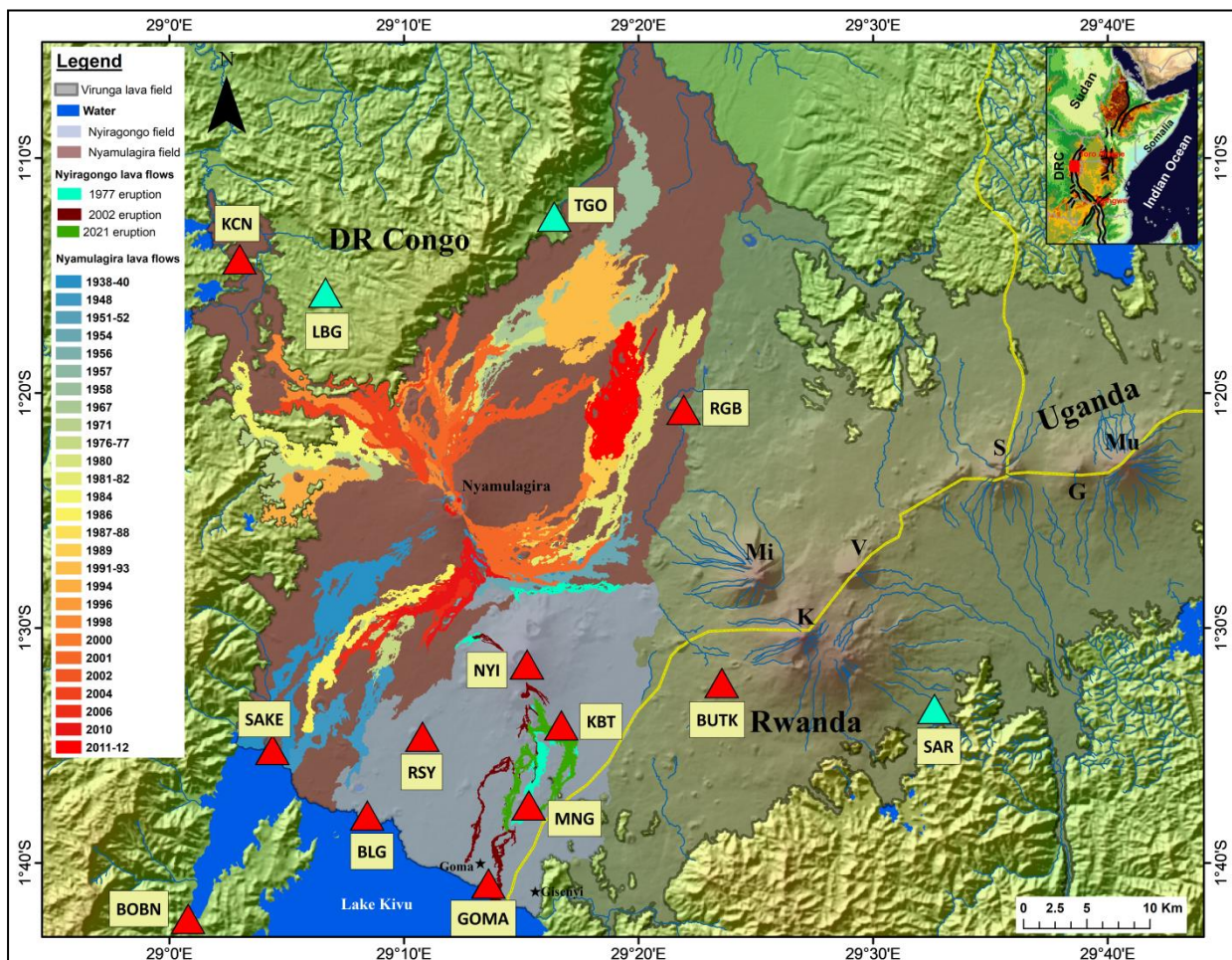


Figure 1. Geological map of the Virunga Volcanic Province showing Nyiragongo and Nyamulagira lava flows since 1938 and Nyiragongo since 1977; with the seismic network of the Goma Volcano Observatory around the active volcanoes. Nyiragongo and Nyamulagira lie in the floor of the rift, while the six others volcanoes of the Virunga; i.e., Mikeno (Mi), Karisimbi (K), Visoke (V), Sabinyo (S), Gahinga (G), and Muhabura (Mu) are perched on the east edge of the rift. The red triangles show the presently operating seismic stations, while the turquoise show stations with technical issues.

The main was the assessment of the magmatic process in the fields of Nyiragongo and Nyamulagira volcanoes. We divide the seismo-volcanic activities into two parts of the year 2021, the first going from January to June 2021, and the second from July to December 2021.

a. Period from January 2021 to June 2021

This semester was characterized by the presence of long-period seismicity which largely dominated the recorded events. It is in the course of this period that occurred the eruption of Nyiragongo volcano on May 22, 2021 around 6:15 PM local time (GMT+2). About a month before the eruption (in April 2021), we recorded in the field of Nyiragongo a swarm dominated by long-period earthquakes accompanied by few earthquakes related to fracturation (e.i., volcano-Tectonic (VT) or hybrids) which were located to the southern flank of Nyiragongo volcano (Fig. 2). This swarm lasted for 4 days, from April 20 to 24, 2021 with an average of 120 earthquakes per day. In addition to these volcano-Tectonic earthquakes recorded in April, three other earthquakes of this category were recorded a few hours before the eruption of May 22, 2021. The figures below illustrate the distribution of the epicenters of the earthquakes located in the fields of these two volcanoes as well as the corresponding level of the tremors.

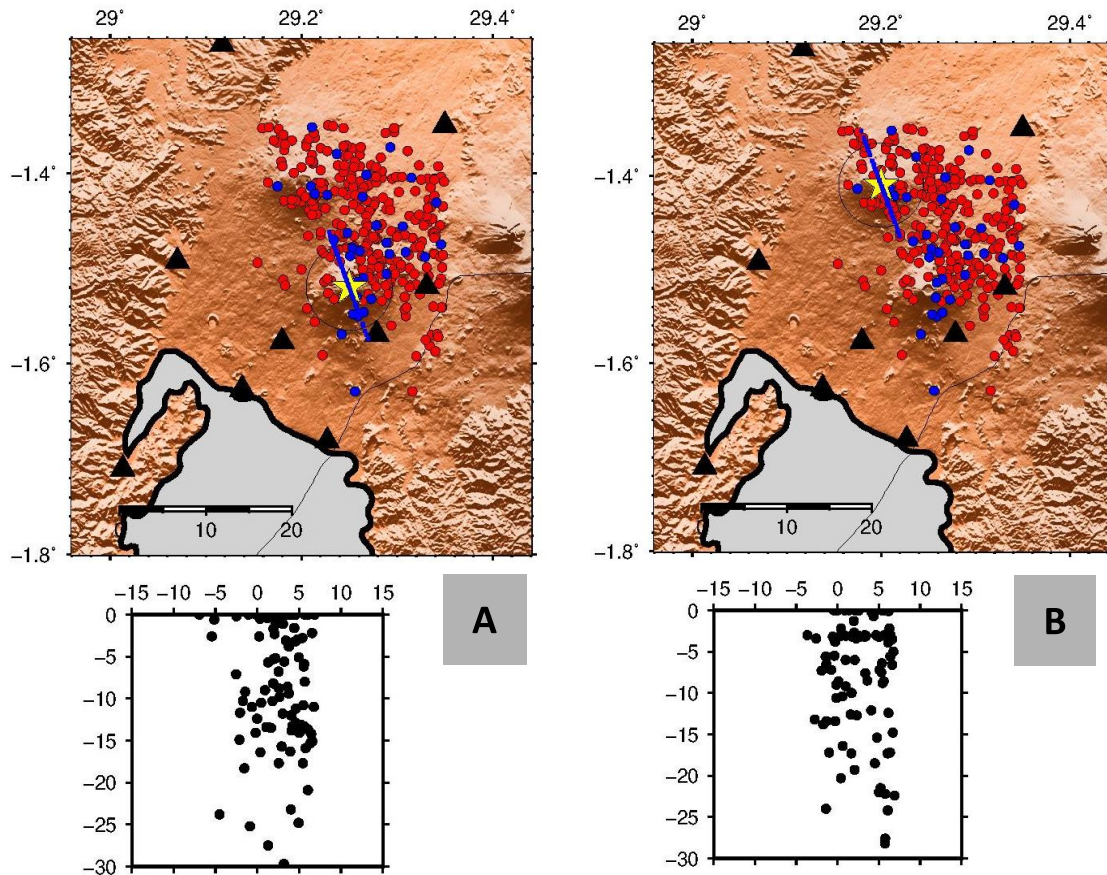


Figure 2. Epicenter distribution of long-period earthquakes in the Nyiragongo (A) and Nyamulagira (B) volcanic fields for the period from January 1 to June 2021. Red dots indicate the long-period events while the blue correspond to the hybrid and Volcano-Tectonic events.

❖ Level of volcanic tremors (RSAM) at Nyiragongo and Nyamulagira volcanoes

The tremors level for the two volcanoes remained almost constant before the eruption, except during the period the swarm was recorded from April 20 to 24, 2021 and that had an average of 120 earthquakes per day as mentioned in the previous section. During this swarm period (April 20 to 24, 2021) a slight increase in the energy was recorded (Fig. 3), while a sudden increase and very significant in the energy was recorded on May 22, 2021 at all stations near Nyiragongo volcano as a result of the eruption (e.g. Fig. 3).

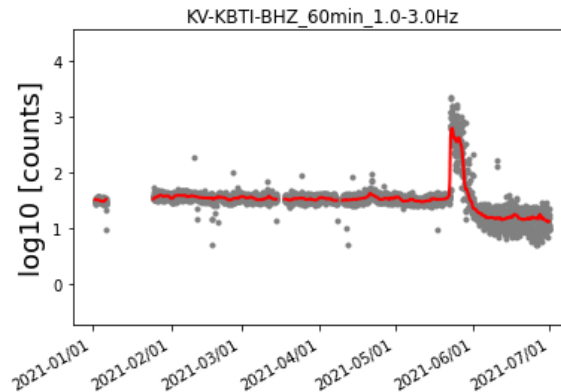


Figure 3. Energy variation for the period from January to June 2021

❖ Regional seismicity during this period

The majority of tectonic earthquakes recorded in the region are concentrated in and around Lake Kivu at depths from 0 to 40 km (Fig. 4). The May 22, 2021 Nyiragongo eruption was followed by a particular tectonic activity characterized by repetitive tectonic earthquake, which initially were felt by the population and subsequently not felt. Later, there was even a continuous migration of the seismic activity from the south of Shaheru crater (located to the south flanks of Nyiragongo summit) towards Lake Kivu where it persisted for more than two months. The largest earthquake recorded during this period was of locale magnitude (MI) 5.3, at coordinates 1.71°S and 29.23°E and at 8 km depth, and which may have initiated the reopening of new cracks and fissures to the south flank of Nyiragongo volcano, including in Goma and Gisenyi cities.

The tectonic earthquakes were recorded in 4 main zones such as lake kivu bassin, lake Edward region (Albertin rift direction), Masisi region (Tananyika rift direction) and Lake Tanganyika region.

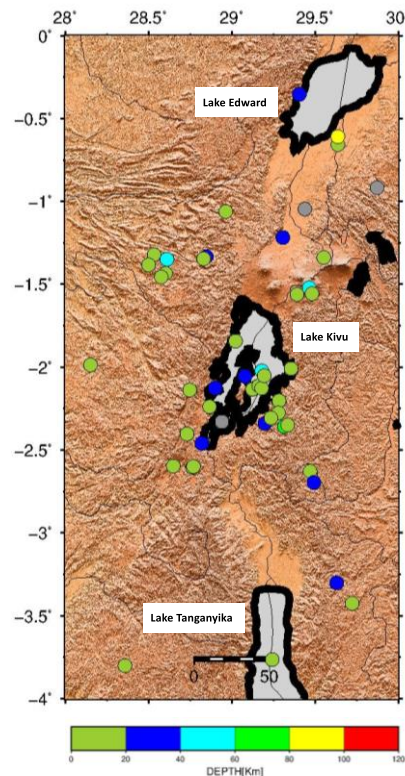


Figure 4. Recorded tectonic earthquakes in the basin of lakes Edward, Kivu and Tanganyika in the period from January 2021 to April 2021.

b. Period from July 2021 to December 2021

This semester was mostly marked by the resume of the seismic activity and the reappearance of the lava lake in the Nyiragongo main crater, three months after its eruption. During this period we recorded more swarms of long-period earthquakes accompanied by hybrid earthquakes related to the renew of effusive activity in the main crater and the beginning of the lava lake formation. The few weeks that followed the eruption, i.e. from end of May to the entire June, the seismic activity was dominated by tectonic swarms. Its only at the end of July that we began to record long-period earthquakes at Nyiragongo. In the week of August 02 to 09, 2021, an unusual seismic activity was recorded in the field of the Mikeno volcano (Fig. 1 shows the location of Mikeno). A few days later, a madflow happened at this volcano which destroyed a large part of the area of Kibumba where several villages are located.

A first swarm of long-period earthquakes accompanied by volcano-Tectonic (VT) earthquakes was recorded at Nyiragongo from August 24 to August 27, 2021. A month after this swarm, i.e. on September 28, 2021, there was the resume of the effusive activity inside Nyiragongo main crater and the beginning of the formation of a new lava lake, coinciding with the recording of

volcanic tremors at a seismic station located at the summit of Nyiragongo. Later on, three other swarms were recorded at Nyiragongo volcano on November 4, November 19-20, and November 27, 2021 during which Hybrid earthquakes recorded. The last swarm of this semester started on the night of December 16 to 17, 2021, characterized by the renew of typically Nyiragongo seismic activity with the recorded volcanic tremors extended to Kibati and Rusayo stations, and on on December 25, 2021 tremors appeared at Bulengo station (Fig. 1). This tremor situation persisted until the end of 2021, and continued for the entire first week of January 2022.

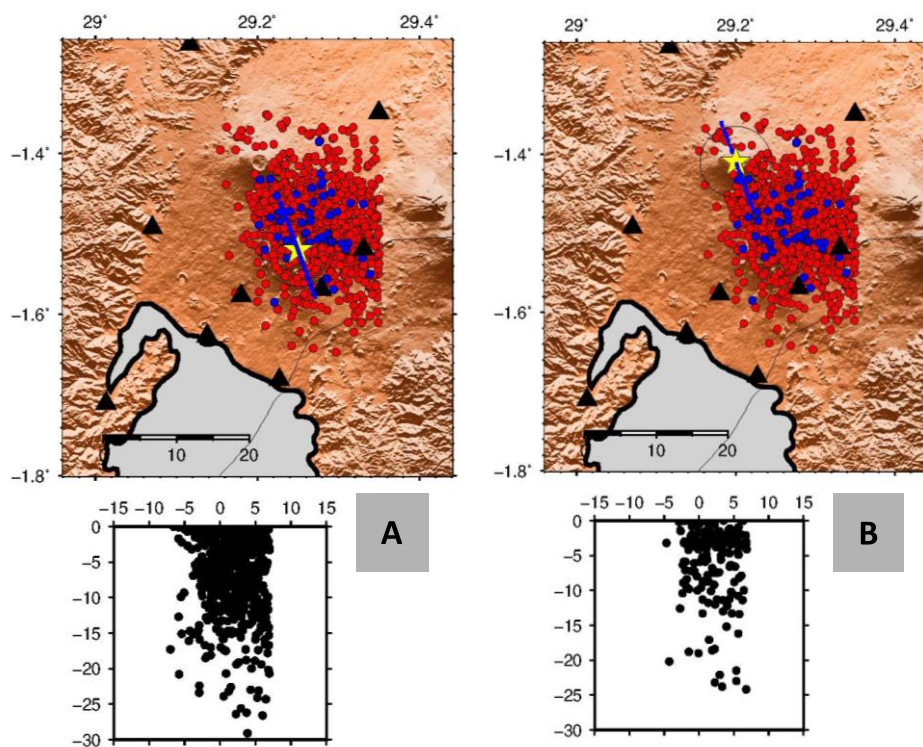


Figure 5. Epicenter distribution of long-period earthquakes in the Nyiragongo (A) and Nyamulagira (B) volcanic fields for the period from July 1 to December 2021. Red dots indicate the long-period events while the blue correspond to the hybrid and Volcano-Tectonic events.

The seismic activity for the period of July to December 2021 was concentrated between the two volcanoes, but more in the field of the Nyiragongo volcano principally at its summit, all being at less than 25 km depth (Fig. 5).

❖ **Level of volcanic tremors (RSAM) at Nyiragongo and Nyamulagira volcanoes**

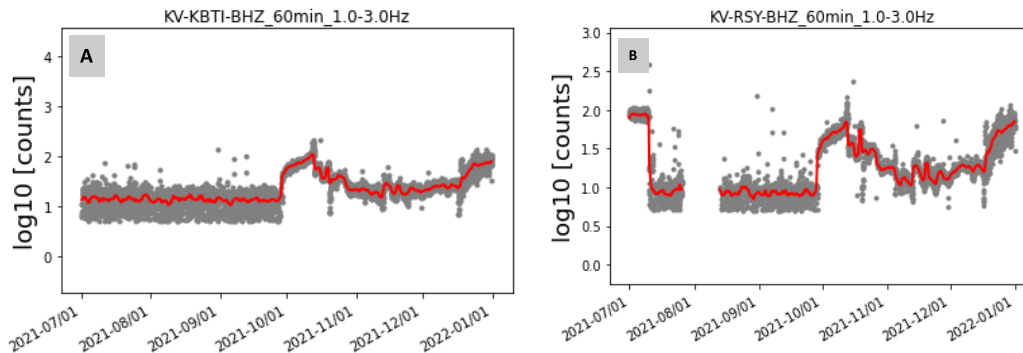


Figure 6. Tremors energy variation for the period from July to December 2021

The second semester was characterized by a double increase in the energy of tremors at Nyiragongo (Fig. 6). The first occurred on August 28, 2021, and was related to the then ongoing effusive eruption inside Nyiragongo main crater, with the lava lake being well established; while the second energy increase occurred on December 17, 2021 during which the tremor level increased at the seismic station located at the summit of Nyiragongo as well as to the other stations located to the southern flank of Nyiragongo (Kibati, Rusayo and Bulengo).

❖ **Level of volcanic tremors at the seismic station located at the summit of Nyiragongo volcano for the entire 2021**

The evolution of RSAM throughout the year 2021 (Fig. 7) shows three major times of rise in the energy level, the first in May, the second in August and the third in November 2021. They correspond to three major eruptive phases observed at Nyiragongo volcano in the course of the year, which are respectively the eruption of May 2021, the reappearance of effusive eruption inside Nyiragongo's main crater (beginning of the formation of the lava lake) at the end of September, and finally the period of renewed tremor activity in the entire Nyiragongo field, more particularly at the stations of Nyiragongo (summit), Kibati, Rusayo and Bulengo.

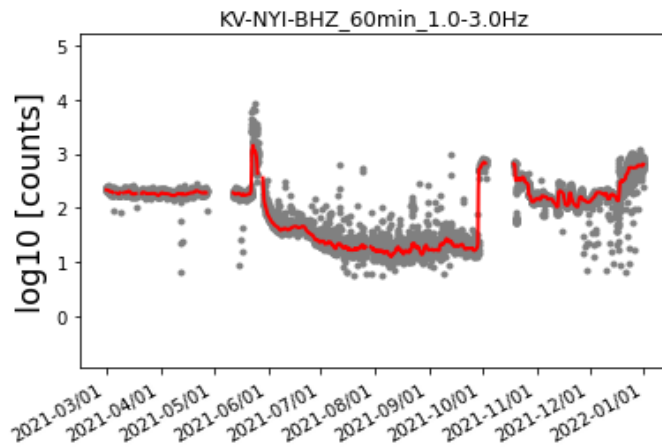


Figure 7. Evolution tremors energy the period from January to December 2021 at the station located at the summit of Nyiragongo volcano

❖ **Regional seismic activity during this period.**

The regional activity dominated by tectonic earthquakes that lasted two and a half months, from from 1 July to 17 September 2021. This tectonic activity was much more concentrated Lake Kivu region(Fig 8A) in the direction of the Nyabyinyu falt which lies under the lake Kivu(Rwanda side) with the Albertine rift direction, particularly in its northern part (Fig. 8B), between 0 and 35 km depth.

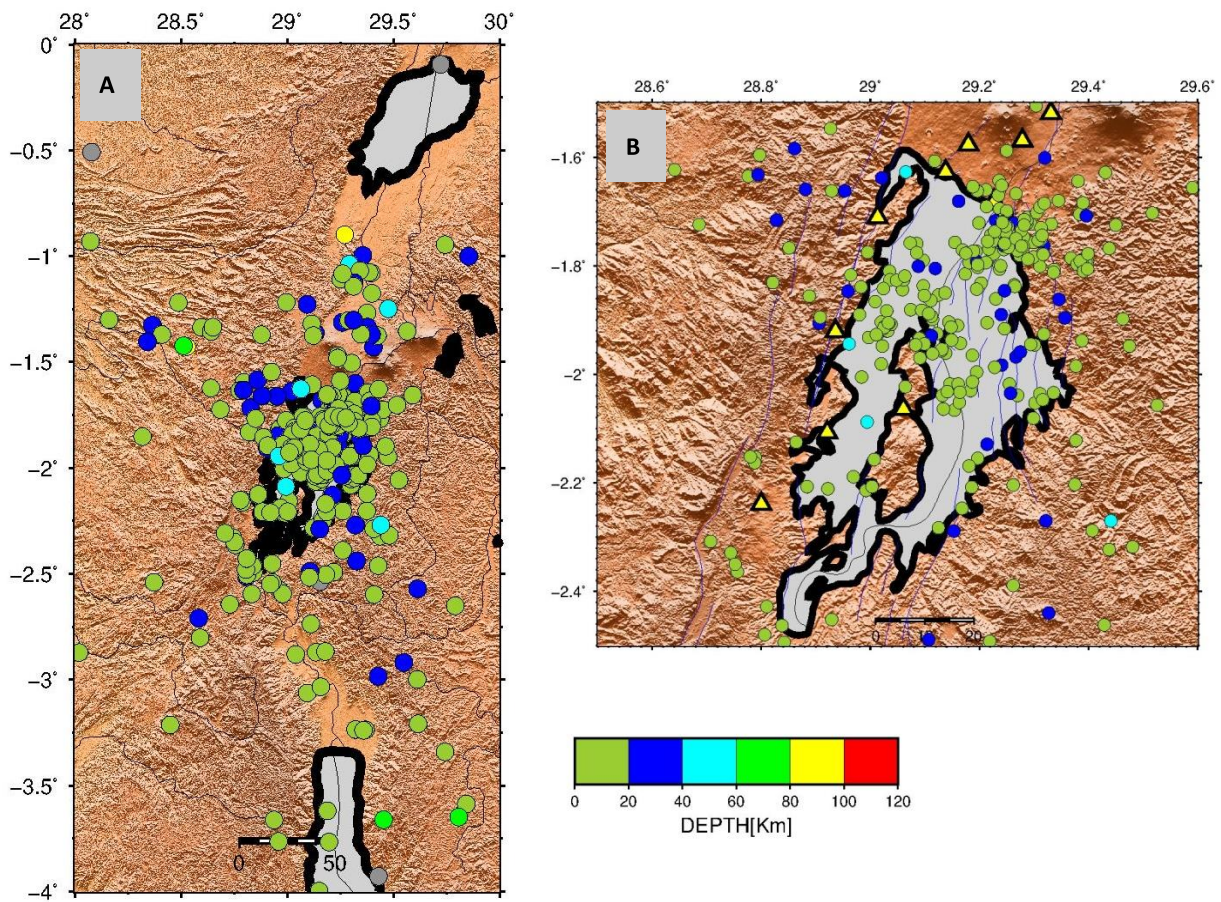


Figure 8. Recorded tectonic earthquakes in the basin of lakes Edward, Kivu and Tanganyika for the period from July 2021 to December 2021

5.1.2. Assessing fractures and fissures created during the Nyiragongo May 2021 eruption

A. Assessment of fractures and fissures on the DR Congo territory

Two main groups of fractures were created during and following the Nyiragongo May 2021 eruption: the first group consist of eruptive fractuieres that were formed at the eruptive sites, while the second group is formed of fractures and iffures that were formed due to the sismicity that followed the eruption (Fig. 9).

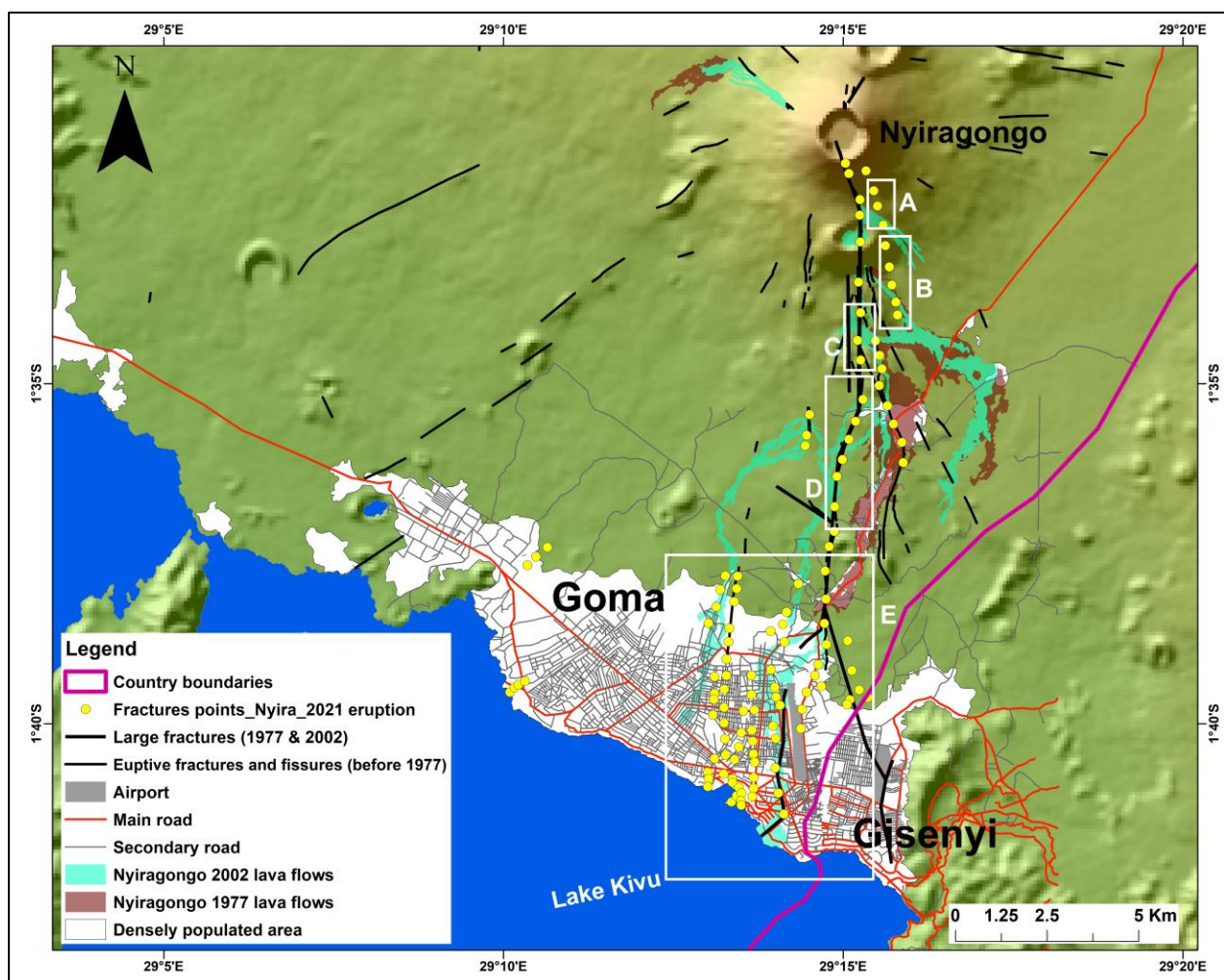


Figure 9. Map showing fractures due to the Nyiragongo eruption of May 2021 and seismic activity that followed the eruption. The yellow dots represent the places where cracks were observed in the field.

The fractures that formed as consequence of magma reaching the surface and that form the eruptive vents include :

- a. **The Shaheru eruptive fracture line:** this fracture is located at about 2 km to the east of the 2002 eruptive fracture of the Shaheru cone, and shown in the map of Fig 9 by the square A. The shaheru fracture extends towards the east side when going to the north (towards Nyiragongo summit), and towards the eruptive site of the Kibati when going to the south.
- b. **The Kibati eruptive fracture line:** This fracture is represented by the dots located in the square B of Fig. 9. This vent produced the eastern lava flow that destroyed the road Goma-Rutchuru road at Kibati, and extends southwards Rwanda.
- c. **The Kaneza eruptive fracture:** This fracture is formed by dots found in square C, and is parallel to that of from Kibati eruptive vent, and also extends southwards towards Mudjoga. The lava flow from this fracture met that from Kibati vent to produce a more large lava flow that took the direction toward Rwanda.
- d. **The Mudjoga-Lemera eruptive fractures lines:** these fractures serie are parallel to the 1977 and 2002 Mudjoga eruptive fractue, at some sites the May 2021 vents are similar to those of 2002. The Mudjoga-Lemera fractures extend southwards towards Bugarura to Munigi villages. These eruptive fractures produced the western lava flow that inveded the northern part of Goma city, distroying houses and roads; and which stopped ~1 km north of Goma's airport.

The fractures and fissures that opened following the seismic activity are located in Goma and Gisenyi cities and the neighboring villages and include (a) those going from the eruptive Mudjoga-Lemera eruptive vents, cross Mabanga district in eastern Goma, follow and reactivated the 2002 fracture that reach lake Kivu (Fig 9). The second group is composed of several fracture lines mostly located in either in Mabanga and Katindo districts, and which go through Mount Goma and reach Lake Kivu. Most of them are newly formed fractures, except few that are in the similar to that of 2002, which are located in Mabanga district. Another group is located to the western districts of Goma, starting from Bujovu and are less dominant.

This group of non eruptive fractures and fissures are found in the square E of Fig. 9, as well as those located to the extrem west of Goma city.

B. Impact of 2021 Nyiragongo Volcano eruption in Rubavu District

Nyiragongo Volcano is located at about 15km from Gisenyi, Rwanda, though in Cyanzarwe sector, of Rubavu District the foot of this volcano is at about 5 km (Fig. 10). The recent recorded volcanic activities include the 1977 and 2002 Nyiragongo eruptions, and latest 2021. On 22nd May 2021 at around 6:30PM, conducting some people from Cyanzarwe sector was temporally displaced. That incident also pushed around 10,000 people from DRC to flee to Rwanda.

Eruption event was followed by a series of earthquakes which caused considerable damages in Rubavu District during 10 days.

About one hour after the eruption, small earthquakes were recorded with an increase in magnitude and frequency of occurrence. From mid night (Kigali Time), 23/05/2021, earthquake of elevated magnitude above ML 4 continued for 10 days. Due to many earthquake affecting the same area, and infrastructures, much damage was observed in Rubavu, Gisenyi, Rugerero and some other sectors in Rubavu District. Though, the earthquake recorded were less than ML 5.4 local magnitude, a single earthquake of this magnitude would normally not cause the observed damage considering that the city is located on volcanic rocks from undocumented historical eruptions. However, recurring earthquakes in short time contributed to significant damage which would be caused by a single event of about ML 6-6.5 single event. Gisenyi and Rubavu Sectors of Rubavu District which is one of 30 districts in Rwanda were much exposed to great damages due to close earthquake epicenters and the reactivated fissure passing through particular properties and infrastructures. As a result of volcanic eruption and earthquakes, existing fissures were reactivated. During reactivation, more than 600 earthquake events were recorded including the strongest being ML 5.3 on 25/05/2021 at 11:03 local time.

Summary of field observation

The observations made indicated the presence of cracks in different places and these joins together to form continuous fissures believed to run from Nyiragongo Volcanic area, through Gisenyi toward Lake Kivu (Fig. 10). A combination of recorded fissure from DRC and Rwandan side will provide a complete set of the continuity of the fractures. Ground fissuring continued to expand for the period of intense earthquake activity, from a single cm scaled fissure to about 40-60m wide zone and 8 Km long. Though general trend of the fissure in Rubavu is between N5-25W, it follows the granitic body of the N-S Rubavu Hill. This is witnessed after passing Rubavu football stadium where the fissure changes its orientation from N-S to about N20W following a similar trend of a change in granitic body. Frankly speaking, the extension of deformed zone did not happen in a single day, rather during 10 days collecting data, new cracks were being observed as earthquakes were occurring.

Other unusual event observed, is the post-eruption event occurred on 28th May, 2021 where Rubavu hot spring water stopped emerging. Later on, after 5 days, the hot spring water returned back. However, some of the hot spring source were still coming with cold water (May be, it was caused by ground fissuring, and dyking event that was ongoing?). The earthquakes recorded migrated from Nyiragongo Volcano in NNW SSE direction and at some point, it changed direction, depicting same observations as observed from the reactivated fissure trend. The earthquake propagation was attributed to dyking event. In Gisenyi sector, about 30 cm

subsidence in a 2-3m wide fissure was observed. The infrastructures such as buildings, and water pipes crossing the fissures were all affected.

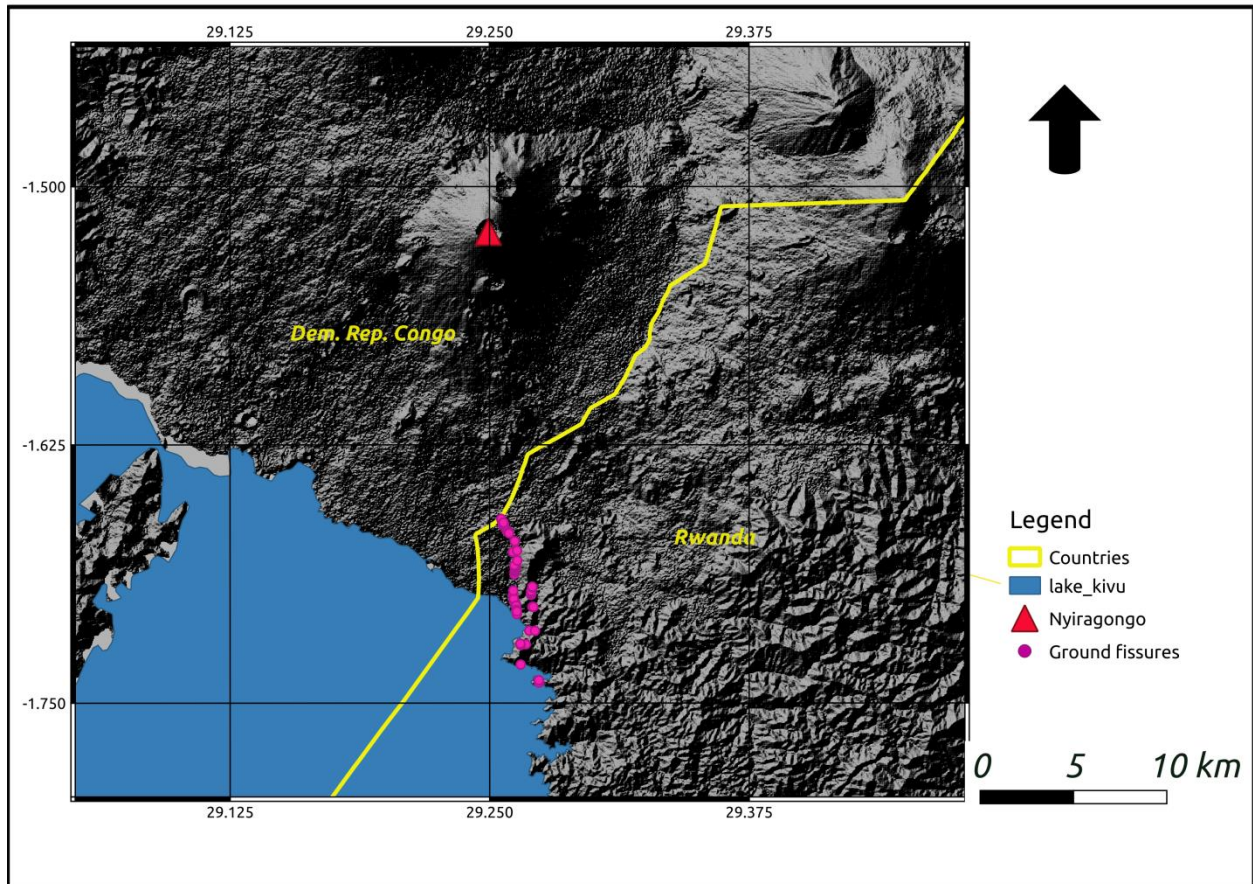


Figure 10. Ground cracks recorded (in purple colour) indicating continuous ground fissure (these data may be supplemented by the ground fissure from DRC side in order to have the full fracture system).

5.1.3. Monitoring CO₂, SO₂ and H₂S concentrations at Nyiragongo summit and the eruptive site of May 2021

A portable MultiGas is being deployed at the summit of Nyiragongo since the resume of the effusive activity inside the main crater (Fig. 11A), as well as at the eruptive vent of May 2021 near Kibati as this site is still emitting gases and characterized with high temperature (Fig. 11B). At the Nyiragongo summit, the new plume bulk composition is in the range of 63.61-82.73%, 36.15- 17.18 % and 0.23- 0.13 % for H₂O, CO₂ and SO₂, respectively.



Figure 11. MultiGas deployment at the summit of Mt Nyiragongo (A) and the eruptive site of May 2021 near Kibati

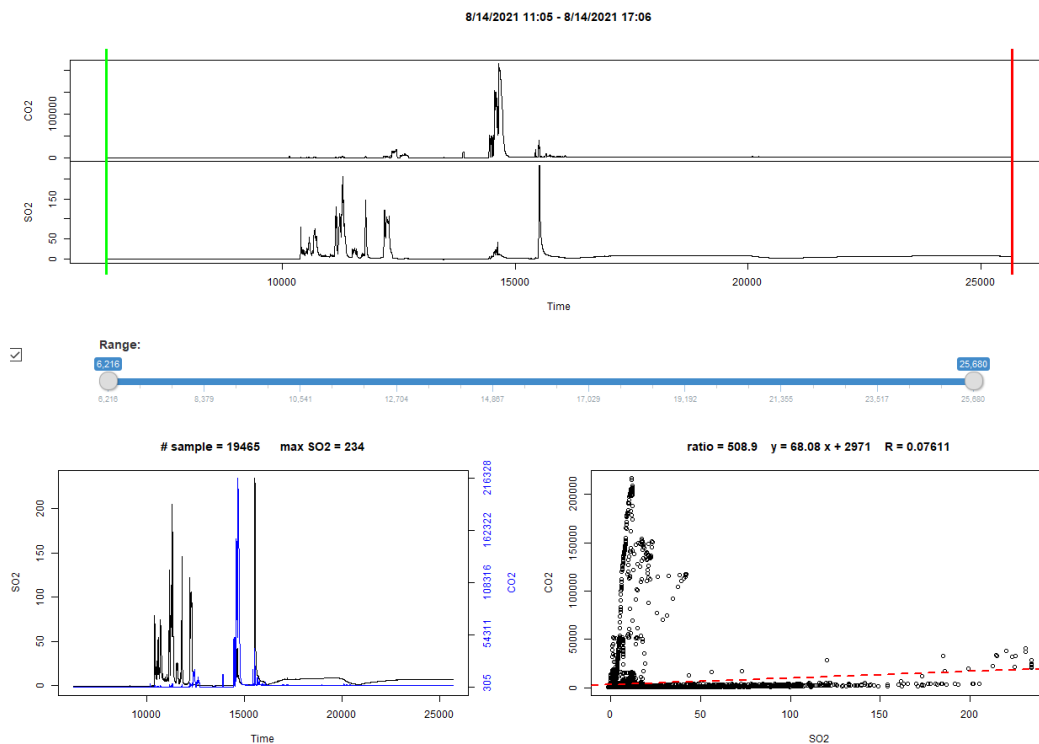


Figure 12. Upper chart: CO₂ and H₂S values as measured at the Nyiragongo 2021 eruptive site located near using a portable MultiGas on August 14, 2021. Lower chart: CO₂ versus H₂S from data selected in the upper chart, i.e. the data found between the vertical green and red lines, which corresponds to the whole measurements of the single campaign.

www.geo-gsnl.org

At the Kibati eruptive vent of May 2021, there have been permanent fumarolic activity with temperature being $\sim 400^{\circ}\text{C}$. We were able to deploy the portable MultiGas at this site since August 2021, and had the possibility to measure the composition of emitted gas.

In August, the gas bulk composition was CO_2 and H_2S dominated with the The gas bulk composition was in the range of 83.64-97.99%, 176-15.79 % and 0.00- 0.57 % for H_2O , CO_2 and SO_2 , respectively. Contrary to the plume measured at the summit, the vent was characterized with the presence of important amount of H_2S , with values that were up to 120 ppm (Fig. 13).

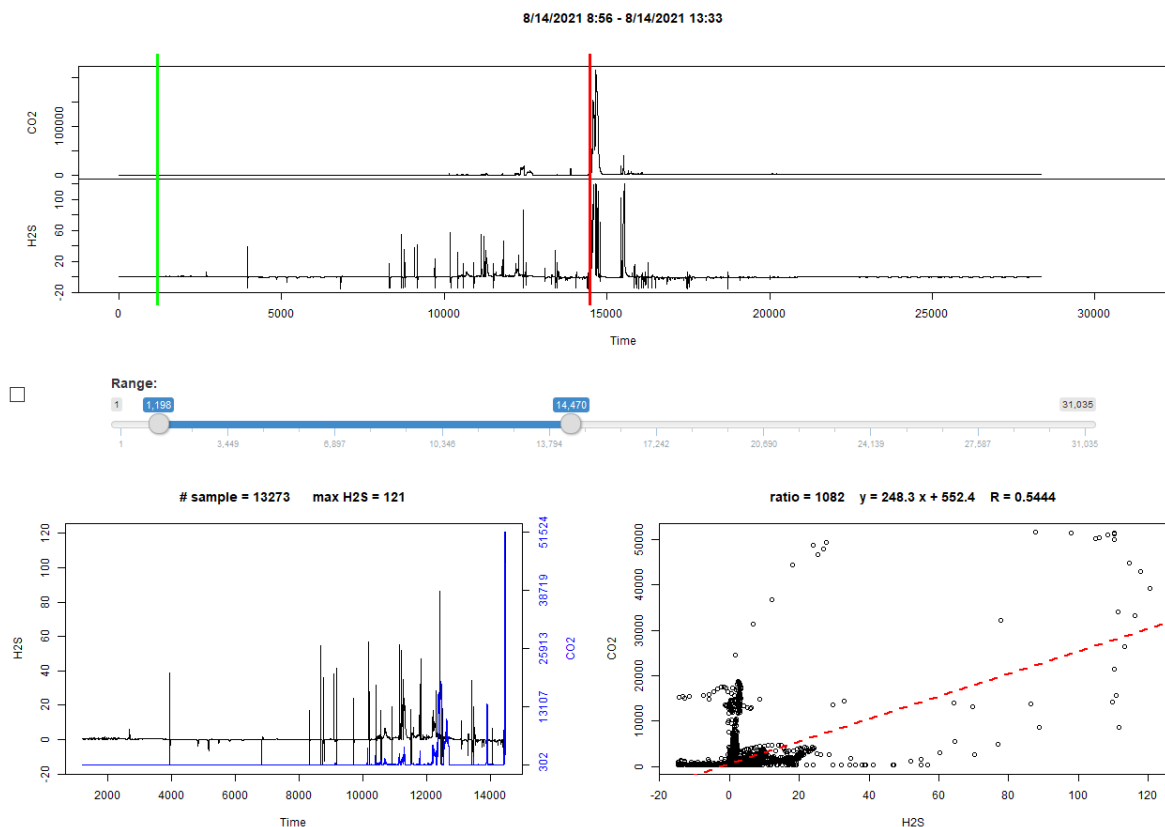


Figure 13. Upper chart: CO_2 and SO_2 values as measured at the Nyraragongo 2021 eruptive site located near using a portable MultiGas on August 14, 2021. Lower chart: CO_2 versus SO_2 from data selected in the upper chart, i.e. the data found between the vertical green and red lines, which corresponds to the whole measurements of the single campaign.

5.1.4. Air quality monitoring before and during the Nyiragongo May 2021 eruption

During the Nyiragongo May 2021 crisis, emitted volcanic plume reached the inhabited area composed of several villages as well as the northern district of Goma city. Further, the air charged of volcanic gases (carbon dioxide, sulphur dioxide and hydrogen sulphide, hydrogen chloride, hydrogen fluoride and carbon monoxide in water vapor) could change the location following the changes in the prevailing wind direction, being hazardous to humans, animals, vegetation and property around. Further, there was volcanic ash falling on a large inhabited area downwind the Nyiragongo Volcano, and going from those located to the the western side of the volcano (e.g. Rusayo) to the south of the volcano (e.g. Kibati), as well as in the entire city of Goma (see Fig. 14 to locate the places).

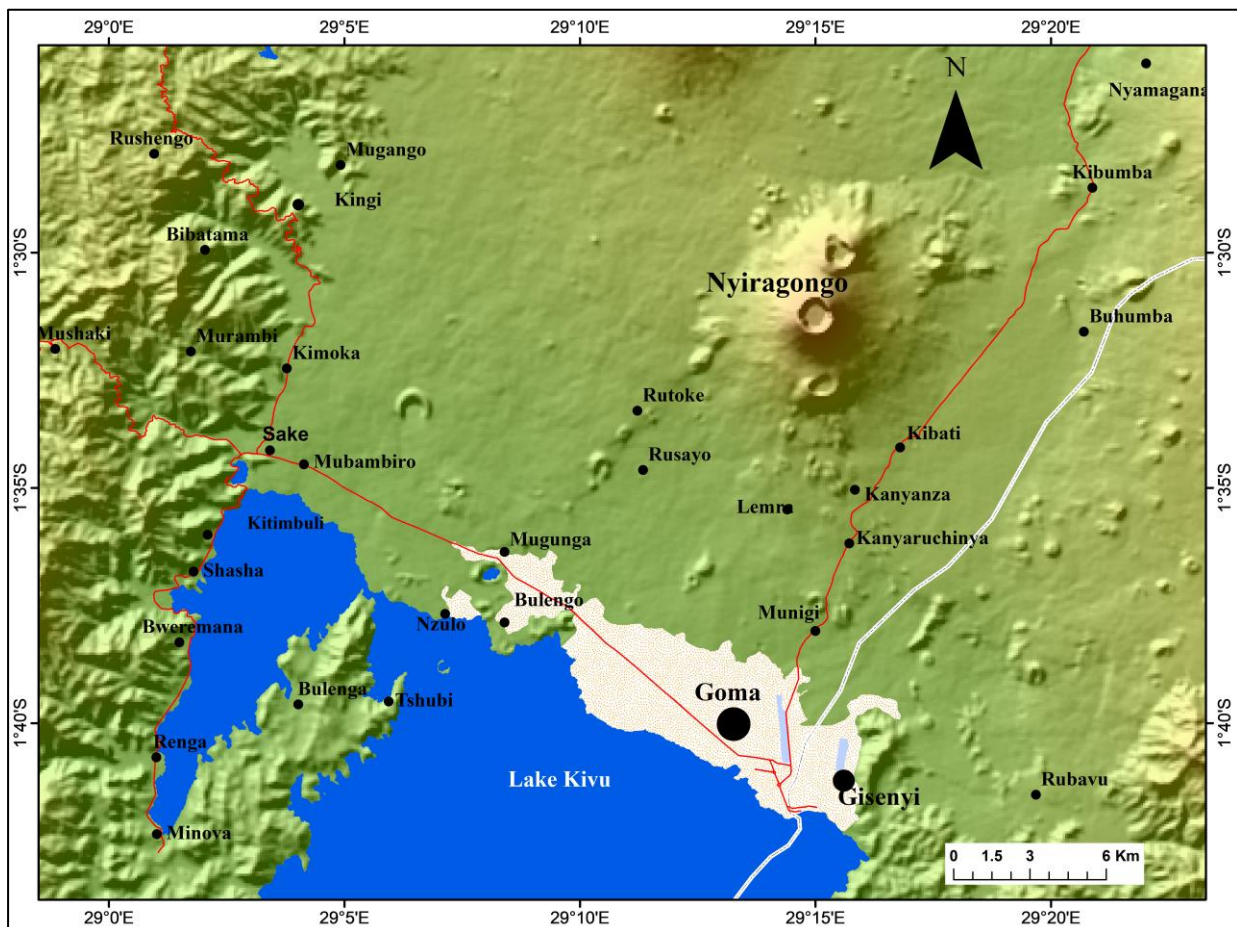


Figure 14. Map showing the location of the cities of Goma (DRC) and Gisenyi (Rwanda), as well as that of main villages located in the field of Nyiragongo and Nyamulagira volcanoes

As known from the literature, fresh volcanic ash is gritty, abrasive, sometimes corrosive, and always unpleasant. Although ash is not highly toxic, it can trouble infants, the elderly, and those with respiratory ailments. Ash can also get in eyes and scratch them, especially when it's windy, be hazardous to grazing livestock. Fortunately, even though ash fell several times especially during the intense seismic activity that caused the collapse of some plateforms or small of their segments in the main crater of Nyiragongo; ash was short lasting as it was removed from the atmosphere through rainwashout. However, the rainwater falling on the hot lava led to the production of a wide steam plume (Fig. 15). Lava interacting with water already happened elsewhere, such as in Hawaii where lava entered the ocean creating large steam plumes (haze). According to measurements and analysis made by the USGS team at this site, the haze sends hydrochloric acid, Hydrofluoric Acid and steam with fine glass particles into the air, their health hazards include lung damage, and eye and skin irritation.



Figure 15. Wide steam plume (haze) being produced and injected onto the atmosphere as a result of rainwater falling on hot lava led in Kanyaruchinya village on May 24, 2021 at 2:25 PM.



Figure 16. Wide steam plume (haze) being produced and injected onto the atmosphere as a result of rainwater falling on hot lava led in Kibati village on May 23, 2021 at 2:30-45 PM, with people crossing the hot lava at the place the Goma-Rutshuru road was cut off by the lava flow. People were crossing in order to reach the other road side toward Rutshuru.

Only on the afternoon of May 24, 2021 at least 7 persons were killed by the steam plume (haze), as they were trying to cross the hot lava flow at Kibati. Fortunately the haze did not reach Goma city according to few measurements we made in the city where the air quality was still of very good quality, almost similar to that made few months prior to the May 2021 Nyiragongo crisis (Fig. 17).

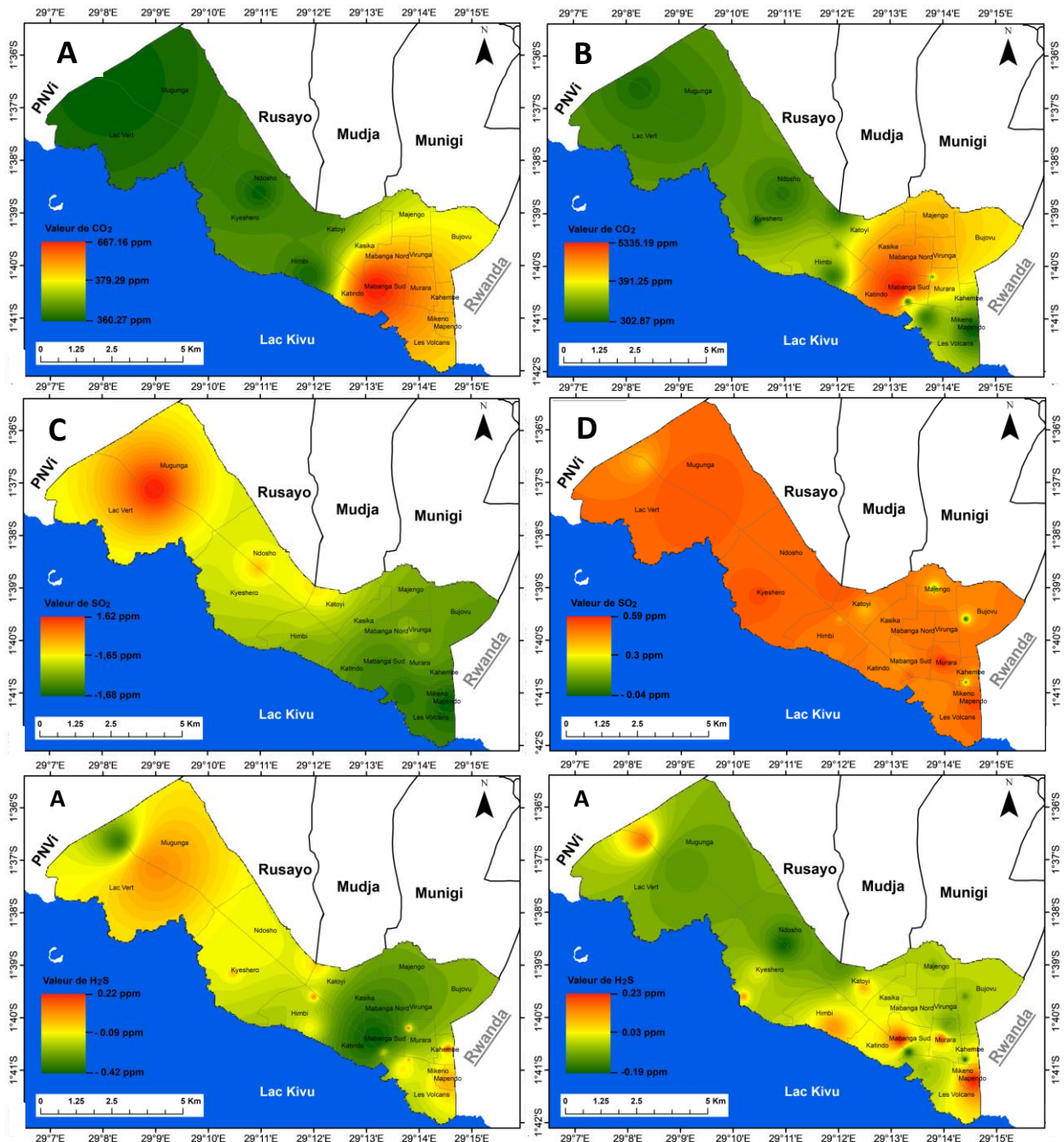


Figure 17. Example of air quality maps developed for carbon dioxide (A and B), sulphur dioxide (C and D) and Hydrogen Sulphide as part of volcanic gases hazards assessment prior Nyiragongo volcanic crisis. The maps were developed in the course of 2020.

Unfortunately the GVO team was not able to map the air quality during the volcanic crisis to produce maps such as those of figure 17, because the team had only one portable MultiGas which was in priority deployed in villages close to the lava flows. Furthermore, few days after the eruption began the intense seismic activity that directed more attention to Lake Kivu as this ground shaking was suspected to break out the lake's stability, which would release the enormous methane and carbon dioxide gases contained in the deep waters of the lake. That said, more attention was paid to ensure the lake remained stable, and in addition to water physico-chemical measurements that were performed; it was important to check if no gas was escaping from the surface of Lake Kivu. Thus, the MultiGas was regularly deployed and air near the lake's water surface was measured for CO₂, H₂S and SO₂ composition (Fig. 18-20).

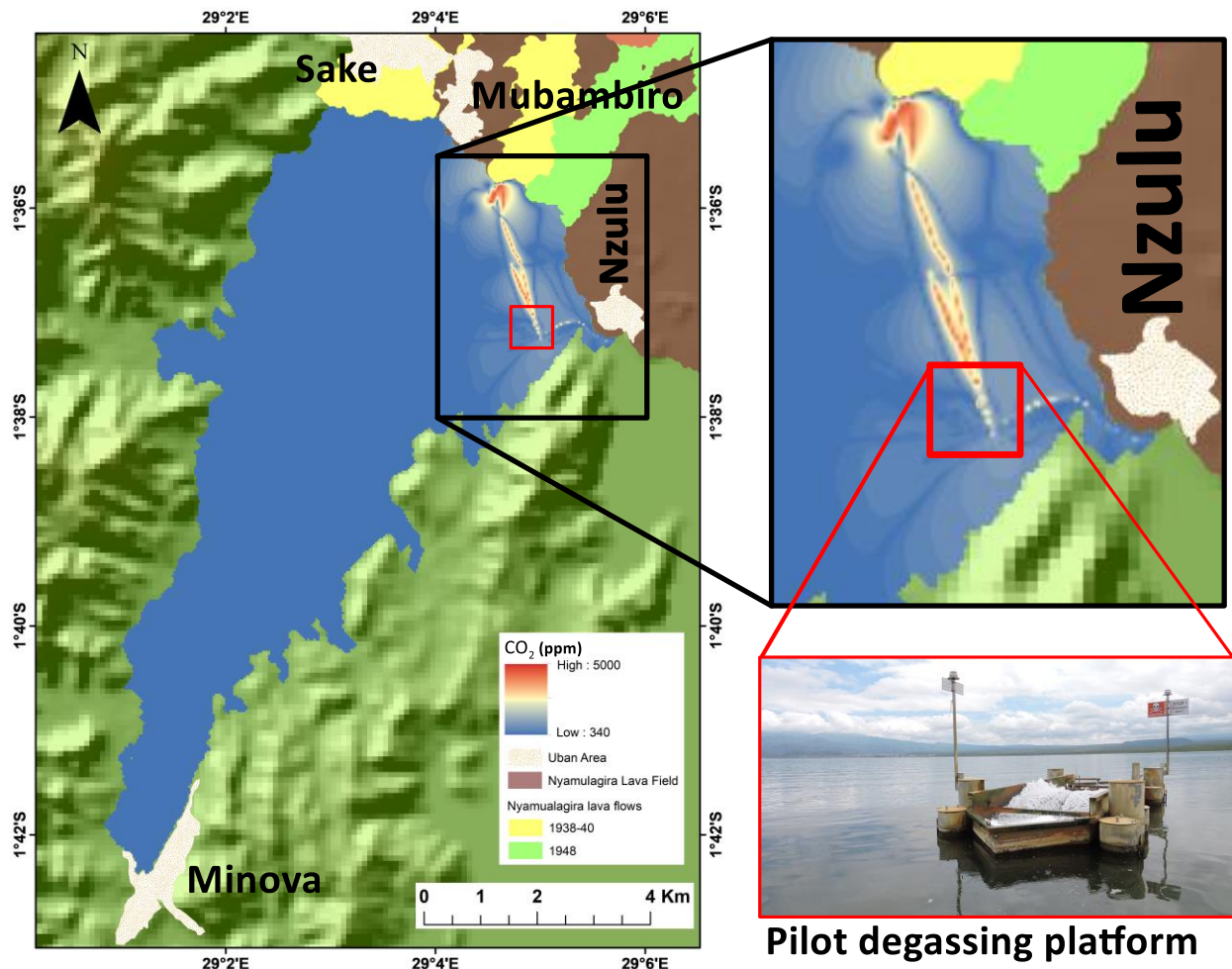


Figure 18. Spatial variation of CO₂ concentration in the air near water surface of Kabuno Bay, a sub-basin of Lake Kivu, during the first half of June 2021. The map was developed using the Inverse Distance Weighted (IDW) interpolation tool of ArcGIS with CO₂ input data series collected by a portable MultiGas placed at the roof of field boat. The CO₂ concentration for most part of the bay is in the range of unpolluted air with values as lower as 340 ppm, while the highest value of 5000 ppm was recorded at the degassing pilot degassing platform that inject gas in the atmosphere, and which dilutes in the air following the main wind direction.

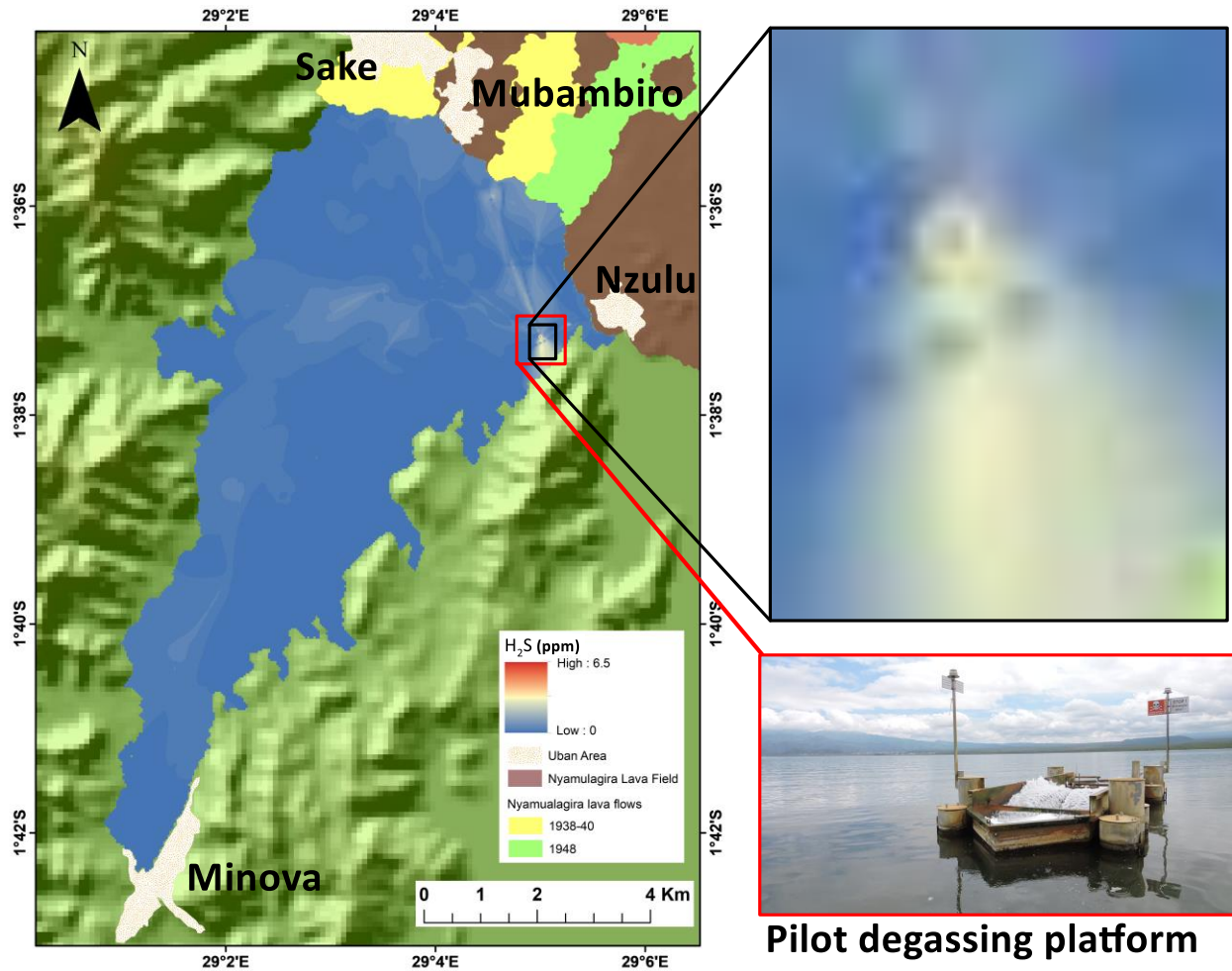


Figure 19. Spatial variation of H₂S concentration in the air near water surface of Kabuno Bay, a sub-basin of Lake Kivu, during the first half of June 2021. The map was developed using the Inverse Distance Weighted (IDW) interpolation tool of ArcGIS with H₂S input data series collected by a portable MultiGas placed at the roof of the field boat. The H₂S concentration for most part of the bay is in the range of unpolluted air with most values being equal to 0 ppm, while the highest value of 6.5 ppm was recorded at the degassing pilot degassing platform that inject gas in the atmosphere, and which dilutes in the air following the main wind direction.

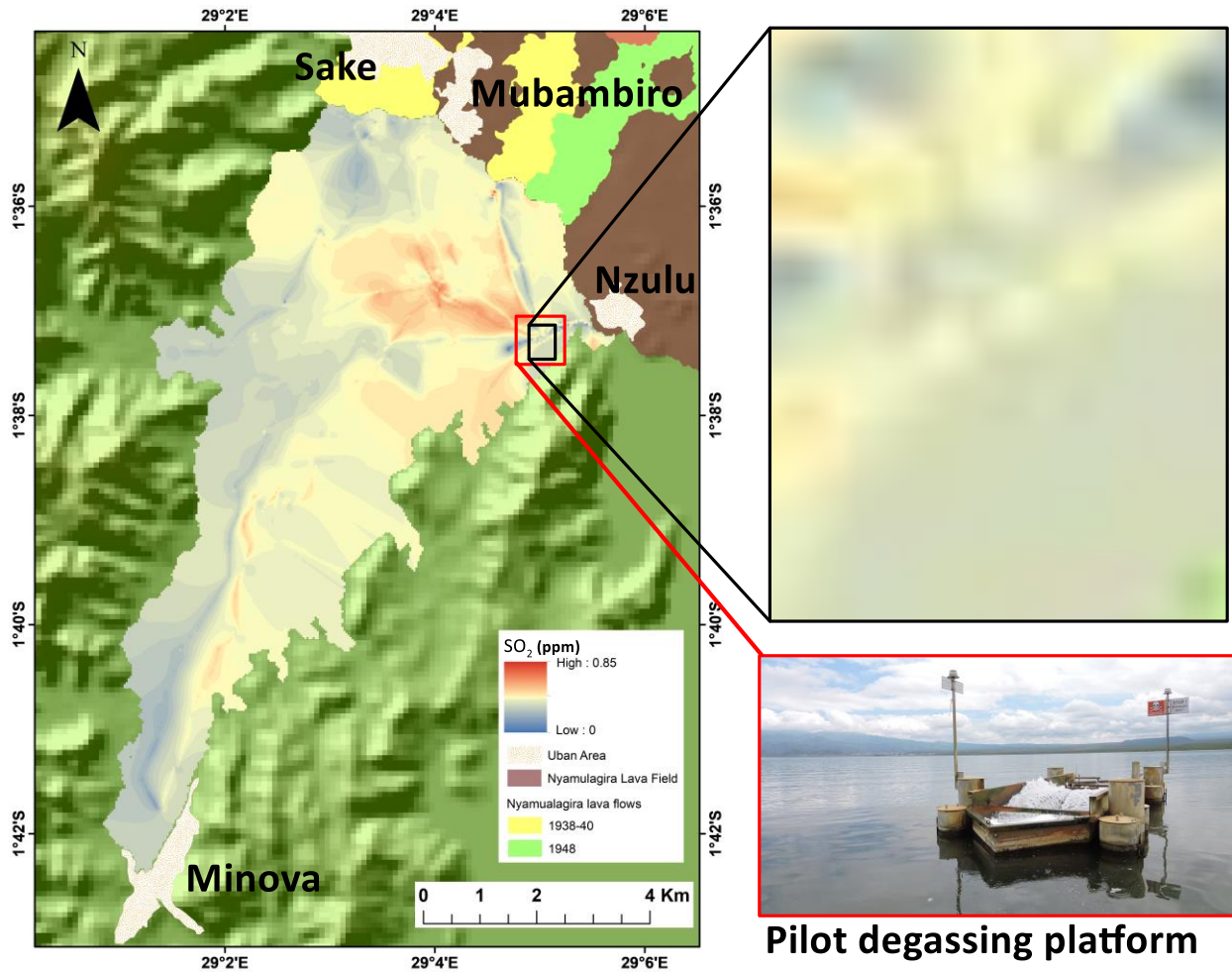


Figure 20. Spatial variation of SO₂ concentration in the air near water surface of Kabuno Bay, a sub-basin of Lake Kivu, during the first half of June 2021. The map was developed using the Inverse Distance Weighted (IDW) interpolation tool of ArcGIS with H₂S input data series collected by a portable MultiGas placed at the roof of the field boat. The SO₂ concentration for most part of the bay is in the range of unpolluted air with most values being equal to 0 ppm, while the highest value of 0.85 ppm was recorded at the degassing pilot degassing platform that inject gas in the atmosphere, and which dilutes in the air following the main wind direction.

The Kabuno bay contains enormous amounts of CO₂ and H₂S with few CH₄, with high concentrations of the two dominant gases being observed at shallow depths of about 15 m which makes the bay too sensitive to an overturn. A plan for degassing Kabuno bay is on the desk of the DRC government, an operation that will reduce the CO₂ and H₂S amounts and hence reduce the risk for an overturn. Since 2017, a degassing pilot platform has been installed in the bay with the plan of installing many others. However, this operation injects the gases into the atmosphere; hence care should be taken as for the health of population living in the coastline of Kabuno and that may be impacted by H₂S and CO₂ injected in the air.

5.1.5. Monitoring Lake Kivu stability during the Nyiragongo May 2021 eruption

Lake Kivu (1460 m, asl; Fig. 21) is a meromictic lake formed during the late Pleistocene while the Virunga volcanic chain was forming, and is located within the western branch of the EARS between the DRC and Rwanda. The lake is in contact with Nyiragongo and Nyamulagira lava flows to its the north (Fig. 21), has a maximum depth of 485 m, contains ~ 580 km³ of water over a surface area of 2,370 km², with water residence time of ~100 years above the major chemocline and 800 to 1,000 years under the major chemocline. The anoxic deep waters of the lake contain 300 km³ of CO₂, 60 km³ CH₄ at 0°C and 1 atm and concentrations increase with depth. Other gases (e.g. H₂S, nitrogen, and argon) are present at low concentrations. Most of the CO₂ dissolved in Lake Kivu is of magmatic origin entering the lake along sub-lacustrine springs and hydrothermal vents, and a few surface rivers from the active volcanic fields. CO₂ is also discharged into the lake as a gas phase that is dissolved into the water column principally along the north shore near the mazuku field. The rest of the CO₂ results from the decomposition of organic matter. CH₄ is derived from bacterial reduction of magmatic CO₂ (two-thirds) and from fermentation of organic material in the sediments (one-third). Because of the large hydrostatic pressure, the dissolved gases accumulate at depth and reach high concentrations that might give rise to a limnic eruption, also known as lake eruption, or lake overturn. Limnic eruptions are geologic processes recognized during the mid-1980s (Zhang and Kling 2006) when the eruptions of Lakes Monoun and Nyos in Cameroon killed ~1700 people and ~3,500 livestock up to 26 km away from the lakes. But Lake Kivu overturn could become the most disastrous lake eruption that has yet occurred in historical time, particularly when considering millions of people at risk.

Lake eruption dynamics depend on gas-liquid conditions and stability (Zhang and Kling 2006) and are driven by the exsolution of dissolved gases from the deep lake waters. The hydrostatic pressure remains the key parameter maintaining dissolved gases in the monimolimnion of Lake Kivu, and controls their dissolution and exsolution. As long as the hydrostatic pressure exceeds the sum of the partial pressures of the dissolved gases, there will not be any gas exsolution and/or limnic eruption unless an external agent upsets the water-gas equilibria. Below are listed and discussed, the internal and external agents that could give rise to a limnic eruption of Lake Kivu based on the local geologic and geodynamic setting.

Nyiragongo May 2021 eruption was followed by an intense seismic activity that persisted for about 2 weeks, with most of their epicenters being located in Lake Kivu particular its northern basin (Fig. 22). The persistent earthquakes series brought the fear of magma rising and accumulating beneath Goma city and Lake Kivu. The latter raised a scenario of a new eruption that could directly start inside Goma city or Lake Kivu, which could have increased the scenario of limnic eruption. It was thus mandatory to monitor Lake Kivu during these intense seismic and volcanic activities. The physico-chemical parameters were thus measured in

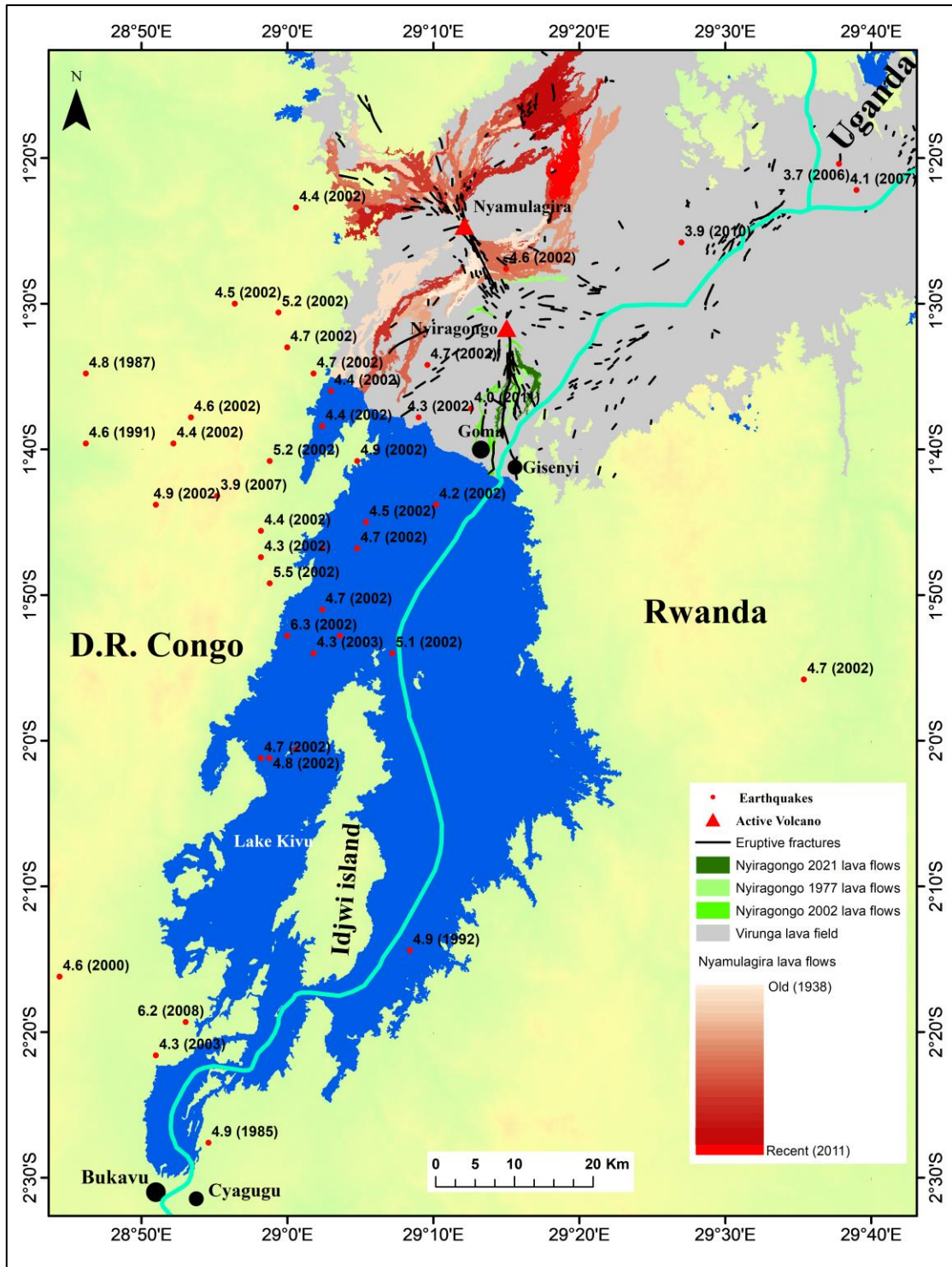


Figure 21. Main towns and cities in the catchment of Lake Kivu where over 2.5 million people live. All these cities could be impacted if Lake Kivu undergoes lake overturn but those located to the north are more threatened. The map also shows the location of the Goma Volcano Observatory seismic network and the main earthquakes ($M_w \geq 3.5$) recorded in the catchment of Lake Kivu from 1985 to 2011 (modified from Balagizi et al., 2018).

Kabuno Bay, a sub-basin of Lake Kivu having high dissolved CO₂ concentrations from the depth of ~ 15 m.

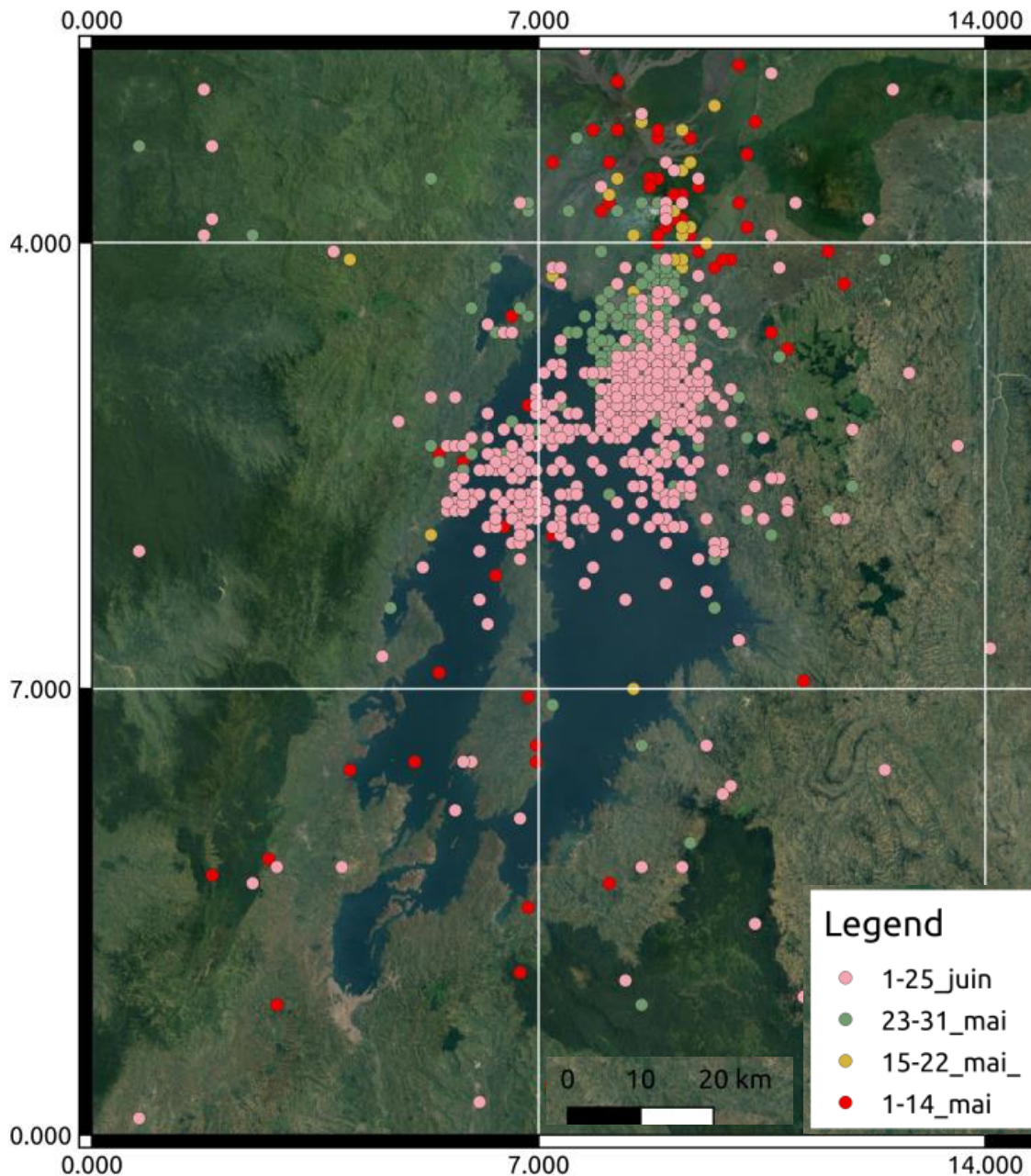


Figure 22. Distribution of epicenters of earthquakes recorded between May 1 and June 25, 2021 in the basin of Lake Kivu.

Some of the obtained results are listed below.

The physico-chemical parameters that were measured included specific conductivity, temperature, dissolved oxygen and pH; the profiles that were generated were compared to those obtained in September 2016.

1°) Specific Conductivity: In the biozone (seasonally mixed layer, as well as due to the wind) it was observed a significant difference in the data from September 2016 and that from May-June 2021 (Fig 23A). This is a season related variation, linked to the less mineralized rainwater input to the surface during the rainy season and which dilute the surface water; and hence to the decrease of the specific conductivity of upper layer. In the permanently stratified layer the values are very close, the slight difference observed at these depths are due to the differences of the equipment that were used during the two field campaigns.

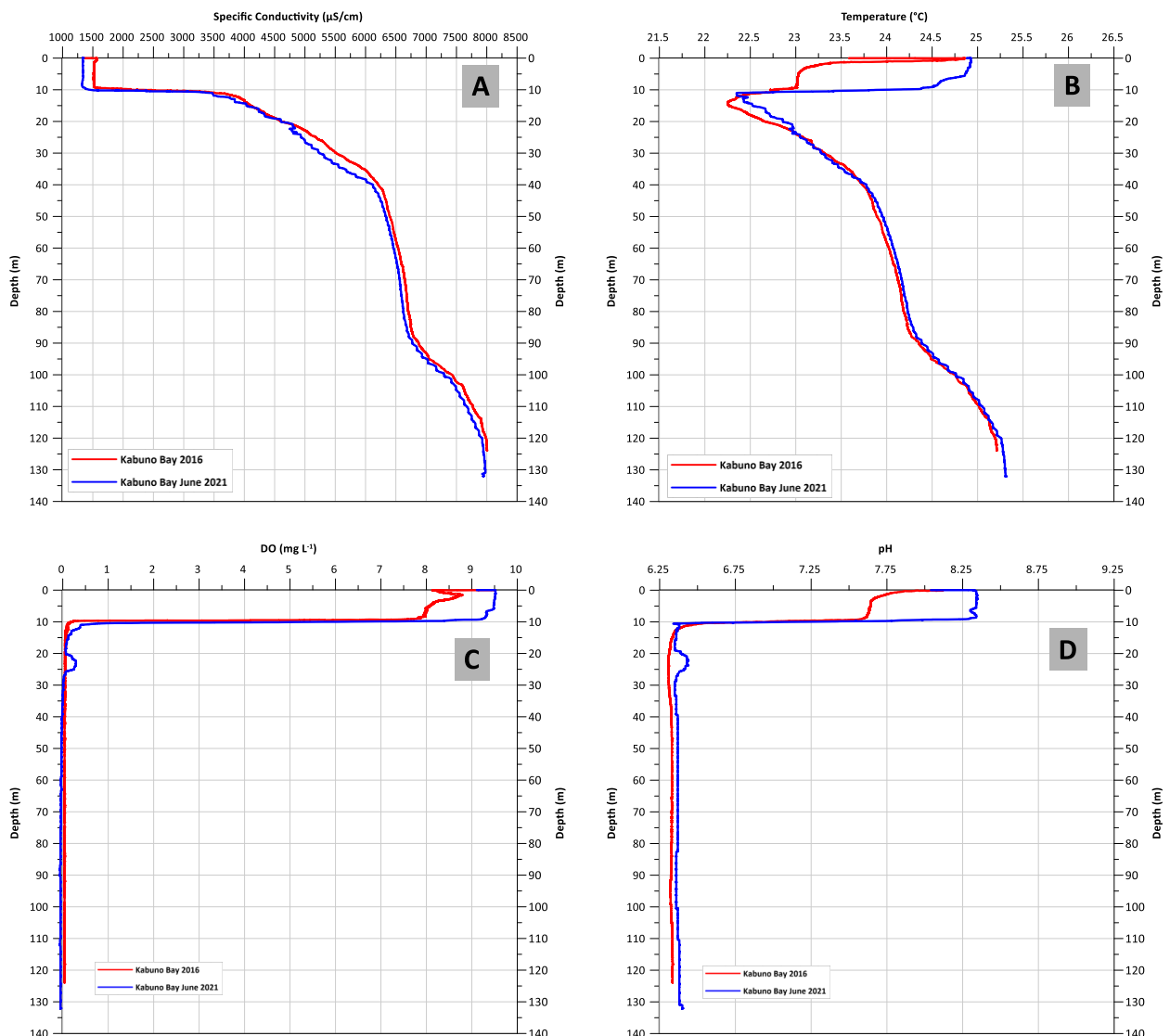


Figure 23. Profile showing the variation of specific conductivity (A), Temperature (B), dissolved oxygen (C) and pH (D) in Kabuno bay (sub-basin of Lake Kivu, Democratic Republic of the Congo), between September 2016 and June 2021.

- 2°) Temperature:** as for the specific conductivity, temperature in the biozone layer is affected by weather conditions and hence is subject to season variation. Thus, a difference of about 2 ° C is observed in the biozone between the measurements made in 2016 and that from 2021 (Fig. 23B). At the remaining depths of the lake, values from the two measurements show very similar values, with slight difference due to the equipment that was used.
- 3°) Dissolved Oxygen:** no anomalies were observed in the dissolved oxygen values, as data from 2016 and 2021 showed large similarities with small differences due to the equipment (Fig.23C). However, it is observed a slight increase of about 0.3 mg L⁻¹ at the depth between 20m and 25 m.
- 4°) The potential of hydrogen (pH):** the pH values from 2021 are very close to that of 2016; the difference of less than one pH unit observed in the biozone was expected (Fig. 23D). In fact, carbon dioxide concentration, photosynthesis activity, respiration and decomposition of organic materials all contribute to pH fluctuations due to their influences on CO₂, and hence to variation of pH levels with season. As for other parameters already discussed, particularly dissolved oxygen, the pH shows a variation in the order of 1/8 pH unit between 20 m and 25 m depths.

The physico-chemical parameters measured during the intense seismic activity that followed the Nyiragongo May 2021 eruption showed any significant changes compared to those measured in 2016. Water samples were collected and their analysis for major and trace elements will reveal more about the potential impact of Nyiragongo eruption on Lake Kivu stability.

References:

- Balagizi C.M., G. Mavonga, M. Kasereka, M. Liotta, M. Manzo, R. Lanari, M. Bonano, C. De Luca, G. Onorato, J. Lukindula, G. Ganci, C. Del Negro, A. Cappello, M. Coltelli, M. Mattia, D. Coppola, R. J. Durrheim, P. Mukambilwa, A. Kyambikwa, N. Mashagiuro, H. Ciraba, J. B. Lowenstern, P. J Kelly, W. McCausland, A. Kies; 2020. Virunga Volcanoes Supersite Biennial Report: 2017- 2019; DOI: 10.5281/zenodo.3910912; <https://zenodo.org/record/3911065#.XxHxQ54zY2w>
- Balagizi M.C. and M. Liotta, 2019. Key factors of precipitation stable isotope fractionation in Central-Eastern Africa and Central Mediterranean. *Geosciences* 2019, 9, 337 <https://www.mdpi.com/2076-3263/9/8/337>
- Balagizi MC, Kasereka M M, Cuoco E, Liotta M (2018a) Influence of moisture source dynamics and weather patterns on stable isotopes ratios of precipitation in Central-Eastern Africa.

- Science of the Total Environment 628–629, 1058–1078.
<https://doi.org/10.1016/j.scitotenv.2018.01.284>
- Balagizi, M.C, A. Kies, M. M. Kasereka, D. Tedesco, M. M. Yalire, W. A. McCausland. (2018b). Natural hazards in Goma and the surrounding villages, East African Rift System. Springer's Journal of Natural Hazards, 93, 31–66,
<https://doi.org/10.1007/s11069-018-3288-x>
- Balagizi, MC., Yalire, M., Ciraba, H., Kajeje, V., Minani, A., Kinja, A., Kasereka, M., (2016). Soil temperature and CO₂ degassing, SO₂ fluxes and field observations before and after the February 29, 2016 new vent inside Nyiragongo crater. Bulletin of Volcanology, 78 (9):1-11, <https://link.springer.com/article/10.1007/s00445-016-1055-y>
- Balagizi MC, Darchambeau F, Yalire M, Bouillon S, Borges VA (2015) River geochemistry, chemical weathering, and atmospheric CO₂ consumption rates in the Virunga Volcanic Province (East Africa), Geochemistry Geophysics Geosystems, 16, 2637- 2660. doi:10.1002/2015GC005999
- Degens ET, Von Herzen RP, Wong HK, Deuser WG, Jannasch HW (1973) Lake Kivu: structure, chemistry and biology of an East African rift lake. Geol. Rundsch., 62 (1), 245-277.
- Ebinger CJ (1989) Tectonic development of the western branch of the East African Rift System. Geol. Soc. Am. Bull., 101, 885–903.
- Kling GW, Evans WC, Tanyileke G, Kusakabe M, Ohba T, Yoshida Y, Hell JV (2005) Degassing Lakes Nyos and Monoun-defusing certain disaster. Proc. National Academy of Sciences 102: 14185-14190. doi: 10.1073/pnas.0502274102
- Pasche N, Schmid M, Vazquez F, Schubert C, Wüest A, Kessler J, Pack M, Reeburgh WS, Buergermann H (2011) Methane sources and sinks in Lake Kivu, J. Geophys., 6,1-16. doi:10.1029/2011JG001690
- Schmid M, Tietze K, Halbwachs M, Lorke A, McGinnis D, Wüest A (2004) How hazardous is the gas accumulation in Lake Kivu? Arguments for a risk assessment in light of the Nyiragongo Volcano eruption of 2002. Acta Vulcanologica., 15 (1-2), 115-122.
- Schoell M, Tietze K, Schoberth SM (1988) Origin of methane in Lake Kivu (East-Central Africa). Chem. Geol., 71, 257–265. doi:10.1016/0009-2541(88)90119-2
- Tassi F, Vaselli O, Tedesco D, Montegrossi G, Darrah T, Cuoco E, Mapendano MY, Poreda R, Huertas DA (2009) Water and gas chemistry at Lake Kivu (DRC): Geochemical evidence of vertical and horizontal heterogeneities in a multibasin structure. Geochem. Geophys. Geosyst., 10 (2),1-22. doi:10.1029/2008GC002191
- Tietze K, Geyh M, Müller H, Schröder L, Stahl W, Wehner H (1980) The genesis of methane in Lake Kivu (Central Africa). Geol. Rundsch., 69, 452-472.
- Zhang Y, Kling GW (2006) Dynamics of Lake Eruptions and Possible Ocean Eruptions. Ann. Rev. Earth Planet. Sc., 34, 293-324. doi:10.1146/annurev.earth.34.031405.125001

5.1.6. Baseline for rainwater chemistry and quality as influenced by Nyiragongo volcano permanent plume

Single rainwater samples were collected in the city of Goma (~ 1,1 million inhabitants, Fig. 24), eastern Democratic Republic of the Congo, from January to June 2013 to draw a baseline for rainwater chemical composition and quality as influenced by the permanent plume of Nyiragongo volcano. This was a better period for a baseline as the neighbouring Nyamulagira volcano, only 15 km apart, had no important degassing from its central crater, and hence the recorded volcanic influence on the rainwater chemistry was solely from Nyiragongo's lava lake which has been active since May 2002. The baseline for the rainwater chemistry and quality is important for this highly populated region where rainwater is the unique potable water source for the inhabitants of many villages surrounding the volcanoes, and for some of the inhabitants of the city of Goma. Our results show that samples collected at the crater rim of Nyiragongo were more acidic with pH ranging from 3.70 to 3.82, while the majority of rainwater samples collected in downtown Goma city and to the northeastern zone of the volcano had pH close to 5.7; which represents the value for rainwater from unpolluted continental areas (Berner and Berner, 2012). However, the pH was as low as 3.93 to the west of Nyiragongo volcano because the volcanic plume is directed westward by the dominant local wind direction. The western part of the city of Goma as well as the small town of Sake and many villages (e.g. Rusayo, Mubambiro, Kingi,...) are located in this zone, and experience endemic fluorosis caused by high fluoride in the available water. The mean F^- in this zone was 0.38 mg/L, while the southern and northeastern zones had mean F^- concentrations on 0.44 and 0.01 mg/L respectively; even though concentrations higher than the WHO guidelines were found in few samples from the western zone (1.69 mg/L) and from the southern zone (3.44 mg/L). Compared to data from Cuoco et al, 2012 obtained during the Nyamulagira 2010 eruption, and from Balagizi et al, 2017 and Liotta et al, 2017 obtained during the intense degassing of both Nyiragongo and Nyamulagira lava lakes; we have noted similarity in the spatial variation of the pH, but samples from the present study showed notable lower concentrations of major elements. This is the case for fluoride which is strictly of volcanic origin. For the other major elements, anthropogenic sources, mainly the traffic and wind-blown dust; or other non-volcanic natural sources influenced their concentrations. Thus, the anions (Cl^- and SO_4^{2-}) and cations (Na^+ , K^+ , Mg^{2+} , and Ca^{2+}) from the present study are either lower compared to that previously reported in the literature for the Virunga, or are both comparable for the zones impacted by anthropogenic activities.

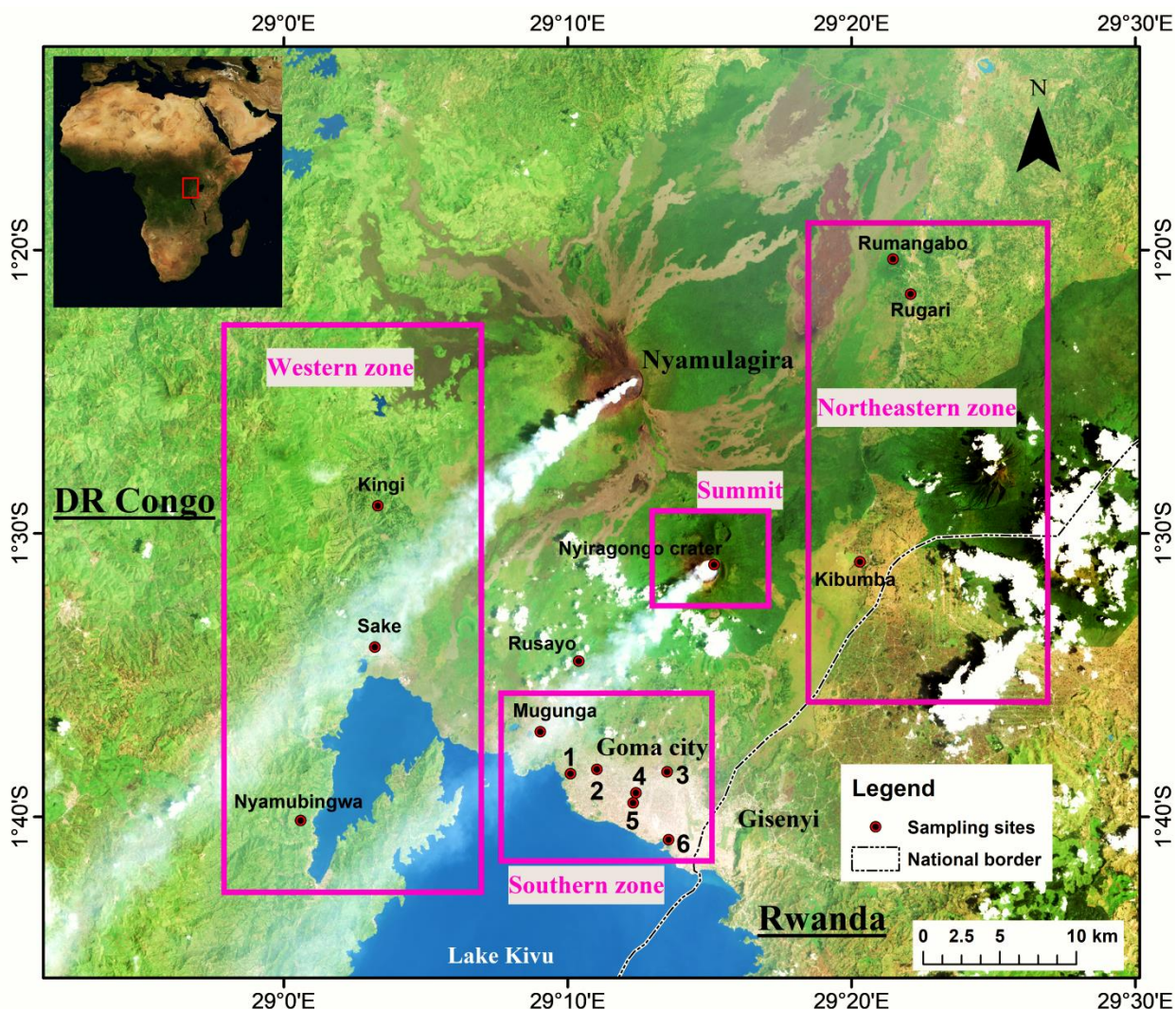


Figure 24. Locations of sampling sites in Goma city, surrounding villages and around Nyiragongo volcanoes situated within the western branch of the East African Rift System, East Africa. In the Southern zone, the numbers correspond to the sites as follows: 1 for Kituku, 2 for Ndosho, 3 for Ngangi, 4 for Kibwe, 5 for Kasika and 6 for OVG.

The main findings of this research are as follows:

- The pH at the crater and west of the Nyiragongo was more acidic than other groups due to the influence of the gas plume in these areas and which is carried by the wind whose preferential direction in the region remains from East to West (Fig. 25A).
- The dominance of F^- and Cl^- anions at the crater of the volcano and SO_4^{2-} anions in the south was noted due to the dissolution of HF, HCl and H_2SO_4 acids in water. Cl^- anion was the most dominant of the all ions and contributed to 20,29 % of the total ionic concentration. Na^+ and K^+ were the most dominant of cations and were of volcanic origin (Fig. 25B,CD).

- Volcanic emissions are the primary sources of dissolved solutes, and their impact decreases with distance. The Virunga region is not industrialized, hence vehicle traffic and soil dust from roads and farms remain the unique anthropogenic sources of pollution.
- Comparing the results of this work with published investigations (Balagizi et al, 2017; Cuoco et al, 2012 and Liotta et al, 2017), we remarked that the atmosphere of the region is less polluted when there is no contribution of the plume of the Nyamulagira volcano from eruption or presence of a lava lake. On the other hand, compared to others non volcanic areas the Virunga region maintains a high concentration of ions of volcanic origin. The mean pH value (3.75) of Nyiragongo volcano is comparable to that obtained at a site located 0.8 km from the Halemaumau crater of Kilauea volcano (3.6) but is high compared to that of La fossa crater in range of (2-3.5) at Vulcano Island (Table 1 and 2). The Virunga region generally could be considered to be an unpolluted area with its mean pH of 5.6 compared to Hawaii Island with mean pH ranged between 4-5 which similarly is proximal to an open system volcano like Nyiragongo (Fig. 26).

www.geo-gsnl.org

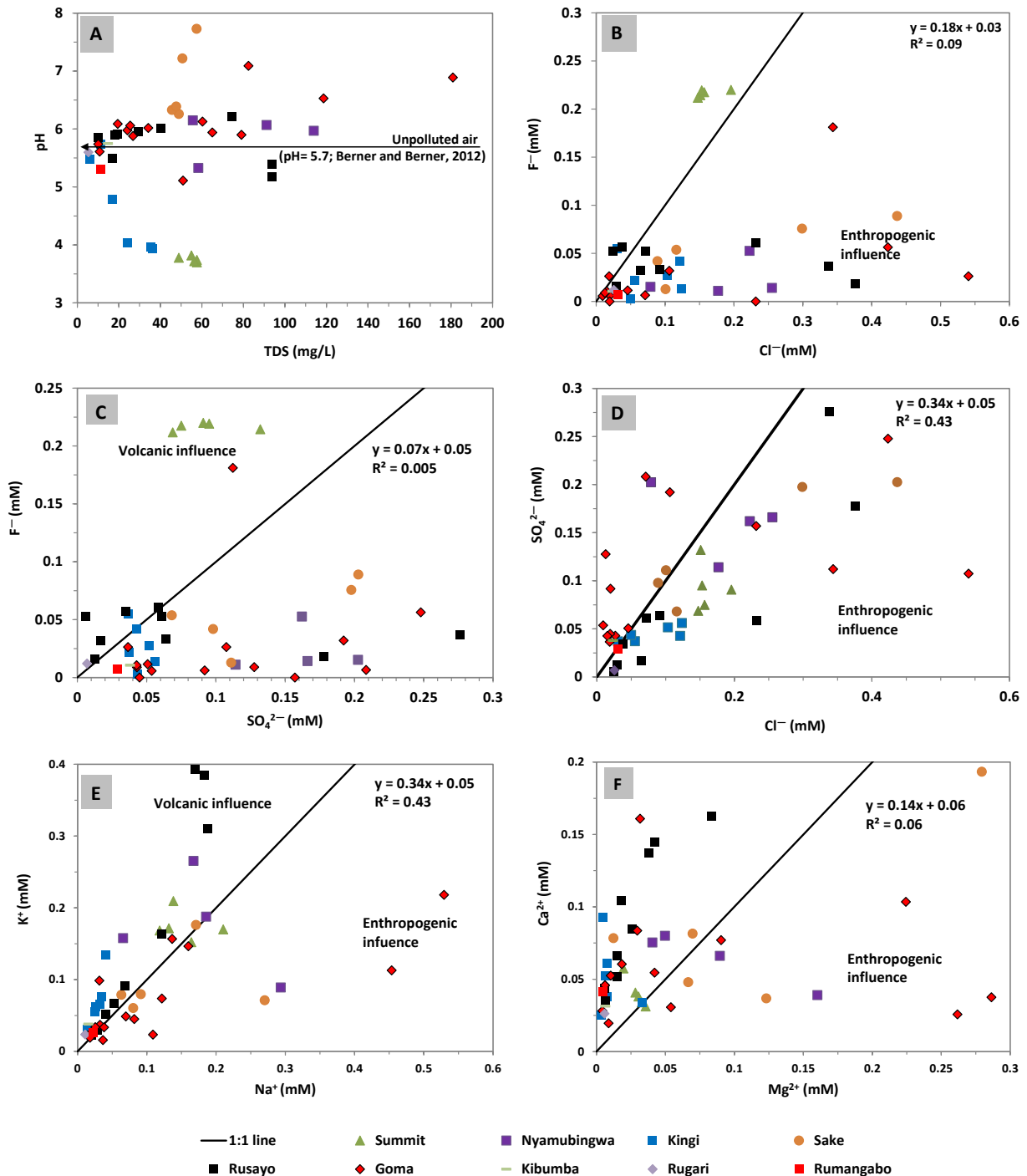


Figure 25. Relationship between total dissolved substances (TDS) and pH (A), F^- and Cl^- (B), SO_4^{2-} and F^- (C), Cl^- and SO_4^{2-} (D), Na^+ and K^+ (E), Mg^{2+} and Ca^{2+} (F) in rainwater collected on a daily basis in the Nyiragongo and Nyamulagira volcanic fields, situated within the western branch of the East African Rift System, East Africa; between January and June 2013.

www.geo-gsnl.org

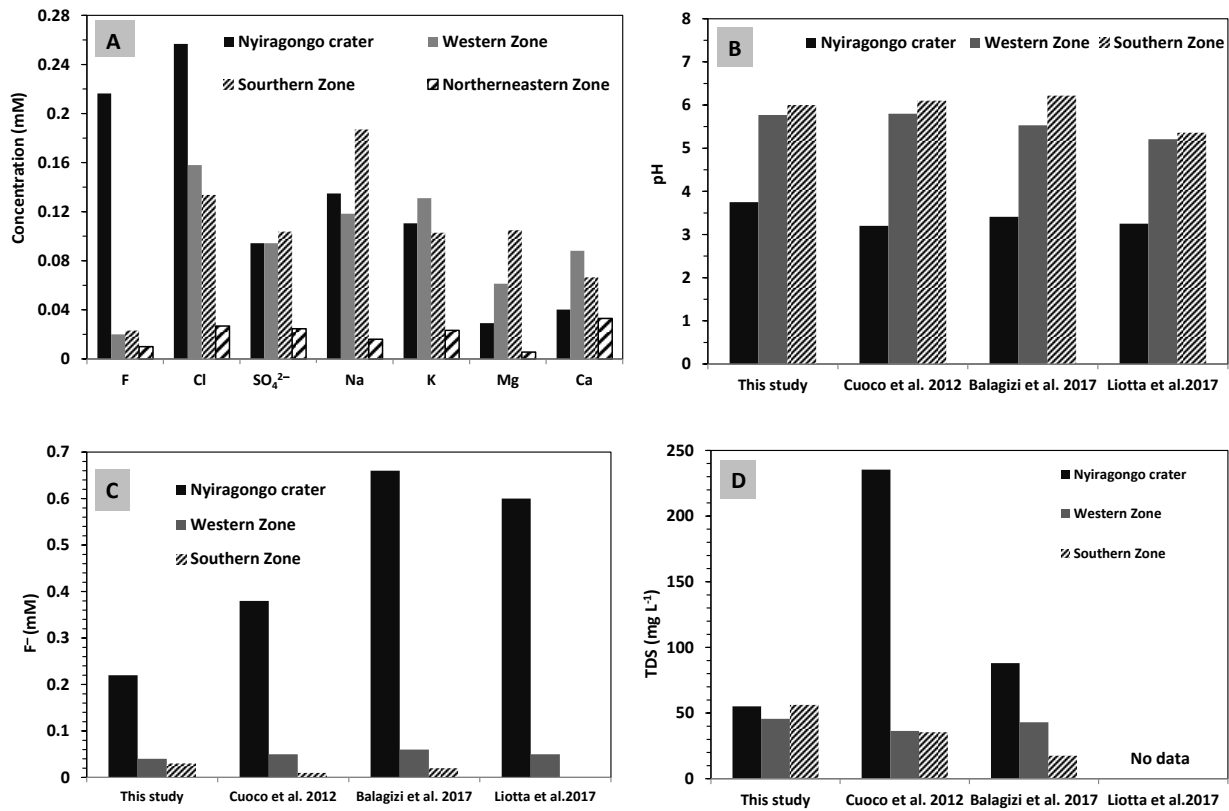


Figure 26. Mean major ion concentrations in different zones (A), comparison of pH (B), F⁻ concentration (C) and total dissolved substances (TDS) (D) means of this study and the previous studies in the Virunga and Nyamulagira volcanic fields, located within the western branch of the East African Rift System, East Africa; between January and June 2013

Table 1. Sampling sites, physico-chemical parameters and major ions concentrations of single rainwater collected in Goma city, on and around Nyiragongo volcano, between January and June 2013

Site Name	Latitude (°)	Longitude (°)	Altitude (m a.s.l.)	Location zone with respect to summit	Sampling Date	E.C. (µS/cm)	pH	F ⁻ (mg L ⁻¹)	Cl ⁻ (mg L ⁻¹)	NO ₃ ⁻ (mg L ⁻¹)	SO ₄ ²⁻ (mg L ⁻¹)	H ₂ PO ₄ ⁻ (mg L ⁻¹)	Na ⁺ (mg L ⁻¹)	K ⁺ (mg L ⁻¹)	Mg ²⁺ (mg L ⁻¹)	Ca ²⁺ (mg L ⁻¹)	TDS (mg L ⁻¹)	Charge balance
Nyiragongo crater	-1.51833	29.2525	3429	Nyiragongo Summit	May 20, 2013	82.00	3.82	4.07	5.36	0.00	12.67	0.00	4.83	5.28	0.47	2.30	54.94	4.27
Nyiragongo crater	-1.51833	29.2525	3429	Nyiragongo Summit	June 8, 2013	73.00	3.78	4.02	5.23	0.00	6.60	0.00	2.73	5.24	0.68	1.63	56.28	9.21
Nyiragongo crater	-1.51833	29.2525	3429	Nyiragongo Summit	June 17, 2013	86.00	3.70	4.13	5.56	0.00	7.20	0.00	3.03	5.33	0.80	1.36	48.91	9.68
Nyiragongo crater	-1.51833	29.2525	3429	Nyiragongo Summit	June 13, 2013	86.00	3.74	4.18	6.94	0.00	8.72	0.00	3.18	6.51	0.74	1.53	57.62	9.81
Nyiragongo crater	-1.51833	29.2525	3429	Nyiragongo Summit	June 1, 2013	84.00	3.72	4.17	5.43	0.00	9.14	0.00	3.77	4.73	0.87	1.25	57.62	9.96
Nyamubingwa	-1.66883	29.00983	1473	Western zone	April 26, 2013	136.00	6.07	0.27	9.05	4.17	15.94	1.57	6.74	2.77	3.89	1.56	58.29	-5.64
Nyamubingwa	-1.66883	29.00983	1473	Western zone	April 20, 2013	87.00	5.33	0.21	6.27	12.79	10.96	0.00	3.85	8.25	0.98	3.02	91.12	-3.78
Nyamubingwa	-1.66883	29.00983	1473	Western zone	May 2, 2013	83.00	6.15	0.29	2.79	1.73	19.44	0.00	1.51	4.91	1.21	3.20	55.61	-4.23
Nyamubingwa	-1.66883	29.00983	1473	Western zone	May 9, 2013	170.00	5.97	1.00	7.89	0.49	15.56	1.84	4.26	5.84	2.17	2.65	113.90	-6.47
Kingi/Kunene	-1.48366	29.05516	2011	Western zone	April 19, 2013	53.00	3.97	0.79	4.30	0.86	4.11	0.00	0.94	4.17	0.08	1.01	36.18	3.79
Kingi/Kunene	-1.48366	29.05516	2011	Western zone	March 19, 2013	17.00	5.74	1.04	1.09	0.74	3.56	0.00	0.57	1.71	0.19	1.53	11.39	3.31
Kingi/Kunene	-1.48366	29.05516	2011	Western zone	May 2, 2013	25.00	4.78	0.41	1.97	0.83	3.58	0.00	0.60	1.94	0.80	1.36	24.12	-9.72
Kingi/Kunene	-1.48366	29.05516	2011	Western zone	April 25, 2013	9.00	5.48	0.05	1.76	0.37	4.19	0.00	0.31	0.95	0.19	2.45	35.51	-5.17
Kingi/Kunene	-1.48366	29.05516	2011	Western zone	March 16, 2013	54.00	3.93	0.26	4.38	1.05	5.39	0.00	0.79	2.35	0.12	3.71	6.03	0.72
Kingi/Kunene	-1.48366	29.05516	2011	Western zone	April 4, 2013	36.00	4.04	0.52	3.66	0.00	4.95	0.00	0.74	2.03	0.15	2.09	16.75	7.65
Sake	-1.56683	29.05333	1511	Western zone	April 24, 2013	73.00	6.26	1.02	4.12	0.05	6.54	0.00	2.09	2.48	1.62	1.92	47.57	-8.82
Sake	-1.56683	29.05333	1511	Western zone	May 25, 2013	68.00	6.33	0.24	3.57	2.90	10.65	0.00	1.84	1.88	0.30	3.14	57.42	7.95
Sake	-1.56683	29.05333	1511	Western zone	April 20, 2013	85.70	7.73	1.69	15.49	0.52	19.46	0.00	6.21	2.21	6.79	7.75	48.91	-4.97
Sake	-1.56683	29.05333	1511	Western zone	May 10, 2013	75.50	7.22	1.44	10.60	0.81	18.97	0.00	3.93	5.48	2.99	1.47	50.59	7.16
Sake	-1.56683	29.05333	1511	Western zone	April 24, 2013	71.00	6.39	0.80	3.16	2.00	9.40	0.00	1.45	2.45	1.69	3.27	45.56	-5.76
Rusayo	-1.57500	29.17316	1671	Western zone	April 8, 2013	140.00	5.39	0.70	11.98	16.46	26.50	0.89	4.21	11.96	2.03	6.52	74.37	6.41
Rusayo	-1.57500	29.17316	1671	Western zone	January 26, 2013	111.00	6.21	1.15	8.24	13.46	5.59	1.01	4.32	9.64	0.93	5.50	40.20	-7.56
Rusayo	-1.57500	29.17316	1671	Western zone	May 1, 2013	44.00	5.95	1.00	2.53	1.79	5.84	1.00	1.56	2.83	0.63	3.40	18.09	-9.16
Rusayo	-1.57500	29.17316	1671	Western zone	May 12, 2013	25.00	5.50	0.61	2.28	0.77	1.61	0.00	0.66	0.92	0.14	1.75	93.80	7.51
Rusayo	-1.57500	29.17316	1671	Western zone	March 26, 2013	27.00	5.90	1.08	1.34	2.53	3.32	0.00	1.20	2.09	0.37	2.66	93.80	-8.23
Rusayo	-1.57500	29.17316	1671	Western zone	March 21, 2013	60.00	6.02	0.63	3.26	9.97	6.12	0.00	2.79	5.07	0.43	4.19	19.43	-7.53
Rusayo	-1.57500	29.17316	1671	Western zone	May 20, 2013	15.00	5.85	0.30	1.04	1.29	1.22	0.00	0.45	0.71	0.16	1.41	29.48	-3.24
Rusayo	-1.57500	29.17316	1671	Western zone	April 5, 2013	140.00	5.18	0.35	13.34	3.46	17.07	0.91	3.89	12.21	1.02	5.79	16.75	-8.01
Rusayo	-1.57500	29.17316	1671	Western zone	April 14, 2013	29.00	5.91	1.00	0.88	2.54	0.56	0.50	0.92	1.60	0.36	2.07	10.05	-9.91

Table 1 (continued)

Site Name	Latitude (°)	Longitude (°)	Altitude (m a.s.l.)	Location zone with respect to summit	Sampling Date	E.C. (µS/cm)	pH	F ⁻ (mg L ⁻¹)	Cl ⁻ (mg L ⁻¹)	NO ₃ ⁻ (mg L ⁻¹)	SO ₄ ²⁻ (mg L ⁻¹)	H ₂ PO ₄ ⁻ (mg L ⁻¹)	Na ⁺ (mg L ⁻¹)	K ⁺ (mg L ⁻¹)	Mg ²⁺ (mg L ⁻¹)	Ca ²⁺ (mg L ⁻¹)	TDS (mg L ⁻¹)	Charge balance
Goma/OVG	-1.68001	29.22583	1501	Southern zone	April 27, 2013	123.00	7.09	0.61	3.77	2.55	18.45	0.00	2.50	0.73	6.36	1.03	10.05	-6.07
Goma/OVG	-1.68001	29.22583	1501	Southern zone	March 26, 2013	15.00	5.74	0.50	0.67	0.80	3.51	0.00	0.84	0.49	0.15	1.84	82.41	-4.74
Goma/OVG	-1.68001	29.22583	1501	Southern zone	May 9, 2013	36.00	5.98	0.17	0.96	1.57	4.13	0.00	0.74	1.15	0.15	1.84	10.72	-7.55
Goma/OVG	-1.68001	29.22583	1501	Southern zone	May 11, 2013	38.00	6.06	0.12	0.70	1.38	8.82	0.00	0.59	1.05	1.02	2.18	24.12	-5.35
Goma/OVG	-1.68001	29.22583	1501	Southern zone	May 10, 2013	40.00	5.88	0.00	0.69	5.67	4.31	0.20	1.88	1.40	0.25	2.10	26.80	-9.07
Goma/OVG	-1.68001	29.22583	1501	Southern zone	May 12, 2013	29.00	6.09	0.20	0.55	1.46	4.10	0.00	0.88	1.04	0.21	0.78	25.46	-3.88
Goma/OVG	-1.68001	29.22583	1501	Southern zone	April 30, 2013	16.00	5.61	0.11	0.33	0.57	5.15	0.00	0.41	0.59	0.10	1.13	19.43	5.76
Goma/OVG	-1.68001	29.22583	1501	Southern zone	May 23, 2013	118.00	5.90	0.00	8.21	13.66	15.07	0.00	3.67	4.56	0.77	6.45	79.06	9.96
Goma/Kituku	-1.64133	29.16833	1479	Southern zone	April 10, 2013	51.00	6.02	0.17	0.45	0.97	12.26	0.20	1.60	1.51	1.31	1.23	34.17	-9.57
Goma/Ndosho	-1.63880	29.18366	1524	Southern zone	April 10, 2013	90.00	6.13	0.12	2.52	1.92	20.00	0.00	2.79	2.29	2.20	3.08	60.30	-6.66
Goma/Mungunga	-1.61666	29.1505	1511	Southern zone	April 12, 2013	97.00	5.94	3.44	12.19	0.48	10.78	0.00	3.14	4.87	5.45	4.14	64.99	1.90
Goma/Ngangi	-1.64016	29.225	1568	Southern zone	April 17, 2013	177.00	6.53	0.50	19.16	0.50	10.32	0.00	12.16	6.78	0.45	2.42	118.59	-9.51
Goma/Kasika	-1.65850	29.205	1522	Southern zone	April 11, 2013	270.00	6.89	1.07	15.01	3.00	23.79	0.30	10.43	3.51	6.96	1.50	180.90	-6.65
Goma/Kibwe	-1.65250	29.20666	1547	Southern zone	April 16, 2013	76.00	5.11	0.22	1.62	8.87	4.87	0.60	0.72	3.07	0.72	3.35	50.92	2.85
Kibumba	-1.51666	29.33816	2026	Northeastern zone	April 13, 2013	22.00	5.75	0.20	0.83	0.22	3.65	0.00	0.35	1.18	0.15	1.26	14.74	-9.40
Rugari	-1.35916	29.368	1565	Northeastern zone	April 14, 2013	8.00	5.60	0.23	0.91	0.57	0.67	0.20	0.25	0.73	0.14	1.05	5.36	-8.37
Rumangabo	-1.33866	29.35766	1602	Northeastern zone	April 11, 2013	17.00	5.31	0.14	1.11	0.73	2.78	0.10	0.51	0.82	0.11	1.66	11.39	-8.10

TDS values calculated from measured specific conductivity after Atekwana et al., 2004.

Charge balances were calculated using values expressed in mmol/L.

Table 2. Comparison of physico-chemical parameters and major ions concentrations of single rainwater collected in Goma city, on and around Nyiragongo volcano, with literature data on rainwater chemistry at Nyiragongo and Nyamulagira volcanoes, as well as some Italian long lasting open system volcanoes

	Zone	pH	E.C. ($\mu\text{S}/\text{cm}$)	F^- (mmol L^{-1})	Cl^- (mmol L^{-1})	SO_4^{2-} (mmol L^{-1})	Na^+ (mmol L^{-1})	K^+ (mmol L^{-1})	Mg^{2+} (mmol L^{-1})	Ca^{2+} (mmol L^{-1})
This study	Nyiragongo crater	3.75 (3.70-3.82)	82.2 (73.00-86.00)	0.22 (0.21-0.22)	0.17 (0.15-0.21)	0.09 (0.07-0.13)	0.17(0.14-0.21)	0.15 (0.13-0.18)	0.03 (0.02-0.04)	0.04 (0.03-0.06)
	Western zone	5.77 (3.93-7.73)	68.09 (9.00-170)	0.04 (0.00-0.09)	0.15 (0.02-0.44)	0.10 (0.01-0.28)	0.10(0.01-0.29)	0.10 (0.02-0.32)	0.05 (0.00-0.28)	0.08 (0.03-0.19)
	Southern zone	6.00 (5.11-7.09)	84.00 (15.00-270)	0.03 (0.00-0.18)	0.13 (0.01-0.54)	0.11 (0.04-0.25)	0.13(0.02-0.53)	0.06 (0.01-0.17)	0.08 (0.00-0.29)	0.06 (0.02-0.16)
	Northeastern zone	5.55 (5.31-5.75)	15.66 (8.00-22.00)	0.01 (0.01-0.01)	0.03 (0.02-0.03)	0.02 (0.01-0.04)	0.02(0.01-0.02)	0.02 (0.02-0.03)	0.01 (0.00-0.01)	0.03 (0.03-0.04)
Cuoco et al, 2012	Nyiragongo crater	3.20 (2.30-5.60)	256.0 (28-1828)	0.38 (bdl-10.21)	0.41 (0.01-7.59)	0.41 (0.01-3.53)	0.16(0.01-1.17)	0.13 (0.01-0.65)	0.03 (0.00-0.54)	0.10 (0.01-0.71)
	Western zone	5.8 (4.0-7.0)	44 (11-115)	0.05 (0.01-0.74)	0.07 (0.01-1.55)	0.06 (0.01-0.20)	0.07(0.02-0.29)	0.04 (0.02-0.30)	0.01 (0.00-0.15)	0.07 (0.01-0.39)
	Southern zone	6.10 (4.90-8.10)	40.0 (5.0-178)	0.01 (bdl-0.08)	0.03 (0.00-0.22)	0.03 (0.00-0.37)	0.04(0.00-0.57)	0.03 (0.00-0.23)	0.02 (bdl-0.26)	0.04 (0.00-0.35)
Balagizi et al, 2017	Nyiragongo crater	3.41 (3.10-3.17)	131 (85-172)	0.66 (0.10-2.64)	0.41 (0.04-1.07)	0.14 (0.05-0.36)	0.33(0.04-1.16)	0.22 (0.04-0.57)	0.11 (0.01-0.46)	0.13 (0.02-0.50)
	Western zone	5.53 (4.06-6.77)	64 (26.33-95.33)	0.06 (0.02-0.17)	0.15 (0.04-0.54)	0.06 (0.03-0.15)	0.04(0.02-0.18)	0.08 (0.03-0.57)	0.05 (0.01-0.40)	0.10 (0.03-0.91)
	Southern zone	6.22 (4.74-7.48)	41 (10-81.5)	0.02 (0.00-0.07)	0.09 (0.02-0.29)	0.04 (0.02-0.09)	0.05 (0.01-0.14)	0.10 (0.02-0.51)	0.03 (0.01-0.06)	0.05 (0.02-0.12)
Liotta et al, 2017	Nyiragongo crater	3.25 (3.11-3.49)	No data	0.60 (0.46-0.63)	0.28 (0.15-0.36)	0.19 (0.14-0.25)	0.08 (0.07-0.10)	0.09 (0.06-0.17)	0.16 (0.01-0.03)	0.03 (0.02-0.05)
	Western zone	5.21 (3.4-6.41)	No data	0.05 (0.00-0.28)	0.12 (0.00-0.42)	0.05 (0.00-0.12)	0.03 (0.01-0.12)	0.04 (0.00-0.16)	0.01 (0.00-0.02)	0.03 (0.00-0.11)
	Southern zone	5.36 (4.96-5.85)	No data	0.00 (0.00-0.00)	0.02 (0.01-0.03)	0.02 (0.01-0.02)	0.03 (0.02-0.04)	0.03 (0.01-0.08)	0.01 (0.00-0.01)	0.03 (0.02-0.04)
Etna*		5.3 (2.0-8.2)	49 (7-2890)	0.01 (bdl-3.42)	0.12 (0.01-11.68)	0.06 (0.01-0.05)	0.08 (0.00-3.13)	0.01 (0.00-1.02)	0.02 (0.00-0.90)	0.05 (0.01-1.50)
Stromboli**		5.6 (3.2-7.6)	No data	0.06 (0.01-5.86)	0.65 (0.16-7.56)	0.09 (bdl-7.10)	0.46 (0.13-3.52)	0.07 (0.01-0.82)	0.47 (0.05-6.75)	0.06 (0.02-1.43)
Vesuvio et Vulcano***		3.6 (1.8-6.9)	No data	0.03 (bdl-1.20)	1.14 (bdl-23.72)	0.38 (bdl-11.09)	0.23 (0.00-1.60)	0.01 (bdl-0.83)	0.07 (0.00-0.70)	0.10 (0.00-0.98)

*Calabrese et al, 2011

**Liotta et al, 2006

*** Madonia and Liotta, 2010

bdl: below detection limit

References:

- Arellano, S.R., Yalire, M., Galle, B., Bobrowski, N., Dingwell, A., Johansson, M., Norman, P., 2016. Long-term Monitoring of SO₂ Quiescent Degassing from Nyiragongo's Lava Lake. <http://dx.doi.org/10.1016/j.jafrearsci.2016.07.002>
- Balagizi, M.C., Kies, A., Kasereka, M.M., Tedesco, D., Yalire, M.M., Mc Causland, W., 2018a. Natural Hazards in Goma and Surrounding Villages, East African Rift System. Nat. Hazards DOI 10.1007/s11069-018-3288-X
- Balagizi M.C., Kasereka M.M., Cuoco E., Liotta M., 2018b. Influence of moisture source dynamics and weather patterns on stable isotopes ratios of precipitation in Central-Eastern Africa. *Sci Total Environ* 628–629:1058–1078. <https://doi.org/10.1016/j.scitotenv.2018.01.284>
- Balagizi, M.C., Kasereka, M.M., Cuoco, E., Liotta, M., 2017, Rain-plume interactions at Nyiragongo and Nyamulagira volcanoes and associated rainwater hazards, Est Africa. *Applied Geochem* 81, 76-89
- Balagizi, M.C., Yalire, M.M., Ciraba, M.H., Vicky, B.K., Minani, S.A., Kinja, K.A., Kasereka, M.M., 2016. CO₂ and SO₂ emissions, temperature variations and field observations before and after the February 29, 2016 new vent inside Nyiragongo crater. *Bull.Volcanol.* 78:64. <https://doi.org/10.1007/s00445-016-1055-y>
- Calabrese, S., Aiuppa, A., Allard, P., Bagnato, E., Bellomo, S., Brusca, L., D'Alessandro, W., Parello, F., 2011. Atmospheric sources and sinks of volcanogenic elements in a basaltic volcano (Etna, Italy). *Geochim. Cosmochim. Acta* 75 (23), 7401e7425. <http://dx.doi.org/10.1016/j.gca.2011.09.040>, 7401-7425
- Cuoco, E., Tedesco, D., Poreda, R. J., Williams, J. C., De Francesco S., Balagizi, C., Darrah, T. H. 2012a. Impact of volcanic plume emissions on rain water chemistry during the January 2010 Nyamuragira eruptive event: Implications for essential potable water resources. *J. Hazard. Mater.* 244, 570–581.
- Cuoco, E., Spagnuolo, A., Balagizi, C., De Francesco, S., Tassi F., Vaselli, O. Tedesco, D., 2012b. Impact of volcanic emissions on rainwater chemistry: The case of Mt. Nyiragongo in the Virunga volcanic region (DRC). *J. Geochem. Explor.* 125, 69–79.
- Madonia, P., Liotta, M., 2010. Chemical composition of precipitation at Mt. Vesuvius and Vulcano Island, Italy: volcanological and environmental implications. *Environmental Earth Sciences* 61, 159–171.
- Liotta, M., Brusca, L., Grassa, F., Inguaggiato, S., Longo, M., Madonna, P., 2006. Geochemistry of rainfall at Stromboli volcano (Aeolian Islands): isotopic composition and plume–rain interaction. *Geochemistry, Geophysics, Geosystems* 7 (N°7) (12 pp.).

5.2. Satellite Data

5.2.1. InSAR analysis of surface deformations between January 2020 and December 2021

a. Syn-eruptive phase

After the occurrence of the eruption at Nyiragongo volcano (Democratic Republic of the Congo, Central Africa) on May 22, 2021, some researchers at INGV were involved to support the GVO community for the emergency phase. At this aim, different methodologies were exploited and among them the two-pass Differential Interferometry SAR (InSAR) technique. Such method allows imaging the occurred ground displacement field due to an event such as earthquakes, eruptions, landslides, etc. by means of remote sensed data. To achieve such results the phase difference between one pre-event and one post-event image is performed using a Digital elevation model to remove the topographic contribution. The Copernicus GLO-30 Public DEM is a global Digital Surface Model (DSM) derived from the WorldDEM. The WorldDEM is based on radar satellite data acquired by the TanDEM-X mission, which was funded by the German Aerospace Center (DLR) and Airbus Defense and Space.

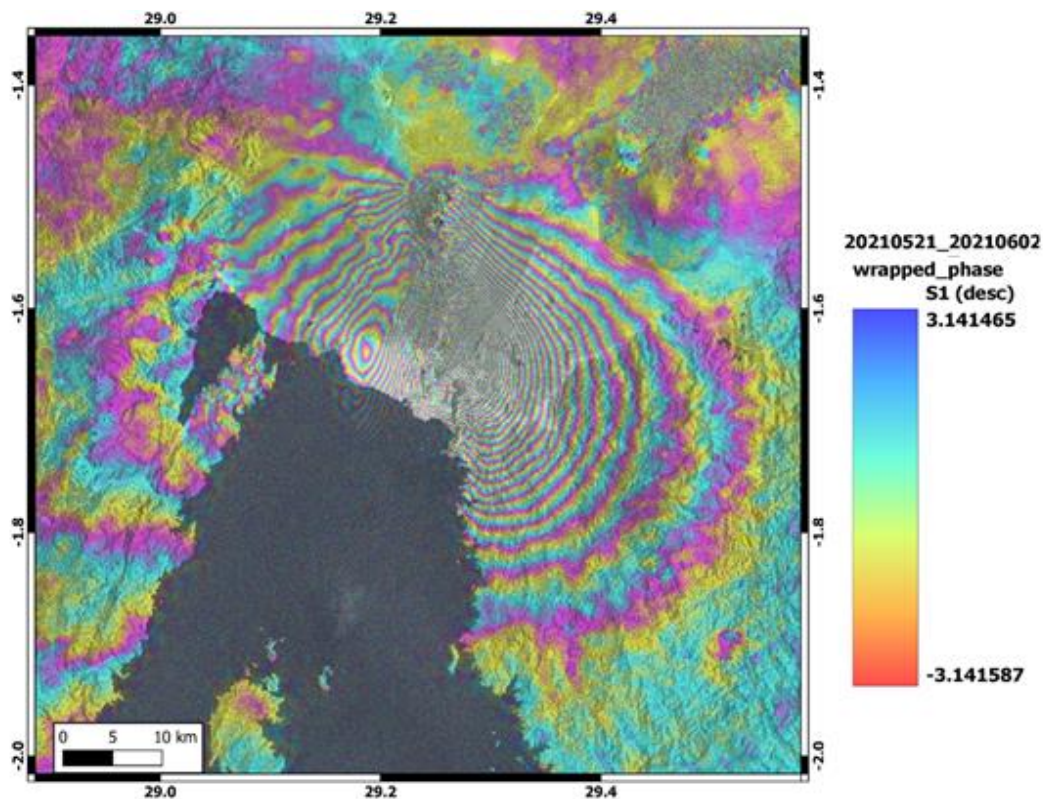


Figure 27. Descending S1 syn-eruptive wrapped phase, covering 21 May 2021 - 2 June 2021.

We applied such a technique using the GAMMA software by means of the Alaskan Facilities Vertex site. We consider two Sentinel-1 (S1, from the European Space Agency, ESA) syn-eruptive pairs along the descending (Fig. 27 and 28, wrapped and unwrapped phase, respectively) and ascending (Fig. 29 and 30, wrapped and unwrapped phase, respectively) orbits. The two displacement maps in Fig. 28 and 30 show a maximum of 0.6-0.7 m Line of Sight (LOS). The opposite colors but similar patterns means that the ground movement is mainly horizontal for geometrical reasons.

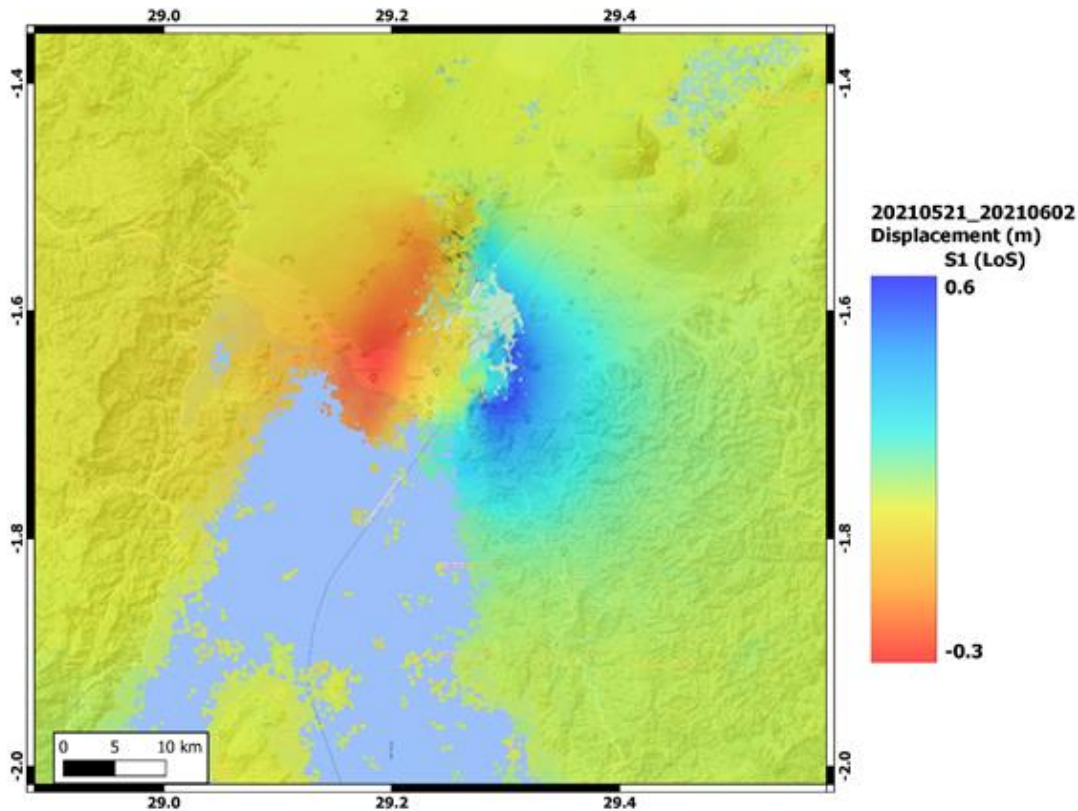


Figure 28. Descending S1 syn-eruptive cumulative displacement (21-05-2021/02-06-2021). Blue color means movement towards the satellite, red away from the satellite, along the LOS direction.

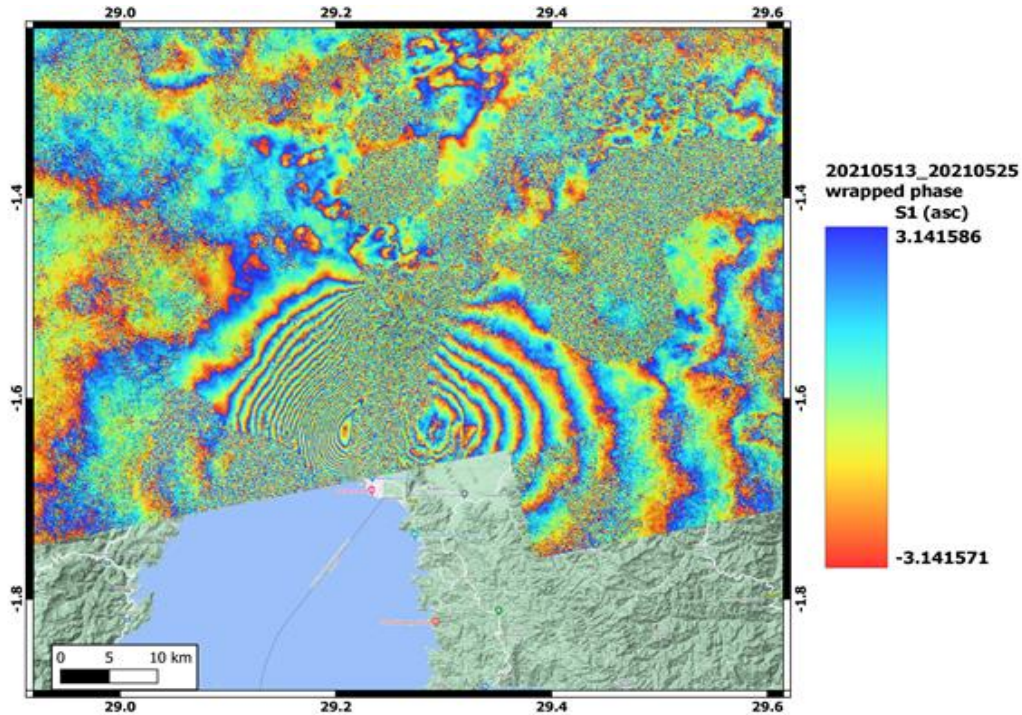


Figure 29. S1 ascending syn-eruptive wrapped interferogram (13-05-2021/25-05-2021).

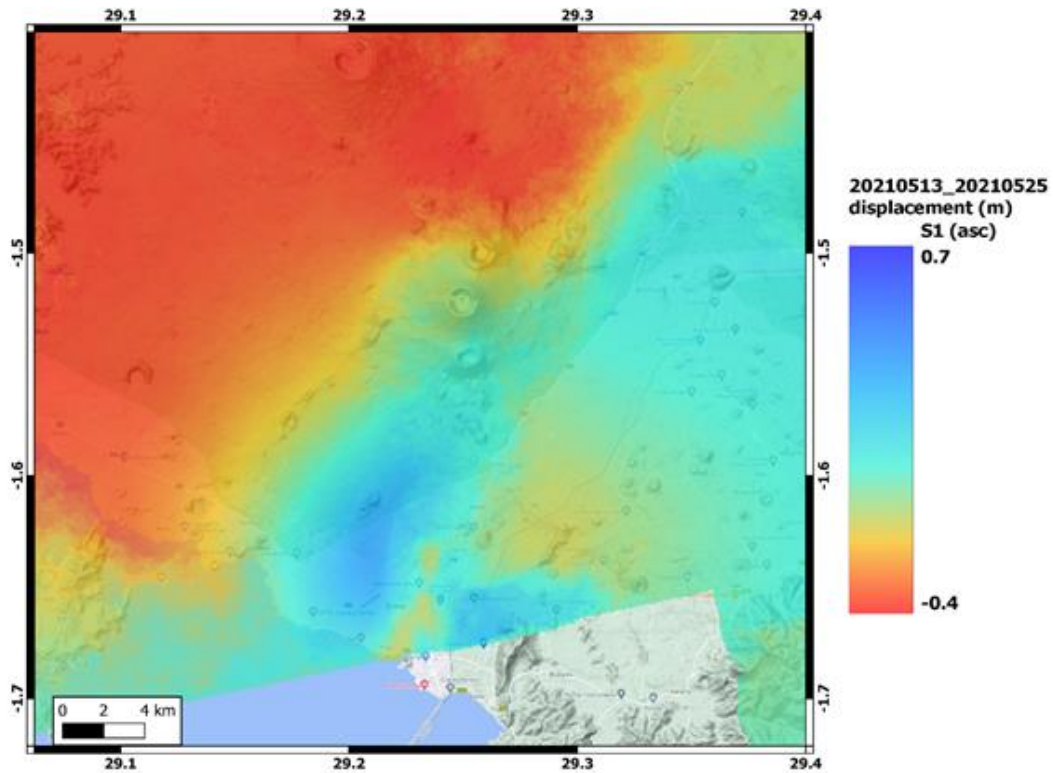


Figure 30. S1 ascending syn-eruptive cumulative displacement map (13-05-2021/25-05-2021). Blue color means movement towards the satellite, red away from the satellite, along the LOS direction.

b. Multi-temporal and multi-sensor analysis for pre- syn- and post- eruptive phases

One of the most important goals in an emergency phase is the possibility to have a continuous monitoring of the surface movement. To achieve such an issue, in the last two decades multi-temporal InSAR methods were developed providing the capability to monitor the possible ground motion in time considering huge SAR images datasets. One of the most popular and nowadays consolidated approaches consists of the Small Baseline Subset (SBAS). In SBAS, all the high-quality interferometric pairs with short spatio-temporal baselines are used, ensuring high temporal sampling rate and high point density. Benefiting from the short spatio-temporal baselines, the influence of temporal decorrelation, spatial decorrelation and DEM error on deformation estimation are all reduced. The outcomes are the mean ground velocity map in the line of sight of the sensor and the relative displacement time series.

We adopt the SBAS algorithm to study the deformation in the post event period analyzing 29 acquisitions along the S1 descending orbit (track 21) in the temporal span 10-11-2020 23-12-2021 (Fig. 31). The 1 arc-second SRTM digital elevation model (30 m) was used to remove the topographic contribution. The final products are geocoded in the WGS84 reference system with a ground pixel resolution equal to 90 m. The temporal interval of the analysis encompasses the syn-eruptive phase. Most of the detected high ground velocity is located in the city of Goma and affects the summit crater of Nyiragongo.

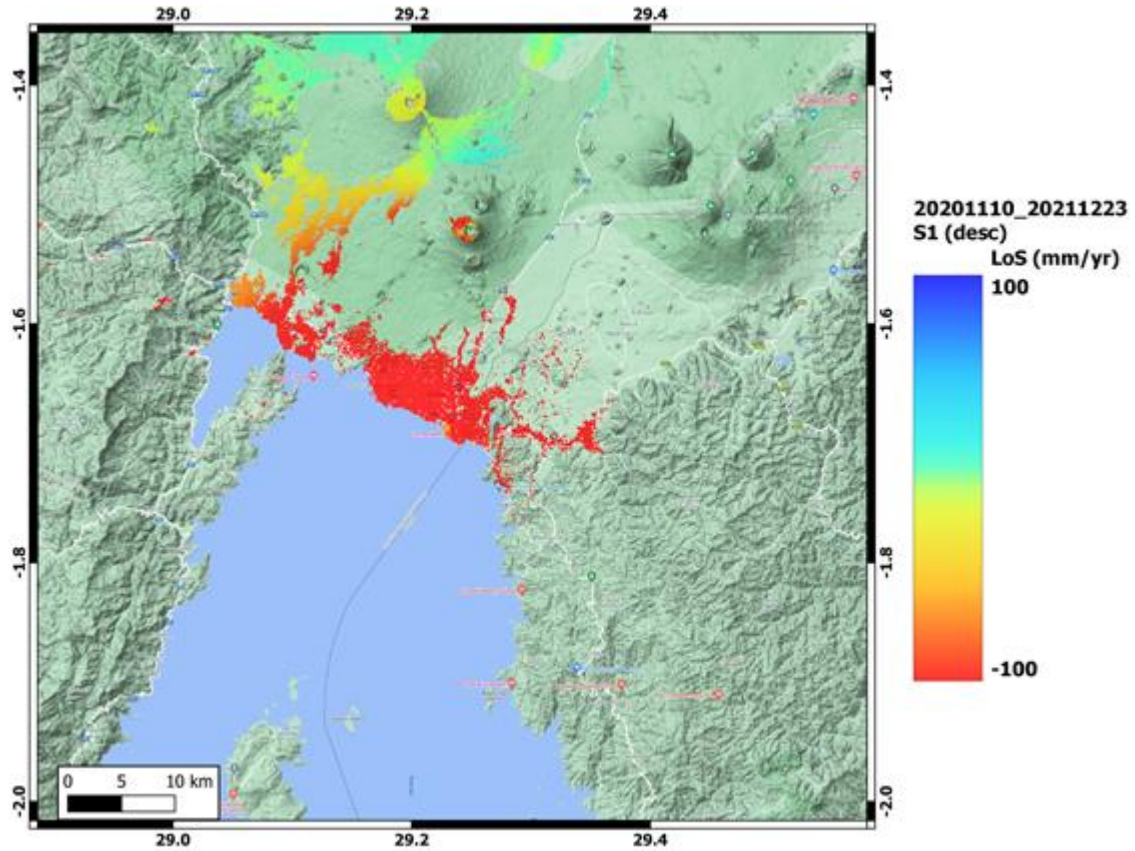


Figure 31. Descending S1 pre- syn- and post- eruptive mean ground velocity map (10-11-2020/23-12-2021). Blue color means movement towards the satellite, red away from the satellite, along the LOS direction.

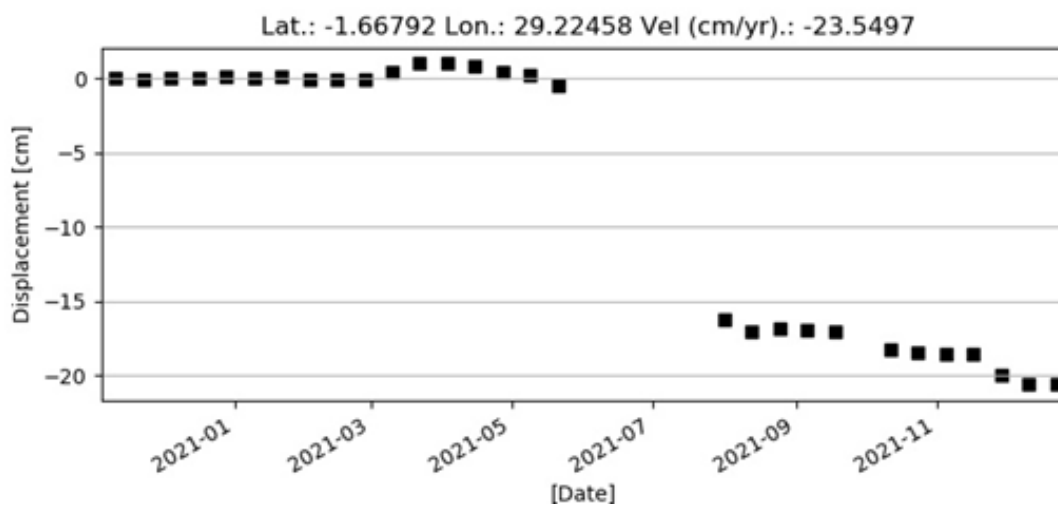


Figure 32. Descending S1 pre- syn- and post- eruptive displacement time series example in Goma city. The syn-eruptive jump in May is evident.

Fig. 32 shows the time series of a pixel located in Goma city. There is no appreciable surface displacement registered before the eruption. The syn-eruptive jump of about -15 cm is evident. Afterwards, the ground continues with a negative movement LOS of about 1 cm/month.

Using the S1 data, we also focalized the time-series analysis on the post-eruptive phase considering a more dense temporal sampling. This study is also aimed at assessing the state of activity of Nyiragongo after the increase of geophysical signals in December 2021. The technique is similar to the analysis presented above. The cumulative displacement field (Fig. 33) from the first post-eruptive date (01-08-2021) until the last processed image (23-12-2021) to better analyze the post-eruptive deformation pattern.

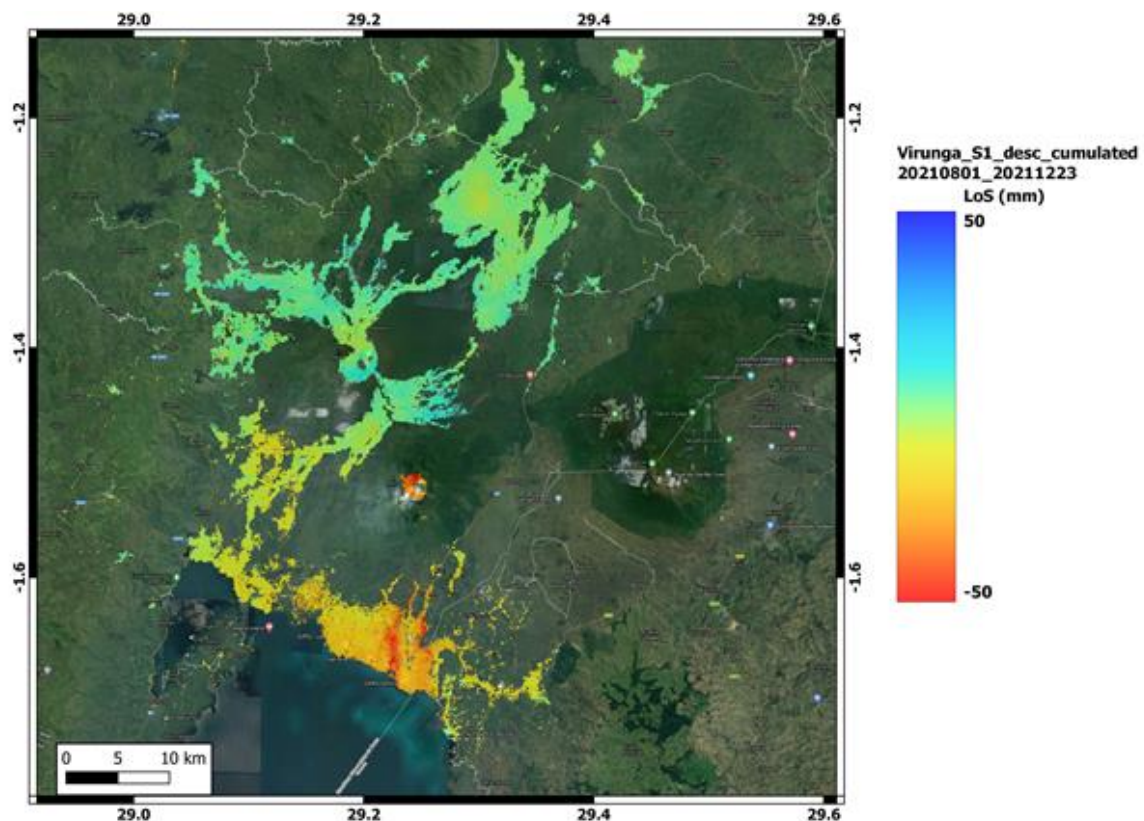


Figure 33. Descending S1 post-eruptive cumulated displacement map. (10-11-2020/23-12-2021). Blue color means movement towards the satellite, red away from the satellite, along the LOS direction.

The results in Fig. 33 show a cumulated displacement of -3 to -5 cm LOS in the eastern side of Goma, reaching lake Kivu, and in the summit crater of Nyiragongo.

We also exploited the possibility of elaborating high resolution COSMO-SkyMed data, provided by the Italian Space Agency (ASI), to study the pre- and post-eruption surface deformation

pattern. In particular we used 24 images to obtain the ground deformation field during the time interval 10-11-2020 / 21-05-2021, until one day before the eruption, and 28 images to analyse the displacements after the eruption, during the 30-05-2021 / 08-12-2021 time span.

Fig. 34 shows the cumulative displacement field from the two COSMO-SkyMed processing: pre-eruption on the left and post-eruption on the right.

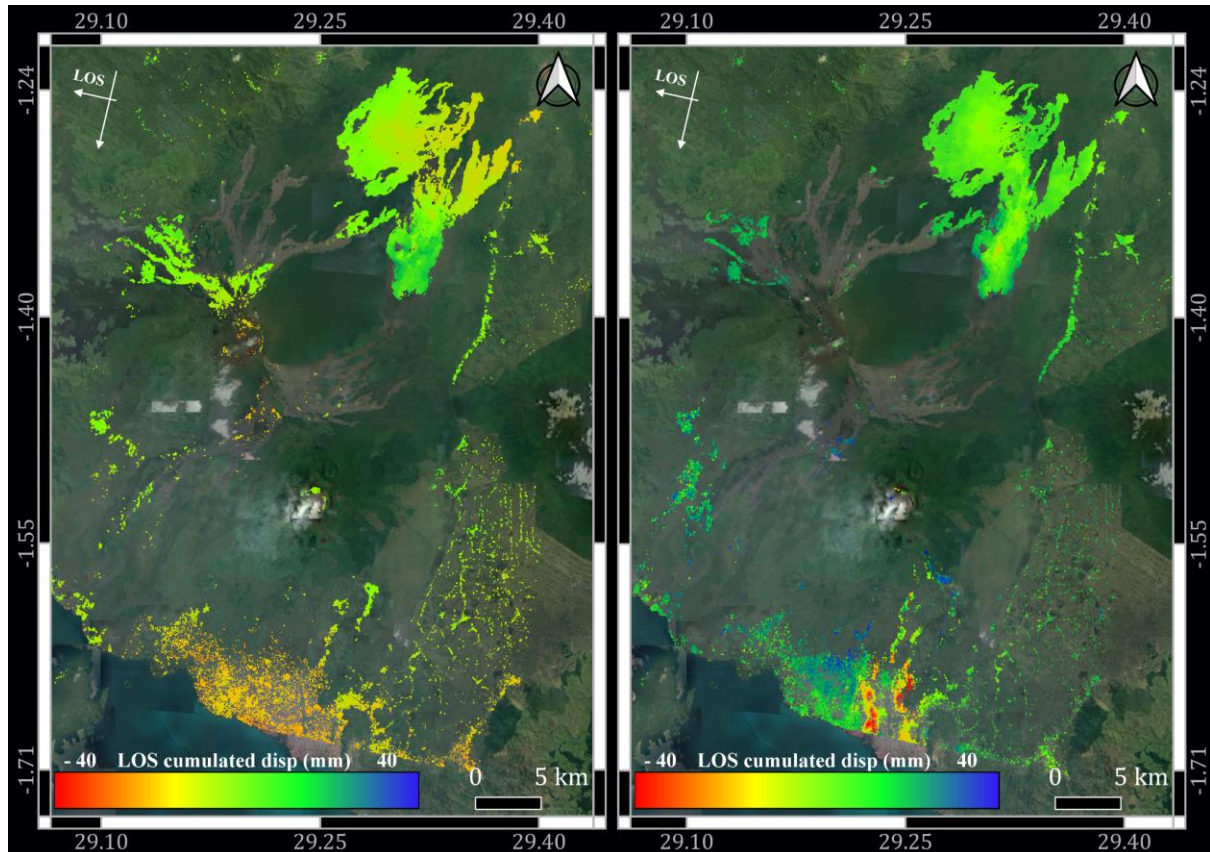


Figure 34. Descending COSMO-SkyMed pre-eruptive (left) and post-eruptive (right) cumulated displacement maps. Blue color means movement towards the satellite, red away from the satellite, along the LOS direction.

The results for the post-eruption phase (Fig. 34 right) show negative LOS cumulative displacements. This result is in accordance with those obtained with descending S1 data (Fig. 33), in the easternmost part of the city of Goma, the LOS displacement values reach -4 cm (see the COSMO-SkyMed displacement time series in Fig. 35).

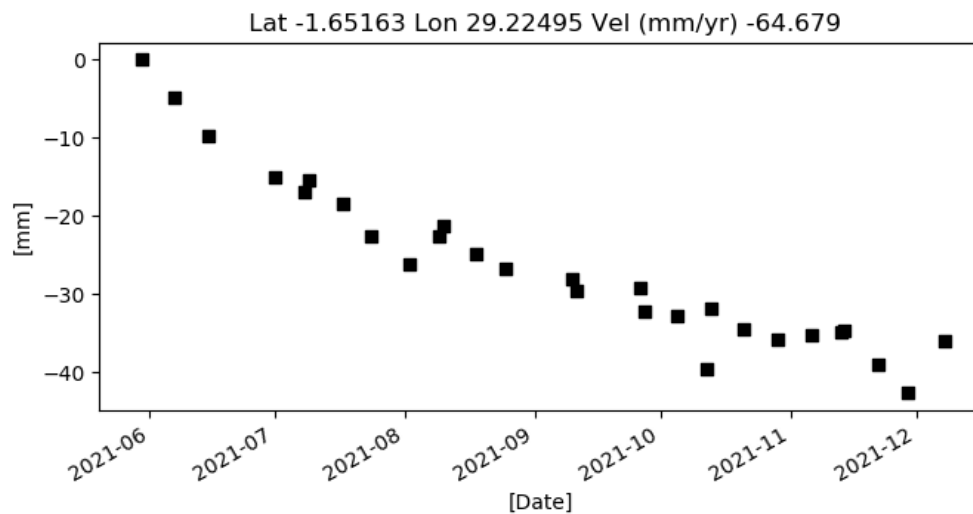


Figure 35. Descending COSMO-SkyMed post-eruptive displacement time-series in the eastern part of Goma city.

5.2.2. Modelling of the Nyiragongo eruption from InSAR data

Modelling of the surface deformation is performed using the VSM (Volcanic and Seismic source Modelling) tool, a python code whose former Fortran version is available here (Trasatti, 2019, http://www.rohub.org/rodetails/volcano_source_modelling_vsm-release/overview. doi:10.24424/ro-id.HRFPNERWFQ).

A dyke model is adopted, combining the syn-eruptive ascending & descending orbits data in section 1 (Fig. 28 and 30). The InSAR results are subsampled with ground step from 300 m to 700 m towards the far field.

The dyke parameters are reported in Table 3. The fit with data is reported in Fig. 36 (ascending orbit) and Fig. 37 (descending orbit). The volume variation associated with the dyke is slightly less than 0.2 km³. The dyke is 18-km-long and 5 km wide. Its top is at 1350 m below the surface, i.e. about at sea level considering the main quote of the lake being 1450 m.

According to the large extension of the syn-eruptive surface deformations, from the volcano through the city of Goma, reaching the lake, the modelling constrains a dyke that extends from the southern flank of the volcano towards south reaching the eastern part of the city close to the airport, and the lake.

Table 3. Mean model from the Bayesian Inference of the ascending and descending syn-eruptive data. TLC is the Top Left Corner of the dyke. Coordinates are in UTM WGS84 zone 35 South.

TLC East (m)	TLC North (m)	TLC depth (m)	Length (m)	Width (m)	Strike (°)	Dip (°)	Opening (m)
751400	9826800	1400	18000	5000	192	82	2.0

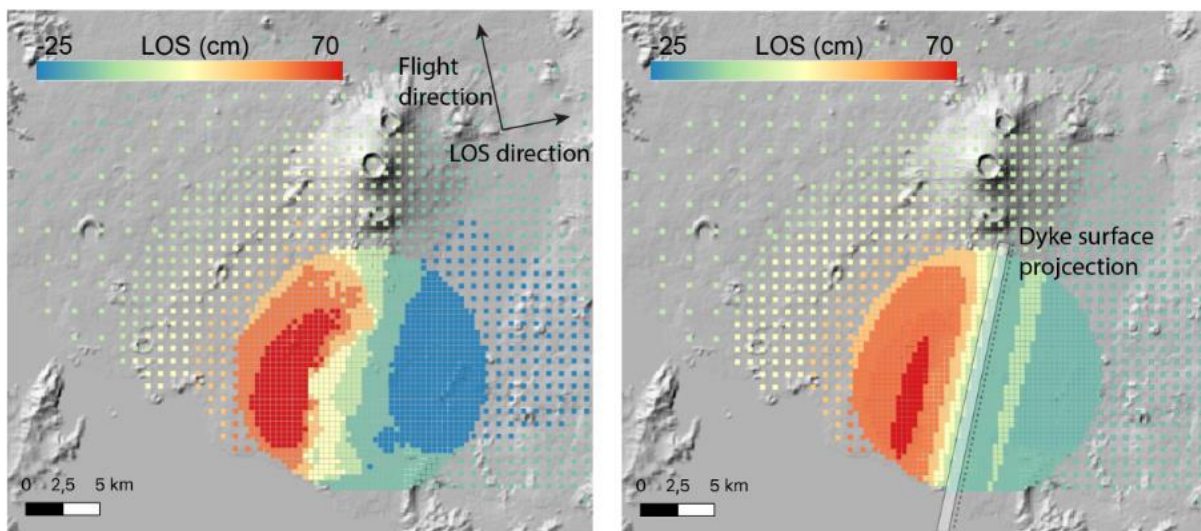


Figure 36. Results of the dyke modelling. Left – subsampled S1 InSAR data in ascending orbit. Right – modelled data. The surface projection of the dyke constrained by the inversion is reported on the right panel.

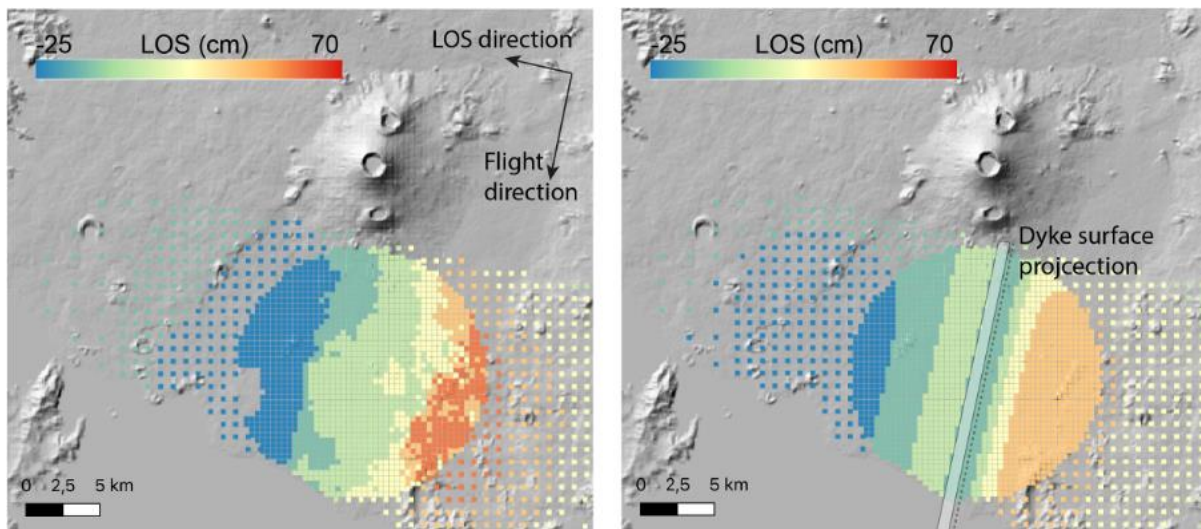


Figure 37. Results of the dyke modelling. Left – subsampled S1 InSAR data in descending orbit. Right – modelled data. The surface projection of the dyke constrained by the inversion is reported on the right panel.

A scheme of the Nyiragongo area with the feeding dyke is reported in Fig. 38.

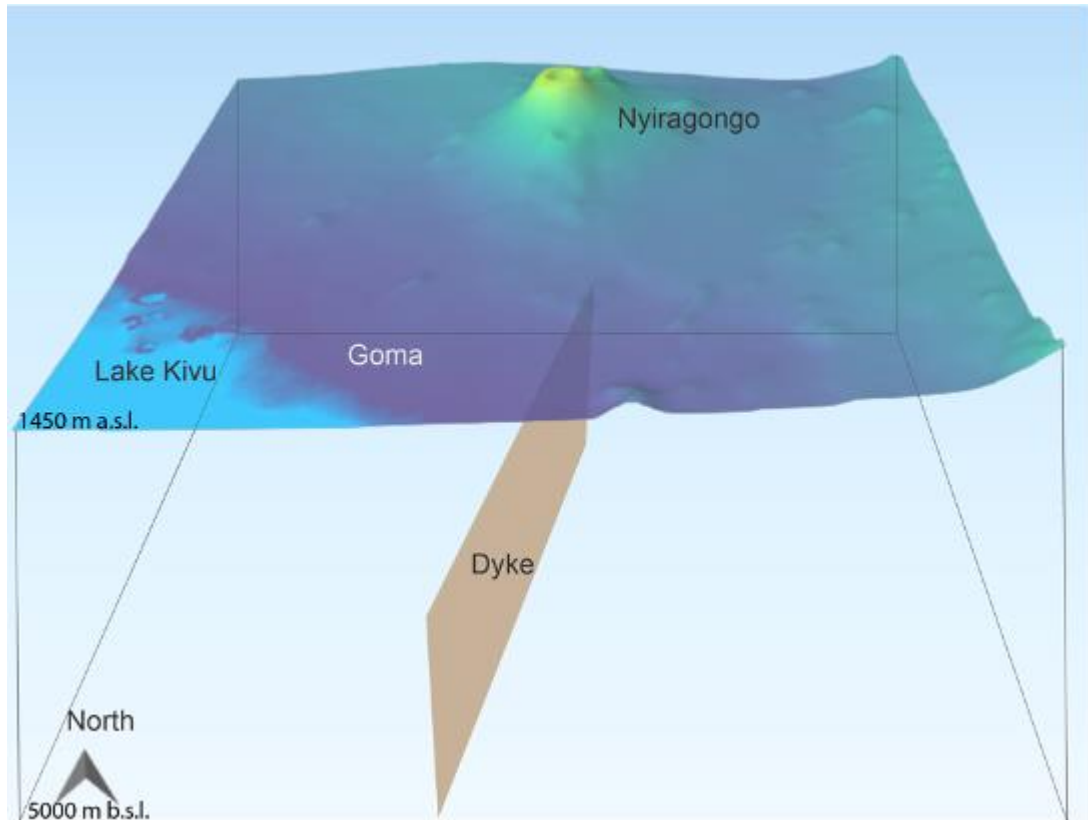


Figure 38. Scheme of the Nyiragongo area with the feeding dyke. The dyke feeding the eruption has been constrained by InSAR data inversion. The dyke extends for 18 km in length and 5 km in depth, reaching 1.3 km below the surface (i.e., it reached about the sea level). Vertical scale 2x.

The information related to the intruding dyke is the result of an inversion process of real data. The results described above are a model and may not necessarily represent the real situation that occurred at Nyiragongo.

5.2.3. Additional analysis of SAR images during the May 2021 Nyiragongo eruption

a. Data and methods

SAR images from COSMO SkyMed (CSK) constellation, provided by the Italian Space Agency (ASI) through the Virunga Supersite initiative, and Sentinel-1 A and B (S1) provided by the European Space Agency (ESA), were used to study the geomorphological changes and ground deformation associated with the May 2021 Nyiragongo eruption and the following dike intrusion. The images were acquired in ascending and descending orbit for both constellations. CSK data in the Virunga volcanic area are acquired in tandem-like configuration, i.e., each 4, 4, 1, and 7 days per orbit, while S1 data are acquired every 6 days per orbit. This comprehensive dataset allowed to follow the volcanic unrest in quasi-real-time (Table 4). Here, amplitude high-resolution images from CSK, wrapped interferograms for both the constellations and S1 deformation maps will be shown. SAR Images were processed using GAMMA software (Wegmüller, 1998). For each orbit, the images were coregistered to the same selected primary image highlighted in Tab. 1. This allows to easier compare the images and to reduce the processing time avoiding to coregister all the single pairs. The SRTM 1 arcsec digital elevation model has been used as a reference for the coregistration of the images, to remove the topographic phase component from the interferograms, and finally to geocode the images processed in radar geometry. CSK amplitude images were multilooked to obtain $\sim 5 \times 5$ m² pixel to reduce the speckle noise while, both CSK and S1 interferograms, were multilooked to obtain $\sim 30 \times 30$ m² pixel size to reduce the phase noise increasing the coherence. Furthermore, interferograms were filtered using the bandpass filter (Goldstin and Wagner 1986). Finally, the minimum cost flow (mcf) algorithm was used to unwrap the interferograms.

Table 4. SAR images used in this report. The * mark the primary images chosen as references for the coregistration process.

CSK		S1	
Asc	Des	Asc	Des
20210516*	20210521*	20210513*	20210509*
20210523	20210522	20210519	20210521
20210601	20210530	20210525	20210527
20210929	20210910	20210531	20210602
20211226	20211231	20210606	20210608

b. Results

b.1. Amplitude images

Unlike optical imagery, the radar signal can pass through the cloud coverage, which is particularly useful in the tropical environment where the Nyiragongo volcano is located. The spatial resolution of CSK's images is high ($\sim 2 \times 2 \text{ m}^2$). Here multilooked amplitude images, with a spatial resolution of $5 \times 5 \text{ m}^2$ (e.g., Fig. 39), have been used to identify some geomorphological features like the lava front (Fig. 40), the emplacement of the eruptive vents, and the development of the fractures (Fig. 41). Furthermore, these images allowed retrieving the collapse that occurred within the Nyiragongo crater and the consequent (temporarily) disappearance of the lava lake (Fig. 42).

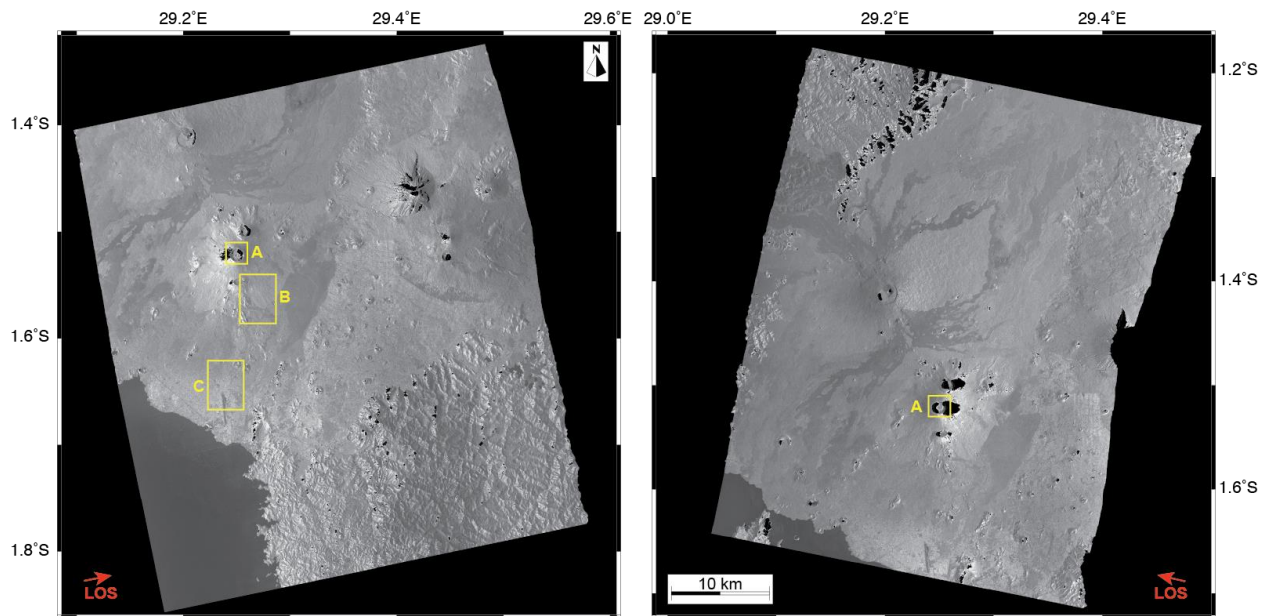


Figure 39. CSK amplitude images acquired in ascending (left) and descending (right) orbit before the eruption onset (May 16 and 22 respectively). The next three figures are the zoom in the areas within the yellow boxes (A = Fig. 4, B = Fig. 3 and C = Fig. 2 respectively).

In Fig. 40 one can see the lava front entering the city of Goma, the image in the middle have been acquired on May 23 at 4:03 (UTC), a few hours before the end of the eruption. The lava covered about 10 km, reaching almost its maximum length, destroying some buildings, and approaching the airport. As shown in the following acquisition, after 8 days, the lava flow mainly widened during the last few hours of the eruption. In Fig. 41 you can see three of the eruptive vents that opened at the beginning of the eruptions, two fractures that opened in a slightly NS direction, the longer on the west (composed of different segments) is $\sim 2 \text{ km}$ long while the one on the east is $\sim 1.5 \text{ km}$ long. They both originated near the new eruptive vents.

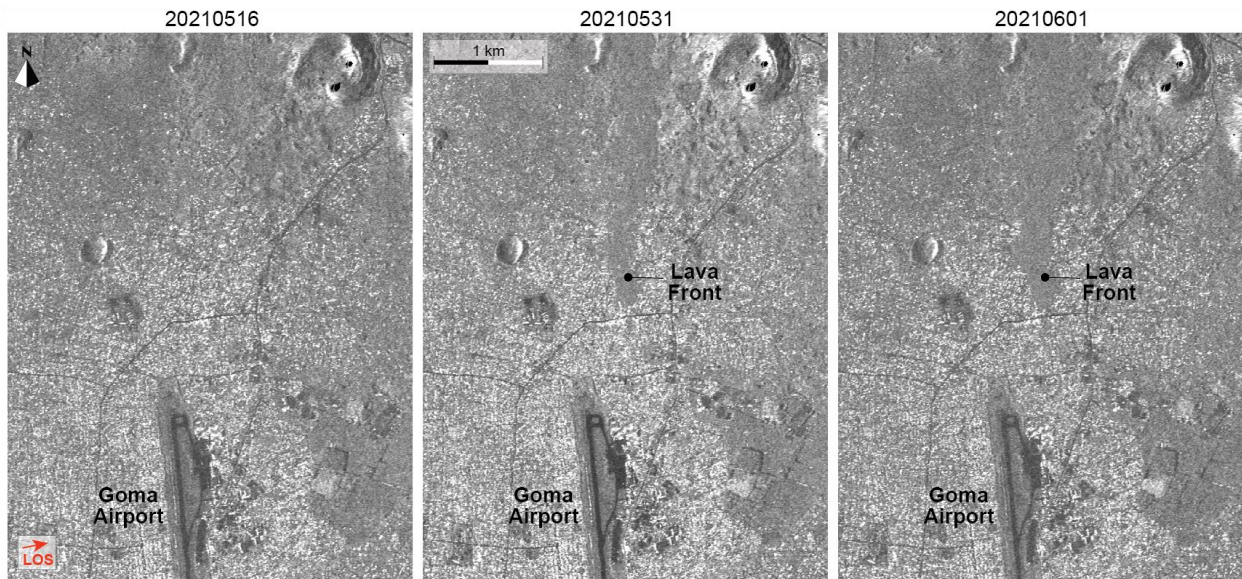


Figure 40. Zoom in the CSK amplitude images (area C in Fig. 39) in ascending orbit that show the evolution of the lava front.

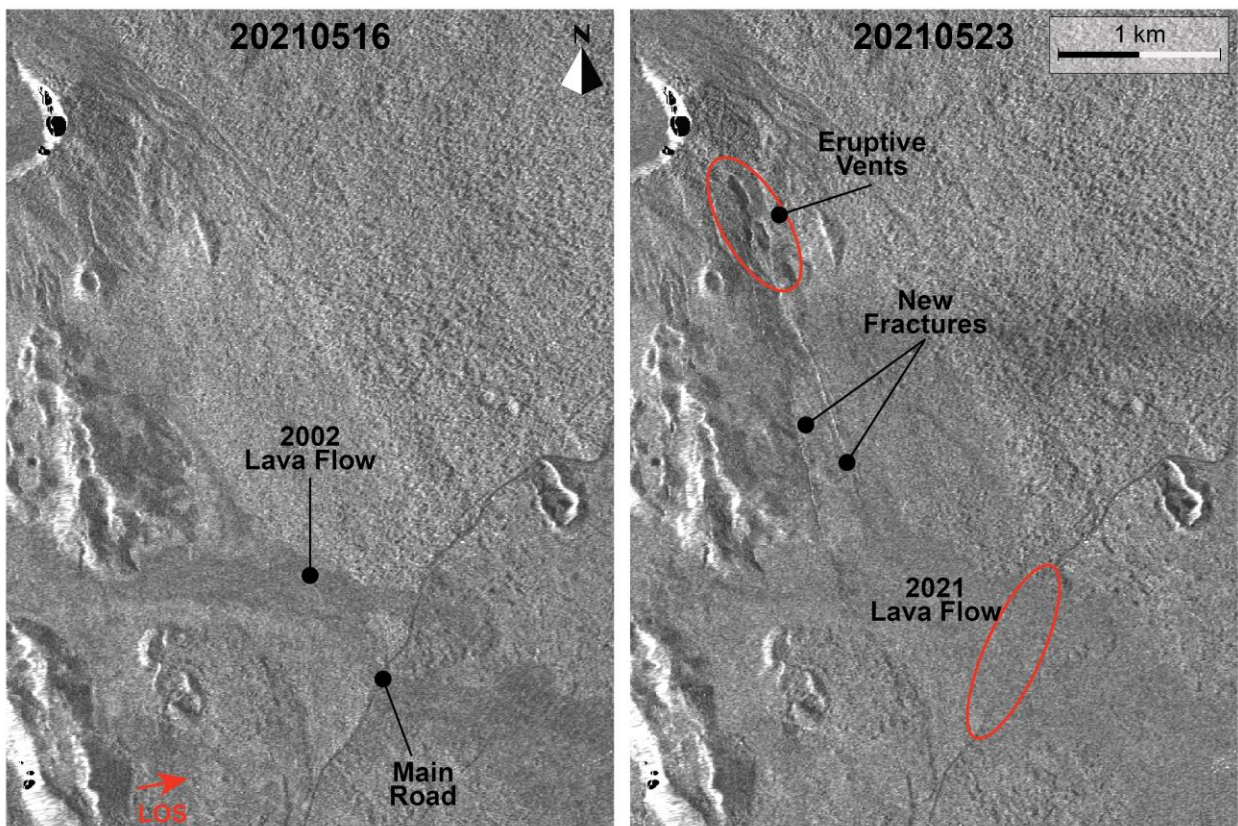


Figure 41. Zoom in the CSK amplitude images (area B in Fig. 39) in ascending orbit that show the onset of a few of the eruptive vents, some fractures and the lava flow that cross the main road.

Also, in the same Fig. 40, it is possible to observe the lava flow that crosses the main road that goes from Goma toward the north, following the border with Rwanda. Finally, in Fig. 42, the shadow cast by the crater rim illuminated by the radar signal provides information about the depth of the crater. Some areas are masked by the software because affected by artifacts due to the steep topography (layover and shadowing – e.g., Hanssen 2000), evaluated using the reference DEM. Before the eruption, the lava lake was visible in the middle of the crater.

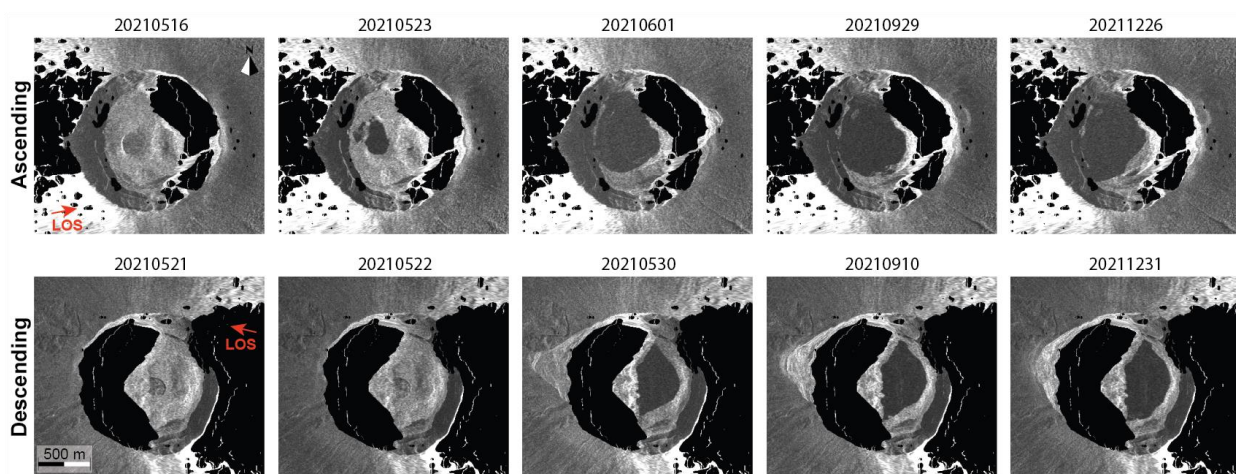


Figure 42. Zoom in the CSK amplitude images (area A in Fig. 39) in ascending (first line) and descending (bottom line) orbits that shows the temporal evolution of the collapses within the Nyiragongo crater. The acquisition dates have been reported

During the eruption, as highlighted on the image acquired on May 23, part of the lava lake rim collapsed. Unfortunately, it is not possible to know exactly when the bottom of the crater collapsed. On the descending orbit, it is also visible that the western part of the crater rim collapsed. Finally, the changes in the shape of the shadow within the crater's bottom, suggest that other collapses occurred even after a few months from the eruption. The first collapse that occurred during the eruptive period, were probably related to the pressure drop within the conduit that fed the lava lake and this probably triggered the entire collapse of the crater's bottom. The rim's collapse is a gravitational process possibly triggered by the seismic activity during the unrest period.

b.2. Wrapped interferograms

Wrapped interferograms provide useful information about the ground deformation pattern and a rough estimation of the displacement amplitude before applying the unwrapping algorithm. Here some interferograms from S1 and CSK for the pre-, co-, and post-eruptive periods will be shown. The co- and a few of the post-eruptive interferograms show that the eruption was accompanied by a dike intrusion. The magma, moved rapidly from the shallow magma reservoir reaching the surface on the southern flank of the Nyiragongo, where several eruptive vents opened. Then, it moved southward below the surface toward Kivu Lake. Thanks to a large amount of SAR acquisitions, it was possible to observe that, while the eruption lasted less than 24 hours, the magma moved southward for a few days (more than 4 and less than 7).

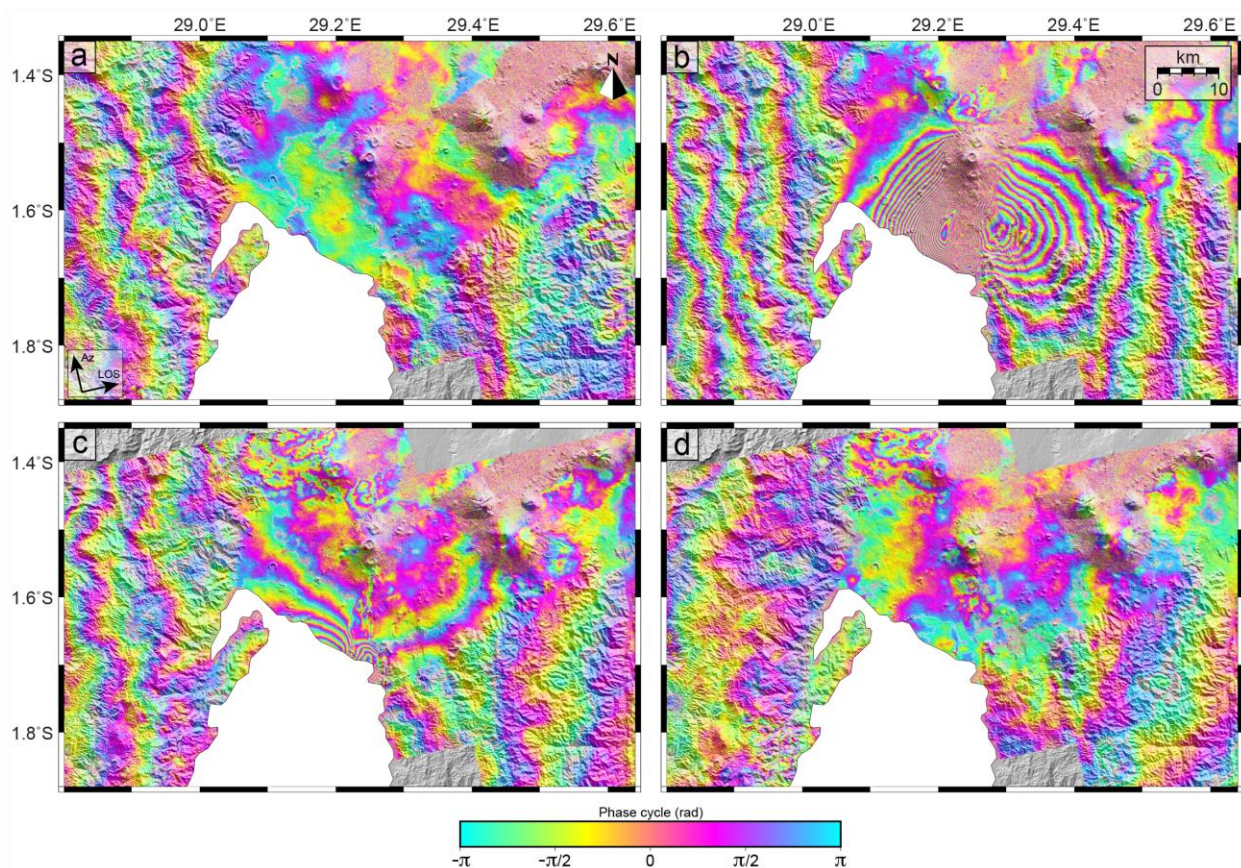


Figure 43. S1 ascending interferograms for the pre-, co- and post eruptive period

Furthermore, the pre-eruptive interferograms don't show clear deformation signals that could be interpreted as an eruptive precursor (such as an inflation of the magma chamber), suggesting that the magma rise was extremely rapid. In Fig. 43 one can see the S1 ascending

interferograms. In a) the pre-eruptive pair (May 13 - 19) shows an orbital ramp but no deformation signal in the area. b) is the co-eruptive pair (May 19-25). Here, there is an evident deformation pattern that consists of three lobes, contoured by concentric fringes. The first on the west is moving toward the satellite (range decrease), instead, the second in the center and the third on the east are moving away from the satellite (range increase). For S1, each phase cycle (fringe), corresponds to a displacement change of ~ 2.8 cm (half of the wavelength of the electromagnetic signal emitted by the satellite). Counting the fringes, it is possible to roughly estimate the total displacement along the line of sight (LOS) of the satellite. On the western lobe, 26 fringes correspond to a maximum displacement of ~ 73 cm between the center of the lobe and the external part. On the eastern lobe, 11 fringes correspond to ~ 31 cm of relative displacement. For the central lobe, it is not possible to count the real number of the fringes; one can see only a few of them because the ground deformation is large and concentrated in a small area causing the signal decorrelation. However, it is visible between the two other lobes and is going from the northern flank of the Nyiragongo and reaching the northern shore of the Kivu Lake. This peculiar deformation pattern is consistent with a NS elongated dike (e.g., Nobile et al., 2012). Indeed, the dike produces extension on his top that results in subsidence at the surface (the lobe in range increase in the middle) and compression of this side that produce a composition of uplift (range increase) and horizontal displacement (that, depending on the looking geometry, could be range increase or range decrease). Since this dike is slightly NS elongated, the western lobe will move toward the west (range decrease for the ascending looking geometry) while the eastern lobe will move toward the east (range increase for the ascending looking geometry). The combination of the vertical and horizontal displacements explains why the amplitude of the displacement on the west is larger (both in range decrease) than the one on the east (they have opposite signs). c) is the post-eruptive pair (May 25-31) and shows that the deformation signal moved south toward the lake. At least part of the side lobes of the dike-induced deformation pattern is visible. Unfortunately, the lake prevents observing the entire deformation signal. However, this information is consistent with the observed seismicity that, after the eruption moved south with several events localized below the northern shore of the lake for several days. In the following interferogram (d - May 31 – June 6), the dike induced signal completely disappeared, only local signal can be identified and could be related to local ground deformation associated with the lava flow compaction (something similar can be observed also in the previous interferogram) or could be an atmospherical artifact (another interferogram could be useful to understand it).

In Fig. 44 on can see the S1 descending interferograms. In a) the pre-eruptive pair (May 9 - 21) no evident ground deformation can be observed. In b), the co-eruptive pair (May 21 - 27) the dike-induced deformation pattern can be observed. In this case, since the satellite is looking toward the west, the relative displacement of the western lobe (~ 31 cm) is smaller than the eastern one (>50 cm, due to the large deformation, not all the fringes are visible). c) span the period May 27 – June 2, the dyke moved toward the satellite, confirming that, after 4 days from

the eruption, the intrusion was still ongoing. Finally, d) is the interferogram between June 2 – 8 and the only observable signal is localized in the area that corresponds to the central lobe in b). This signal could be an artifact or since it is in range increase could be subsidence produced by the volume contraction of the dike or to the viscoelastic relaxation of the crust. Further analysis is needed to better understand this signal.

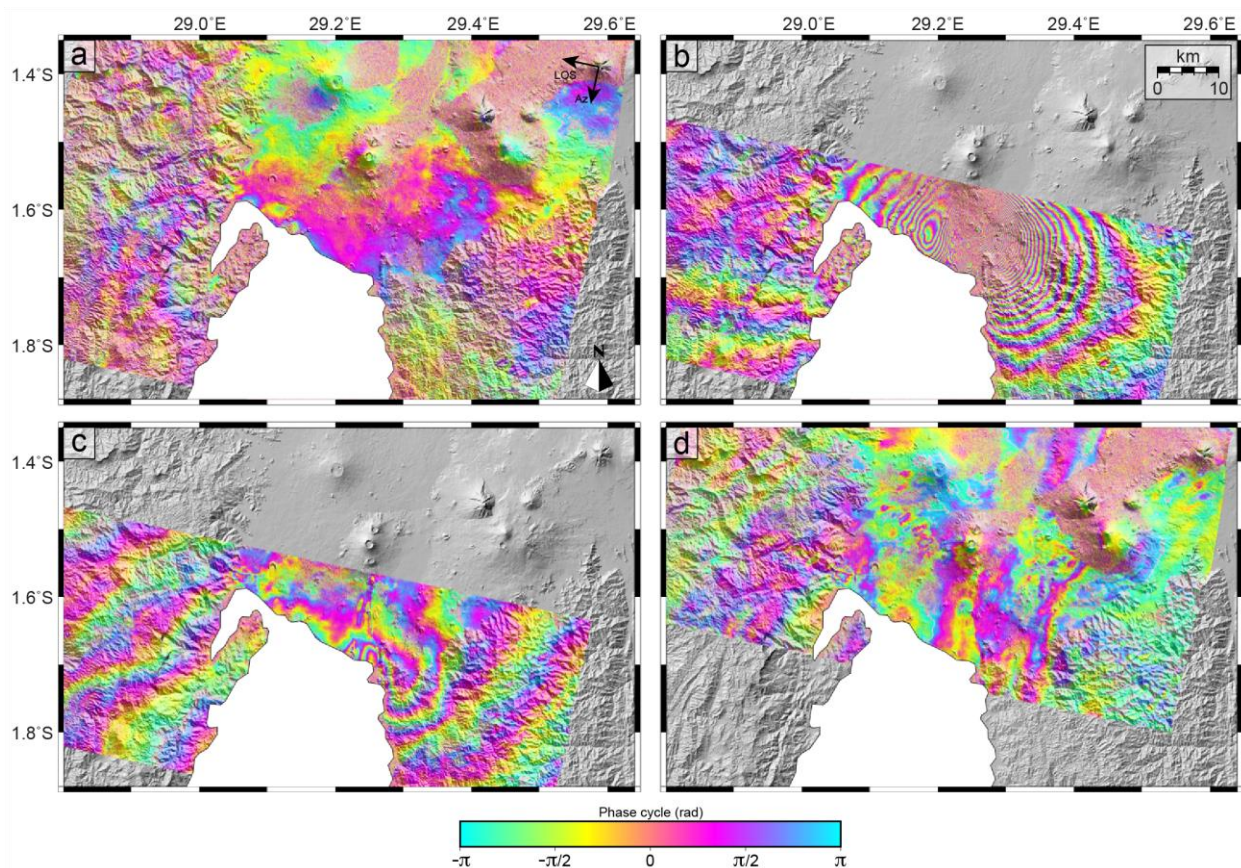


Figure 44. S1 descending interferograms for the pre- (a), co- (b) and post-eruptive (c and d) period

CSK in descending orbit, acquired an image on May 22 at 15:37 (UTC), only a few hours before the beginning of the eruption. The interferogram in Fig. 45 has been processed using this image as secondary and the one acquired on May 21 as primary. Zooming on the area where the eruptive vents opened, it is visible a signal in range increase (2 fringes - ~ 3 cm – CSK signal wavelength is 3.1 cm). This could be some subsidence associated with the beginning of the dike intrusion that produced some extension at depth or, more likely, an artifact due to tropospheric noise. Indeed, another signal in range increase with a similar amplitude is visible south, above Goma. All the interferograms with the image acquired on May 21 used as secondary don't show this signal while, all the interferograms processed with the image acquired on May 22 as primary will show the dike-induced deformation (e.g., Fig. 46c). This prevents the artifact from

being confirmed. Still, if this is a deformation signal, it would be started after May 21 (acquisition time 15:37 UTC) in an uninhabited area where no monitoring instruments are installed. Furthermore, the SAR images were provided a few days after the eruption so this data couldn't be used as an early warning system. Fig. 46 shows two ascending (a & b) and 2 descending (c & d) CSK interferograms.

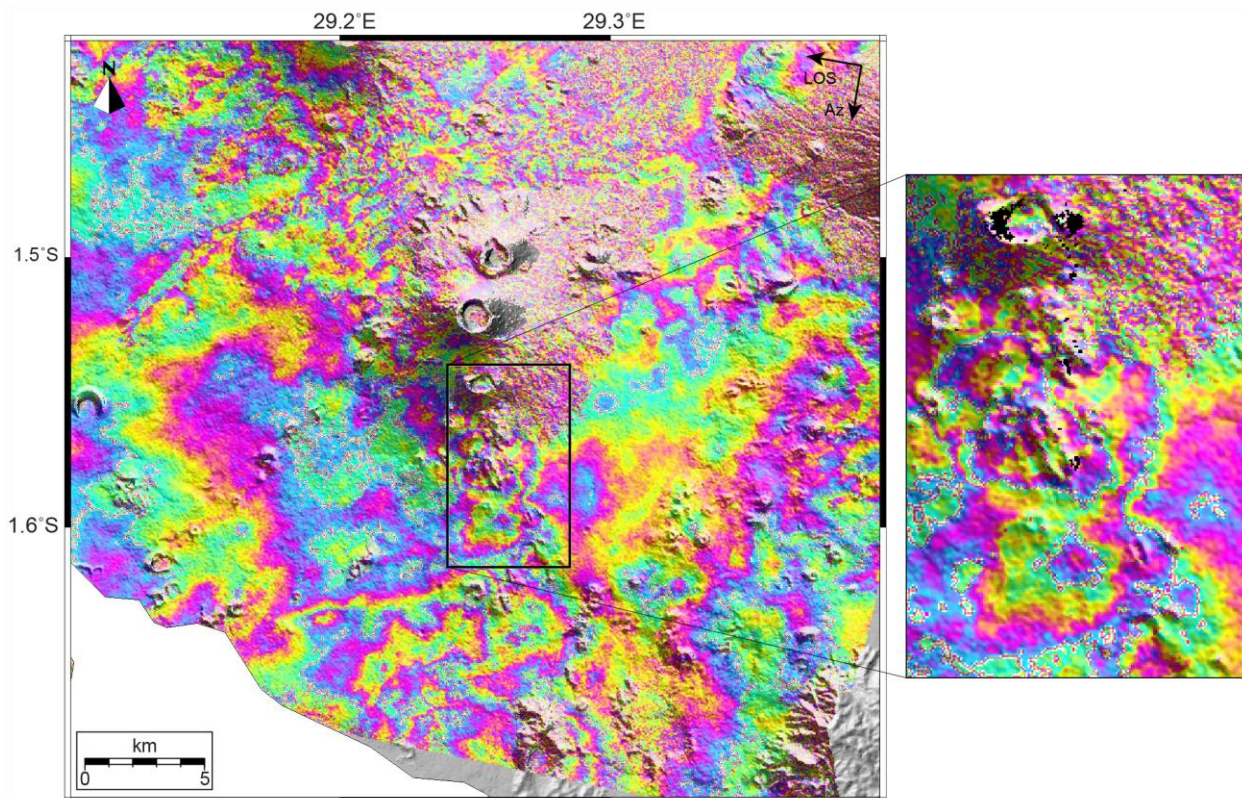


Figure 45. CSK interferogram 20210521-20210522. Zoom on the eruptive vents area

As written before, the CSK wavelength is shorter than the S1 one. This increases the coherence loss issue when measuring large displacements concentrated in small areas. However, in a, b, and c, the deformation pattern with 3 lobes is visible even if it is not possible to correctly count all the fringes. The interferogram in a) covers only the first part of the eruptive period (until 4:03 UTC of May 23). Compared with the following interferogram in b), it is clear that a large part of the dike-induced deformation occurred along with the eruption and that the dike started to move immediately southward. Finally, in the interferogram d that shows the post-diking deformation, there is some residual signal on the top of the area where the dike intruded suggesting that probably the dike started to cool by the beginning of June. Some other local signals could be associated with lava compaction.

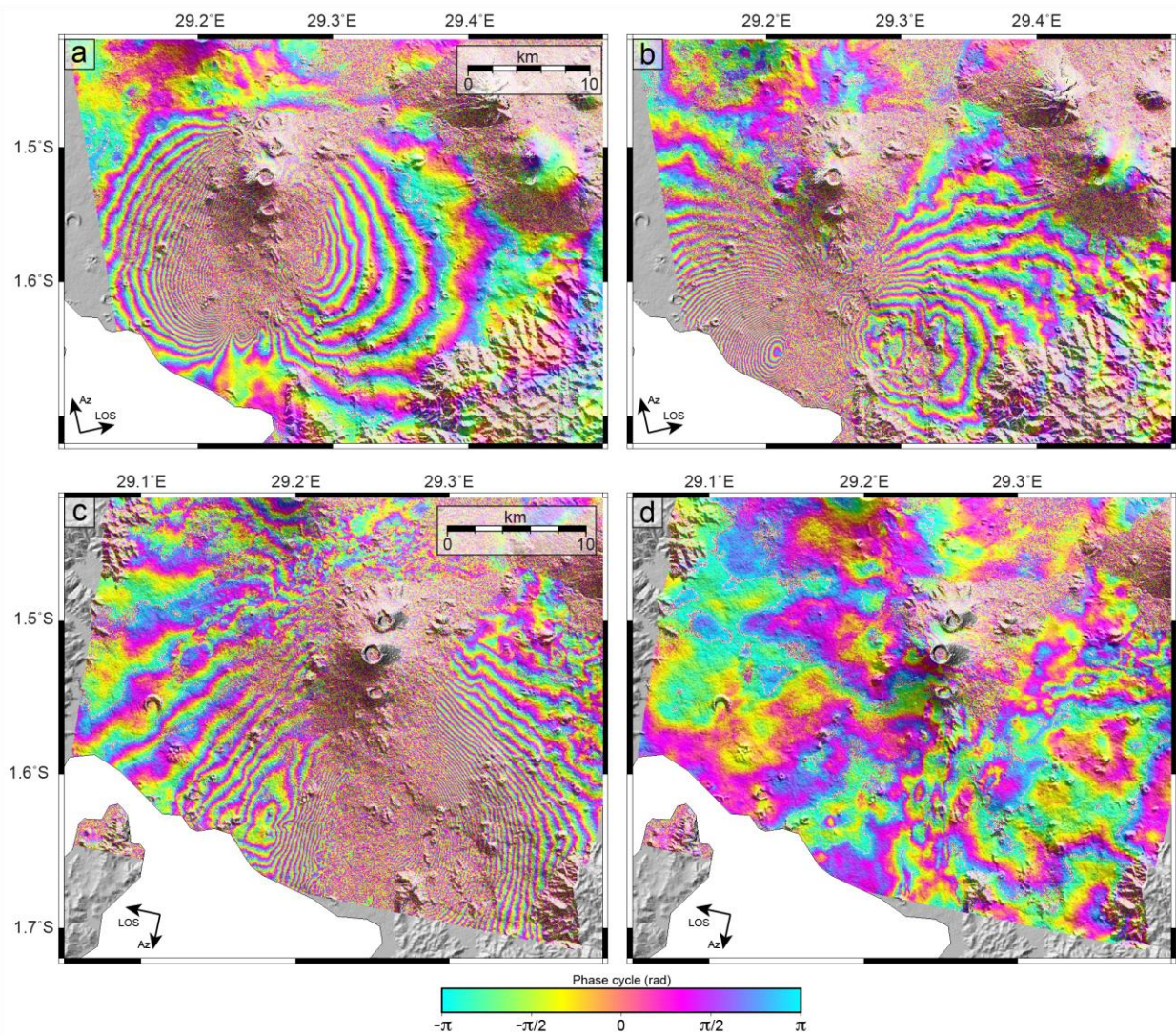


Figure 46. CSK interferograms in ascending (a & b) and descending (c & d) orbits. a) span the first hours of the eruption. b) cover the last part of the eruption and the intrusion period. c) span the entire intrusion period. d) shows the post-intrusive signal.

b.3. Deformation maps

To unwrap the interferograms, the mcf (Werner et al., 2002) algorithm uses the coherence as weight. This reduces the reliability of the measured deformations in areas with low coherence values like where the signal is large and concentrated in small areas. Furthermore, the Nyiragongo volcano is surrounded by a very dense forest that completely prevents to retrieval of a coherent signal in large areas. Finally, isolated coherent patches are subject to large misestimations of the deformation because the algorithm cannot correctly count the fringes since there are some missing. Here only two S1 unwrapped interferograms, converted to deformation maps will be shown (Fig. 47).

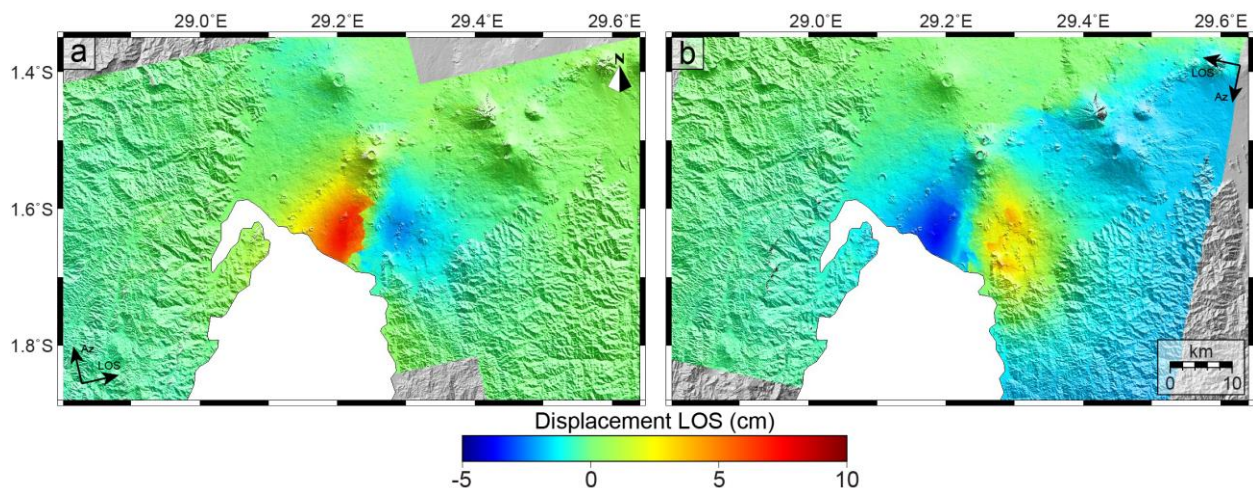


Figure 47. S1 LOS deformation maps.

Indeed, thanks to the larger wavelength, S1 interferograms are more coherent. Both the interferograms cover the entire intrusive period. In a) the S1 ascending interferogram covers the period May 19 – 31. Two clear lobes of signal are observable, one on the west is moving toward the satellite (red – positive signal) of up to 8 cm while the eastern lobe is moving away from the satellite (blue – negative signal) up to 3 cm. Between the two lobes, there is an area with a small deformation. This corresponds to the lobe in the middle in range increase in the interferogram in Fig. 43b, which, since it's not coherent due to the large displacement cannot be correctly unwrapped. Furthermore, the sharp boundaries of the western lobe suggest the presence of some unwrapping artifacts. In Fig. 47b, the descending interferogram covers the period May 21 – June 2. Also here, two lobes of deformation are visible.

The one on the west is moving away from the satellite (blue – negative signal) up to 4 cm while the one on the east is moving toward the satellite (red – positive signal) up to 5 cm. Also here,

the lobe in the middle is not visible. Since the signs of the lobes in the two interferograms shows the opposite behavior, it is possible to assume that a large part of the displacement occurred along the horizontal component. It would be possible to combine the two images to retrieve the near-vertical and near-east-west components of the deformation but, since both unwrapped interferograms are affected by large errors, the estimation will not be precise.

References

Goldstein, R.M.; Werner, C.L. Radar interferogram filtering for geophysical applications. *Geophys. Res. Lett.* 1998, 25, 4035–4038.

Hanssen, R. (2001). *Radar interferometry: Data interpretation and error analysis (Vol. 2)*. Springer, Dordrecht. doi: 10.1007/0-306-47633-9.

Nobile, A., Pagli, C., Keir, D., Wright, T. J., Ayele, A., Ruch, J., and Acocella, V. (2012), Dike-fault interaction during the 2004 Dallol intrusion at the northern edge of the Erta Ale Ridge (Afar, Ethiopia), *Geophys. Res. Lett.*, 39, L19305, doi:10.1029/2012GL053152.

Wegmüller, U. (1998). *SAR Processing, Interferometry, Differential Interferometry and Geocoding Software*. presented at EUSAR'98, 25-27 May. Friedrichshafen, Germany, VDE-Verlag.

Werner, C., Wegmüller, U., & Strozzi, T. (2002). Processing strategies for phase unwrapping for INSAR applications. presented at Procs. EUSAR Conf. Cologne, Germany

5.2.4. Pléiades data processing in the Virunga area

In the framework of the Virunga Supersite, different Pleiades triplets have been acquired since 2019. During 2020-2021, several acquisitions were made through those areas poorly covered in 2019, moreover for different parts we have redundancy of acquisition (Fig. 48a).

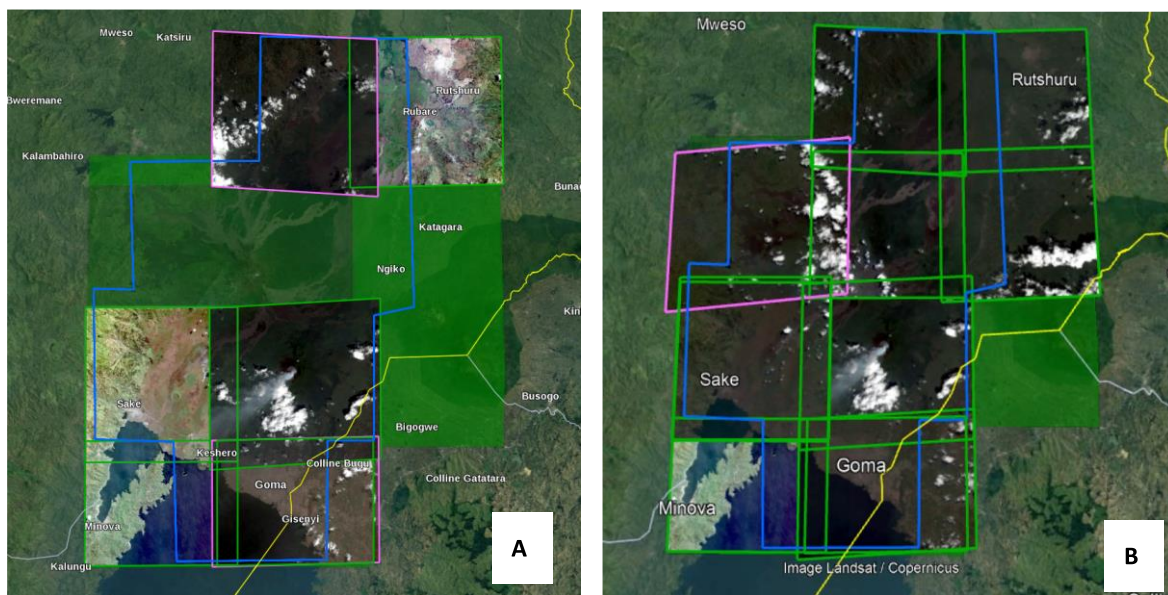


Figure 48. Pléiades images acquired in 2020 and 2021 (a) and since 2019 (b). The blue area highlights the Region of Interest, while each green square represents a different acquisition.

The Region of Interest (ROI, blu line) extends over an area of 2,032 square kilometers. From 2019 to 2021 the whole area was covered by nineteen Pleiades acquisitions (green squares) (Fig 48b). It is worth noting that both the Nyiragongo and the Nyamulagira summits are partially covered by clouds.

The 3D processing of the tri-stereo Pléiades imagery was performed at INGV, Osservatorio Etno, using the free and open source MicMac (Multi-images Correspondances, Méthodes Automatiques de Corrélation) photogrammetric library developed by the French Institut Géographique National (Rupnik et al., 2017). MicMac is based on the principles of photogrammetry and consists of three main steps:

- 1) Tie points recognition and matching between images;
- 2) Calibration and orientation, recognizing relationships between viewpoints and objects;
- 3) Correlation, producing dense matching for 3D scene reconstruction.

As result of this processing, a Digital Surface Model (DSM) composed by different patches was retrieved at the spatial resolution of 1 meter. Areas covered by clouds result necessarily in holes in the final product. The nominal absolute location accuracy of Pléiades-derived digital surface model is 8.5 m (Oh and Lee, 2014), this value is often an upper bound (Ganci et al.,2019). GPS points are required in order to evaluate the accuracy of the DSM in the Virunga area. Figure 1 shows a new DSM produced in the area of Goma city.

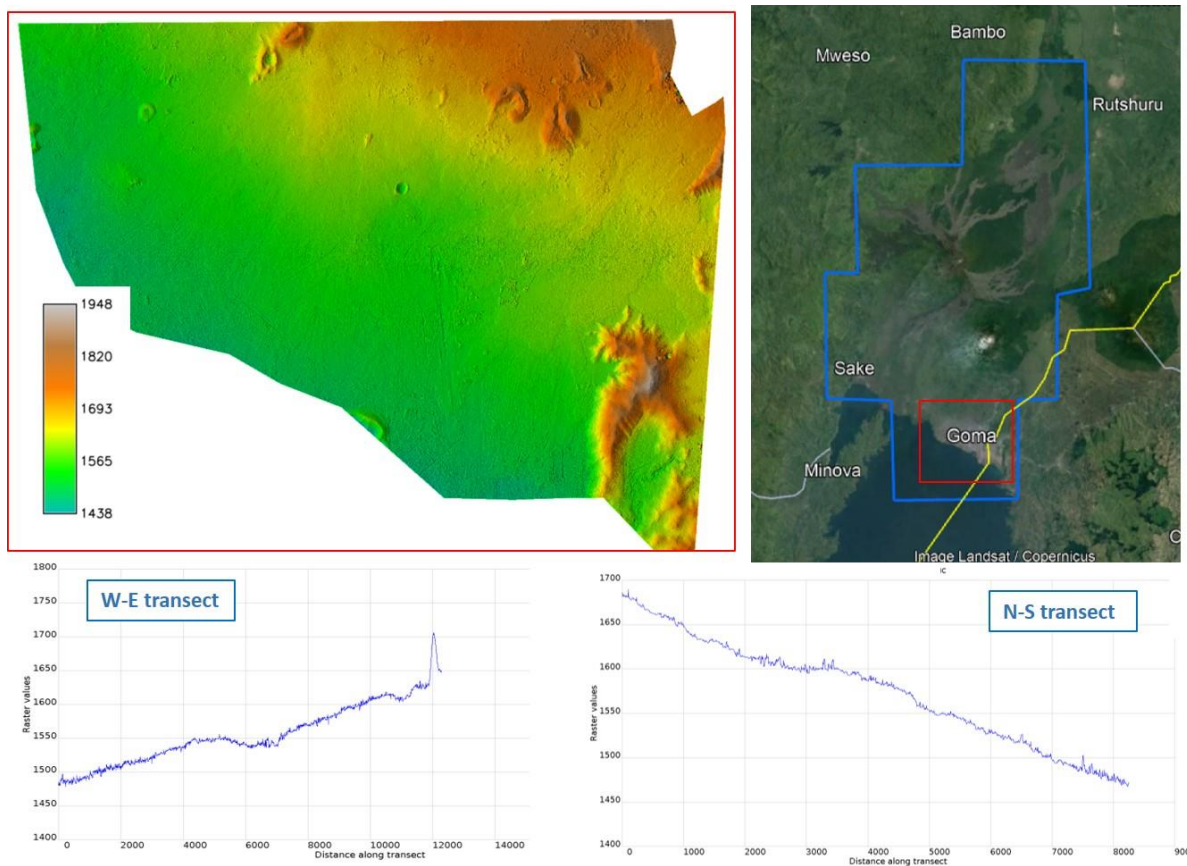


Figure 49. DSM in the area of Goma city. In the lower part two transects in the West-East (lower left) and North-South (lower right) direction are shown.

An ad hoc acquisition program was set after the Nyiragongo 2021 eruption on the area covered by the lava flow and on the Nyiragongo summit. This program provided other two acquisitions one on 1 August 2021 and the other one on 12 November 2021. We produced two DSMs, one for each acquisition. Unfortunately, the DSM produced with the acquisition of November had a poor quality, so it was discarded.

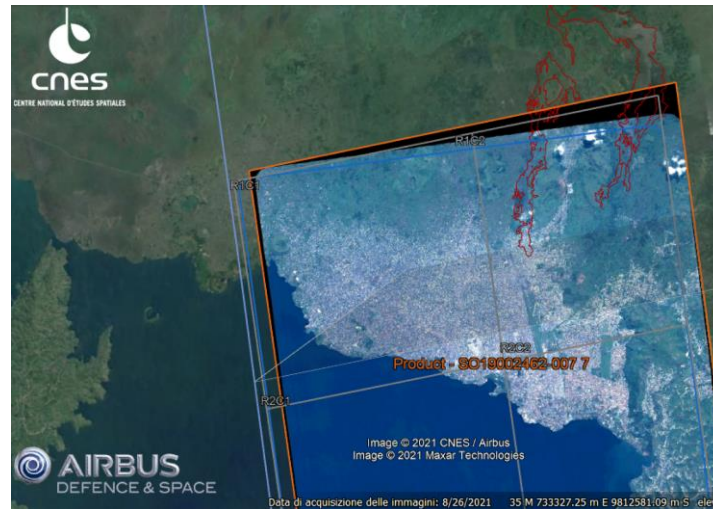


Figure 50. Pléiades image acquired on 1 August 2021 in the area of Goma. The red contours show the lower parts of the lava flow fields emplaced in May 2021

The acquisition of 01/08/2021 overlaps with that of 03/07/2019 in the Goma area (Fig. 50). The two 1-meter DSMs produced by using the MicMac photogrammetric library were aligned using the Nuth and Kääb (2011) algorithm and the difference was computed in correspondence of the lava flow field emplaced on 21-22 May 2021 (Fig. 51). Due to the vertical accuracy of the Pleiades derived DSM, usually around 1 meter, we argued that the lava flow thickness was very low, often under 1 meter, with some exceptions in the front area reaching 3 meters (Fig. 51).

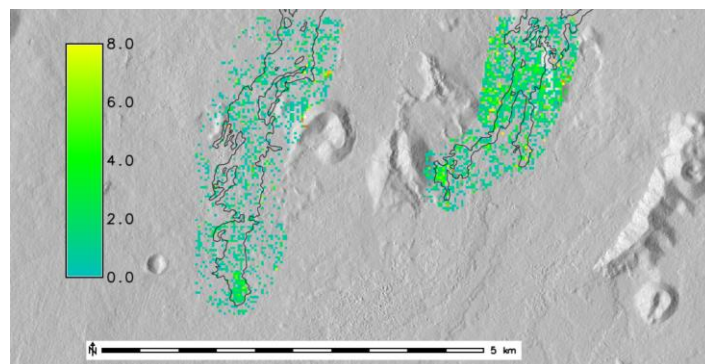


Figure 51. Difference between the two Pléiades-derived DSMs (1 August 2021 - 3 July 2019) in the southern portion of the lava flow emitted in May 2021. The legend shows the lava thickness in meters.

From the Pléiades image acquired on 12 November 2021 (Fig. 52a), we extracted the entire lava flow field that measures about 10 km² (Fig. 52b). By considering an average thickness of lava ranging from 0.8 to 1.5 meters, a total volume of 12±4 million cubic meters is thus obtained.

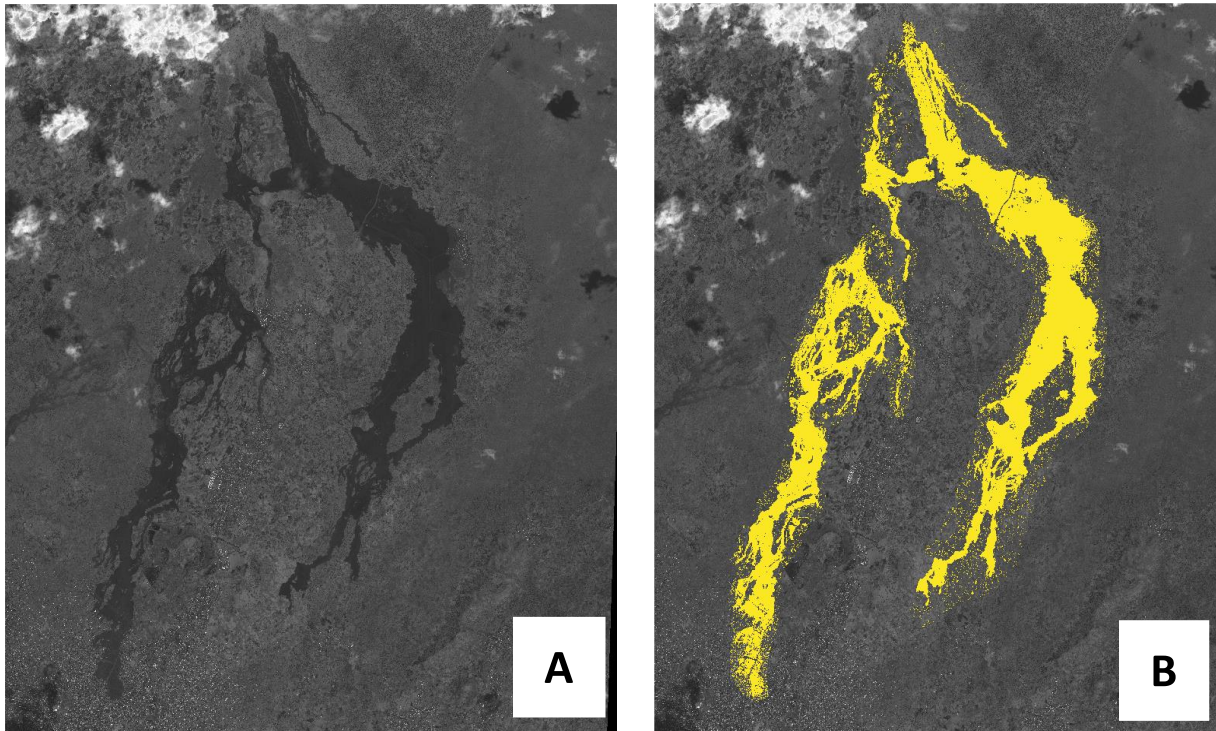


Figure 52. a) Pléiades image acquired on 12 November 2021; b) Lava flow field emplaced in May 2021 as retrieved from the Pleiades image (yellow area).

❖ COSMO-SkyMed data processing for lava flow mapping in the Virunga area

In the framework of the Virunga Supersite, data acquired by the COSMO-SkyMed SAR satellite constellation of the Italian Space Agency (ASI) are available, at INGV, Osservatorio Etneo those images were processed in order to retrieve the lava flow area emitted during the 2021 Nyiragongo eruption. Because a thick layer of volcanic and meteorological clouds prevented to clearly observe the lava flow field, especially in the first period after the eruption, SAR images were the unique way to derive this information.

Three ascending images, acquired before the eruption, at its end and after it (20210516, 20210523 and 20210601) have been preliminary processed through the Sentinel Application Platform (SNAP) which is an open source common architecture for ESA Toolboxes, ideal for the exploitation of Earth Observation data. Each pair of images has been analyzed through the Multi-Temporal and Coherence (MTC) color composite approach that combined SAR amplitude and coherence analysis, being its general goal the detection of changes between two multi-temporal datasets (Boccardo et al. 2015).

For each pair, the MTC images have been obtained combining the following bands: R= Intensity of the master image (first acquisition date); G= Intensity of the slave image (second acquisition

date); B= Interferometric coherence map between the master and slave images. The MTC images have been exported in geotiff format and analyzed through the ESRI arcgis software for manually delimiting the area interested by the new lava flow. Fig. 53 and 54 show the images obtained from the 20210516- 20210523 pair and 20210516- 20210601 pair, respectively.

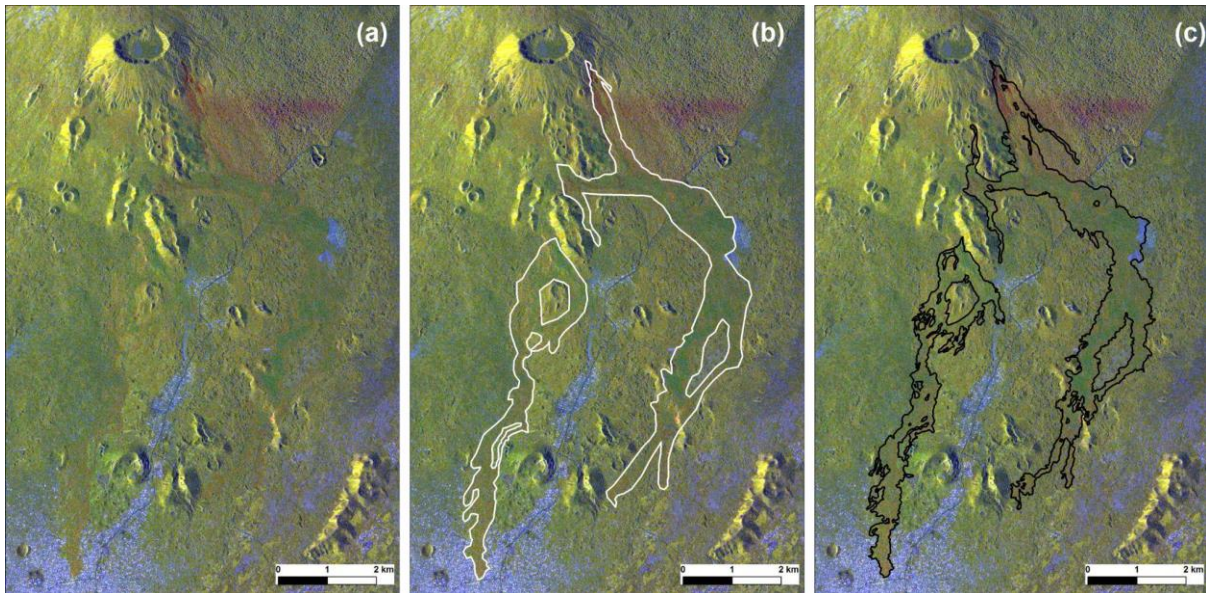


Figure 53. (a) MTC color map from the 20210516- 20210523 pair; (b) lava flow manually delimited on (a); (c) lava flow, updated as of 20210530, downloaded from the website <https://emergency.copernicus.eu/mapping> overlapped to (a)

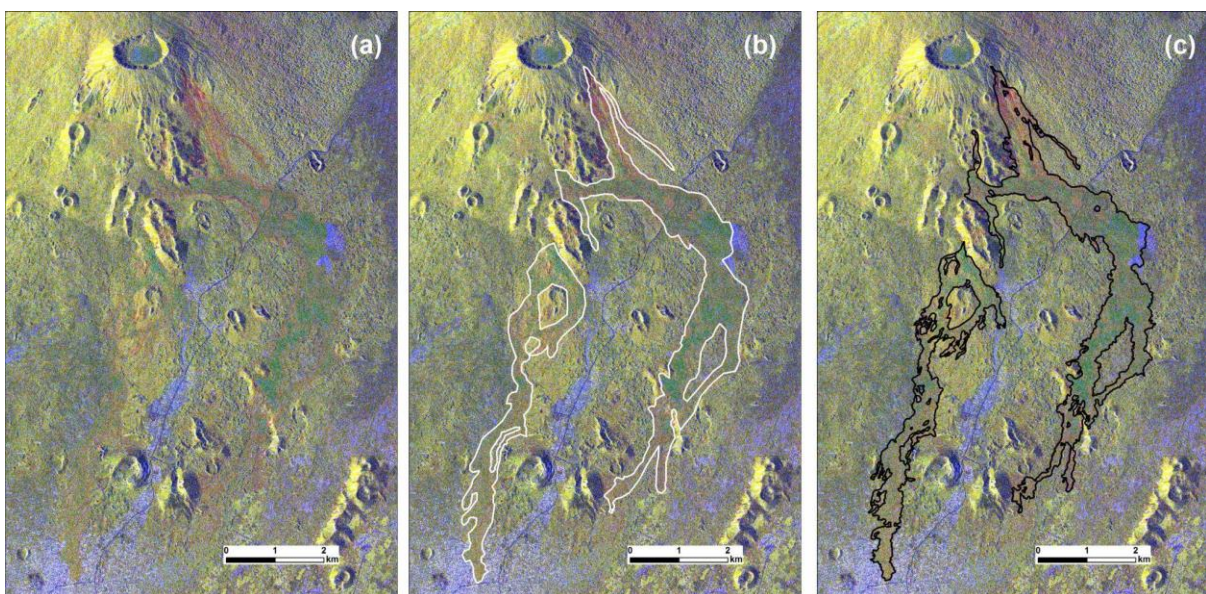


Figure 54. (a) MTC color map from the 20210516- 20210601 pair; (b) lava flow manually delimited on (a); (c) lava flow, updated as of 20210530, downloaded from the website <https://emergency.copernicus.eu/mapping> overlapped to (a)

It was tricky to map the new lava flow on the MTC images because also the areas adjacent to it decorrelated. The little lava flow to the NE of the upper vent cannot be easily recognized in Fig. 52, updated as of 20210523, whereas it is clearly evident on Fig. 53, updated as of 20210601. However, it is not possible to define whether it further propagated between 23 May and 1 June or whether it is not possible to identify it on the first map which is quite disturbed in the area of that flow. In fact, on Fig. 53b we mapped a much shorter bifurcation than that measurable on Fig. 54b. Further processing and analysis of the images will therefore be necessary.

References:

- Boccardo, P., Gentile, V., Tonolo, F. G., Grandoni, D., Vassileva, M. (2015). Multitemporal SAR coherence analysis: Lava flow monitoring case study. 2015 IEEE International Geoscience and Remote Sensing Symposium (IGARSS), 2699-2702, doi: 10.1109/IGARSS.2015.7326370
- Oh, J., and C. Lee (2014). Automated bias-compensation of rational polynomial coefficients of high resolution satellite imagery based on topographic maps, ISPRS J. Photogramm. Remote Sens., 100, 12–22.
- Ganci, G., Cappello, A., Bilotta, G., Herault, A, Zago, V., Del Negro, C. (2018). Mapping Volcanic Deposits of the 2011–2015 Etna
- Nuth, C. and A. Kääb (2011). Co-registration and biascorrections of satellite elevation data sets for quantifying glacier thickness change, *The Cryosphere*, 5, 271-290, doi:10.5194/tc-5-271-2011
- Ganci G., Cappello A., Bilotta G., Herault A., Zago V, Del Negro C. (2018). Mapping Volcanic Deposits of the 2011–2015 Etna Eruptive Events Using Satellite Remote Sensing, vol. 6, 83, doi:10.3389/feart.2018.00083.
- Rupnik, E., Daakir, M., Pierrot Deseilligny, M. (2017). MicMac – a free, open-source solution for photogrammetry. *Open geospatial data, softw. stand.* 2: 14. doi:10.1186/s40965-017-0027-2.

❖ **Delineating the lava flows from Mount Shaheru and other vents near Nyiragongo**

During the heightened unrest of Nyiragongo May - June 2021, the USGS-USAID Volcano Disaster Assistance Program (VDAP) supported the Observatoire Volcanologique de Goma (OVG) with satellite remote sensing information and imagery that were collected from a variety of resources. A list of routine resources that VDAP used to contribute timely information includes:


- ASTER night-time thermal,
- Sentinel-1 SAR,
- Sentinel-2 SWIR multispectral bands,
- Landsat8 VNIR, TIR,
- the MIROVA online webtool for thermal output timeseries of MODIS and S-2 SWIR,
- the NASA EarthView online webtool for daily distribution of thermal alerts from VIIRS and MODIS,
- DigitalGlobe WorldView high-resolution optical images for vapor and gas plume and weather cloud presence (with occasional views of the ground surface to look for lava flows/lava lake),
- Meteosat-8 nighttime “fire” layer in the online RAMMB-CIRA SLIDER webtool.

In addition, VDAP was able to take advantage of a temporary access to two commercial SAR: ICEYE and Capella. These platforms were testing calibrations and to help validate their data, they supplied imagery to VDAP for a short-term project. This was a new data resource, and the timing was very fortuitous. These data may become available to US government under contract shortly.


The International Charter for Space and Major Disasters (the “International Charter”) was started 23 May 2021 and ran for approximately two weeks. Information products and summaries from during that time are available here: <https://disasterscharter.org/web/guest/activations/-/article/volcano-in-congo-the-democratic-republic-of-the-activation-713->. This activation allowed for expedited and prioritized sharing of satellite data for a short, intense period of time from a multitude of global satellites including DLR’s TerraSAR-X (Germany), SAOCOM (Argentina), Radarsat Constellation Mission (Canada), PAZ (Spain), CosmoSkyMed (Italy), Pleiades (France) and others. These data provided the backbone for identifying and delineating the lava flows, fissures, and new volcanic vents near Nyiragongo. The digitized GIS lines were created as shapefiles (.shp) and as GoogleEarth files (.kml).


An additional source of data was JAXA PALSAR through a collaborative relationship that VDAP holds with NASA Jet Propulsion Labs investigators who contributed INSAR information (deformation patterns). These data are not part of the International Charter but were made available through friendly connections. VDAP didn't get the original data, but the processed INSAR results were shared readily, helped determine the extent of dike propagation towards Lake Kivu shoreline and tied in the smaller lava flows NW of Nyiragongo, and helped to confirm interpretations and timing from other SAR sources too.

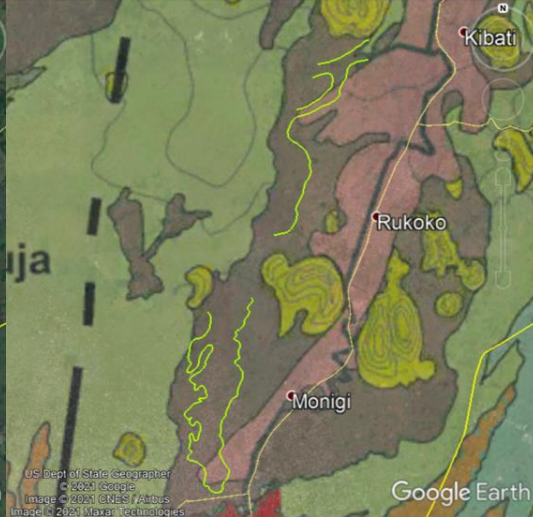
Some of the early, preliminary delineation of the new lava flows was done by other foreign academic colleagues and shared with us as seen here,




Nyiragongo Southeast Rift Zone and May 2021 Lava Flow extends > 5.5 km:
Preliminary mapping derived from ICEYE imagery 23 May 2010 UTC







Data Credits:
Lava flow linework (left inset image): Susanna Ebmeier and Edna Dualeh at the University of Leeds (UK) using ICEYE imagery.
The geologic map (right inset image) from Platz, T., 2002. *Nyiragongo volcano, DR Congo* – Mineral chemistry and Petrology. PhD Dissertation, University of Greifswald, Germany, 96p.

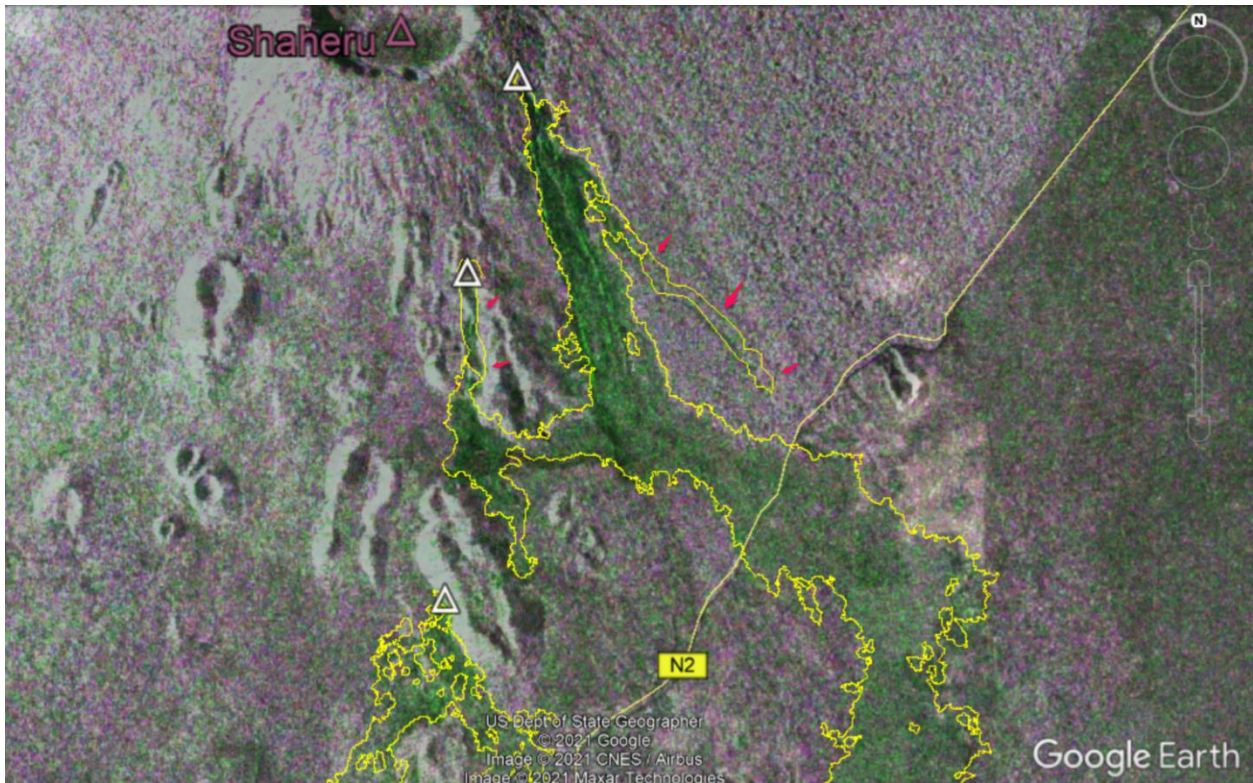


Building on the initial linework done by Susanna Ebmeier and Edna Dualeh at the University of Leeds, the UNITAR-UNOSAT group took the lead through their value-added provider role in the International Charter for a majority of the lava flow GIS analysis line work. VDAP, also contributed some lava flow delineation with fissure and vent locations for a combined effort in GIS.

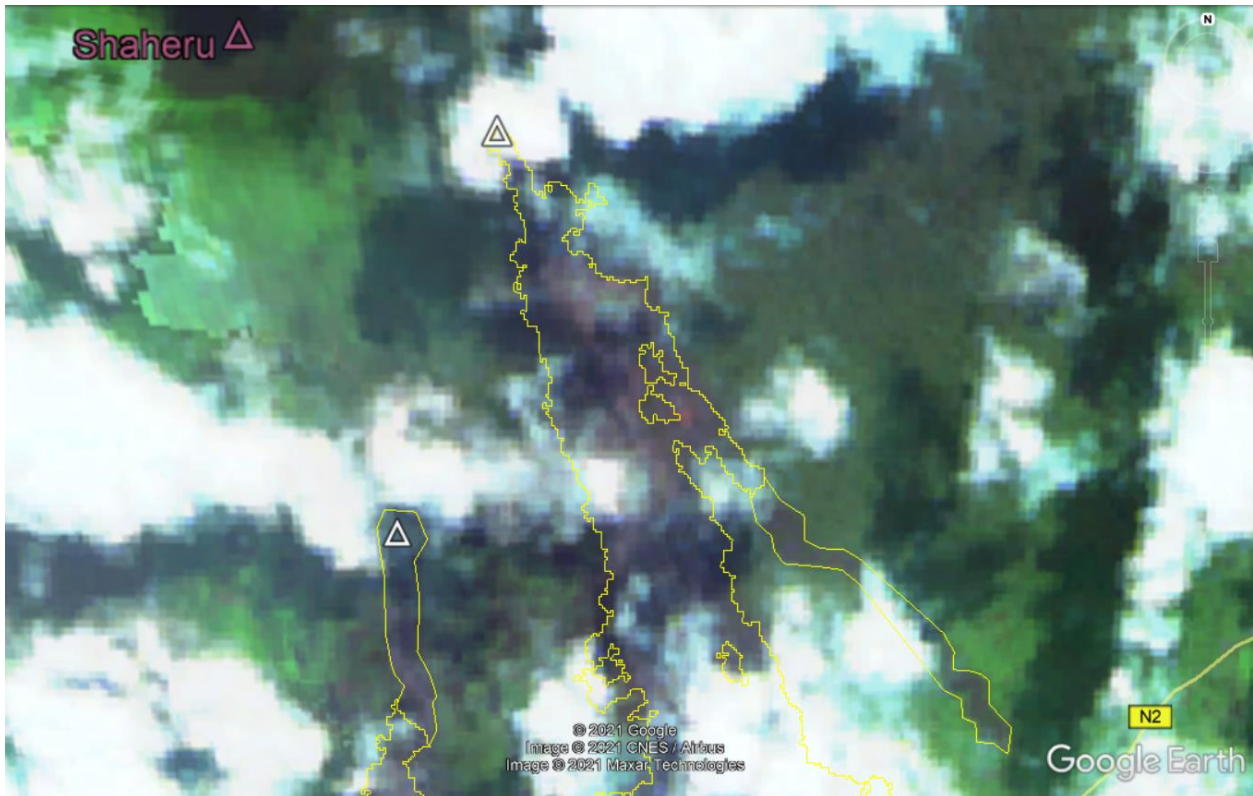
During the course of the unrest, some newer remote sensing techniques were used where a multi-band image is made from two SAR images from different days to tease out changes. The change detection work identified that the lava lake level in the Nyiragongo main crater underwent a significant change between two SAR image dates. This helped to encourage additional tasking of SAR which can “see through” weather clouds whereas in the multispectral high-resolution optical imagery, the lava flows were persistently obscured by those clouds.

Further exploring of SAR imagery using various polarization combinations as image bands really helped to delineate the lava flows.

Iteratively using a series of SAR imagery (here below: 27 May 27 SAOCOM red, green, blue (RGB) bands assigned with VH, VV, VH polarizations) and SWIR (here below: 27 May Sentinel-2 bands 12,11,4), the linework came together collaboratively.

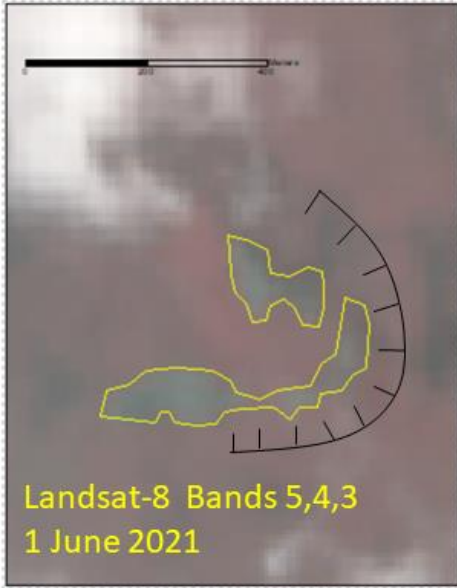


An early SAR image that did not fully capture the full extent of the lava flows was supplemented with an optical multispectral SWIR image (here). The white triangles are three new volcanic vents.



It is worthwhile to point out that this line work represents a best effort at the time with the data available. Follow-up field verification when field safety permits would validate this GIS linework.

Finally on the northwest side of Nyiragongo, a thermal anomaly detected with VIIRS thermal alerts using the NASA EarthView online tool was noted 24 May. A drone flight on 26 May confirmed this. Reviewing archive satellite imagery ensued to try to pin down the timing of these flows. The anomaly was initially determined to have appeared sometime after 8 March. Follow-up attention to this area began to limit the timing. Eventually, it was determined that the lava flow must have appeared before 24 May (the VIIRS anomaly identification) and after 22 May (Sentinel-2 VNIR that shows the absence of lava in this location although area is partially obscured by clouds). Finally, a false-color VNIR Landsat8 image on 1 June further helped to map out details of the lava flow lobes when there were fewer clouds. This was further corroborated with multiple INSAR analysis images that show the lava flow location coincides with the northern terminus of dramatic deformation patterns.

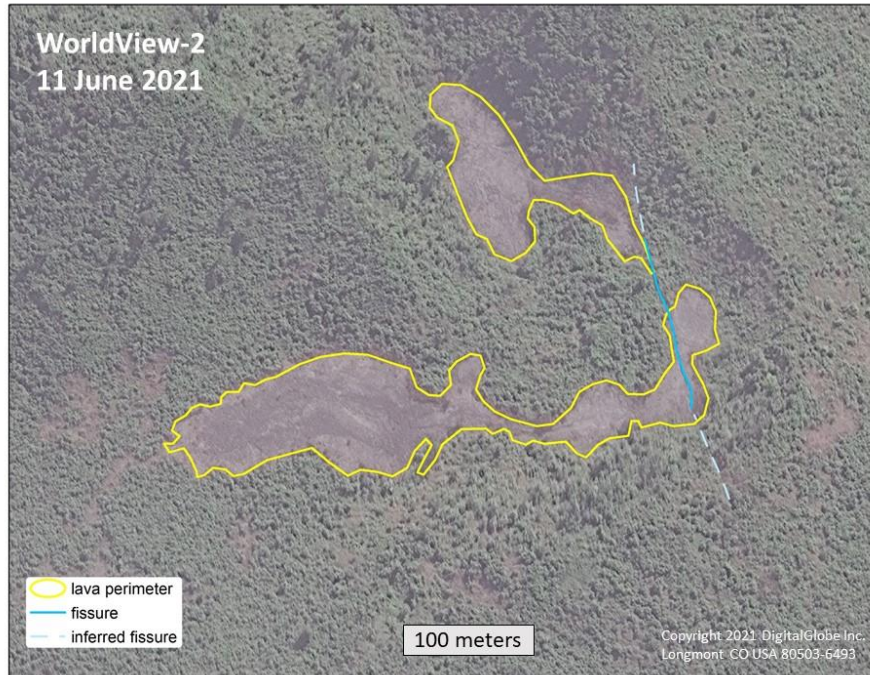


Nyiragongo Volcano, DRC

Lava flow lobes were first observed with VIIRS nighttime thermal radiance 24 & 27 May sensors on NOAA-20 and Suomi-NPP. Anomalies confirmed using Landsat-8 false-color VNIR with 1 June image (left panel). Actual date of effusion is not certain but presumed prior to 24 May. The lava flow lobes sit within an older scoria cone whose crater opens to the west and sits 3.2 kilometers NNW of Nyiragongo Volcano. Area of lava is ~30,000 square meters.



And after 11 June with a high-resolution commercial image, the fissure locations were added and lava flow lines were refined. Again, the GIS line work ought to be corroborated in the field as the tree line and shadows prevents a perfect view of the ground surface.



**Lava flow and fissure
north-northwest of
Nyiragongo Volcano,
Democratic Republic of
the Congo**

Lava flow lobes effused from a fissure some time between 22 and 24 May constrained by observations from Sentinel-2 and VIIRS. The lava flow lobes sit within an older scoria cone whose crater opens to the west and sits 3.2 kilometers NNW of Nyiragongo Volcano. The area of the lava flows is ~31,000 square meters.



5.2.5. Contribution of the satellite monitoring system MOUNTS to the surveillance of Nyiragongo and Nyamulagira volcanoes (DRC)

a. MOUNTS monitoring system

MOUNTS (Monitoring Unrest from Space, www.mounts-project.com, Valade et al. 2019) is a satellite-based volcano monitoring system, exploiting the diversity of sensors on-board the polar-orbiting Sentinel spacecrafts (ESA Copernicus). The synergistic use of radar (Sentinel-1 SAR), short-wave infrared (Sentinel-2 MSI) and ultraviolet (Sentinel-5P TROPOMI) payloads allow for surveillance of surface deformation, emplacement of volcanic deposits, detection of thermal anomalies, and emission of volcanic SO₂. Deep Learning "plugins" are incorporated to assist specific processing tasks, such as the automatic detection of large deformation (INSAR) and SAR speckle filtering. The system is openly inspired by the MIROVA system, whereby volcanic activity is visualized through the systematic display of geo-referenced images and time-series of the above mentioned parameters at several tens of active volcanoes worldwide. It is now regularly used by several volcano observatories and monitoring agencies, highlighting the usefulness of such an integrated interdisciplinary approach, where systematic processing and visualization of EO products can support both scientific and operational communities for volcanic risk assessment and management. The description of the system can be found in Valade et al. (2019). The development of MOUNTS was funded from 2017-2019 by Geo.X (Research Network for Geosciences in Berlin and Potsdam). From January 2021 to January 2023 it is partially supported by the UNAM PAPIIT funding (project IA102221).

b. Nyiragongo Volcano

The May 2021 eruption of Nyiragongo was characterized by the drainage of the summit lava lake, the emplacement of a lava flow on the slopes of the edifice, the intrusion of a dike (initiating from the edifice and propagating towards the South), as well as the drastic reduction of SO₂ emissions and thermal anomalies in the days following the eruption onset. These important observations were captured through the multidisciplinary system MOUNTS.

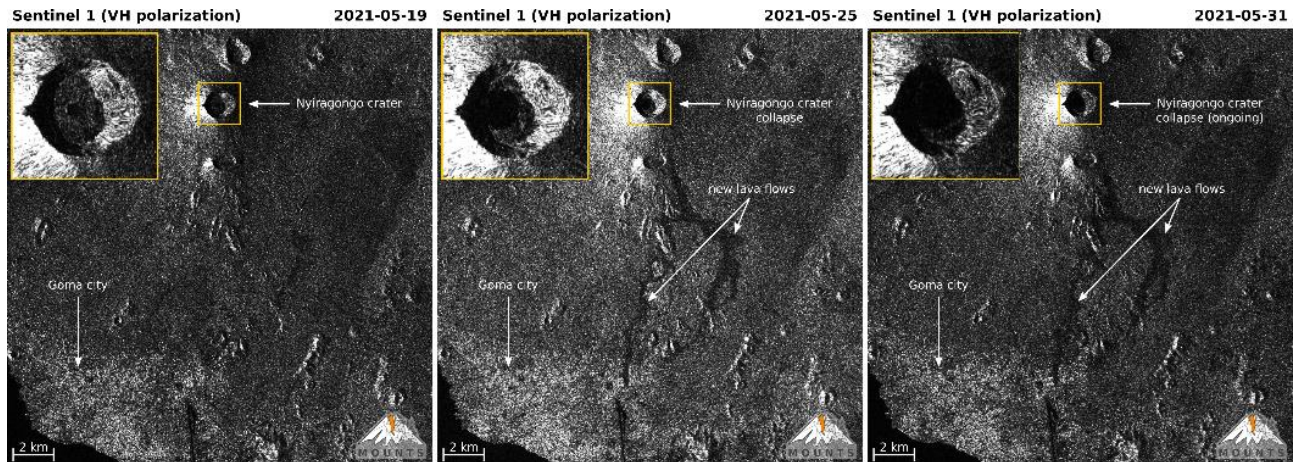


Figure 55. Sentinel-1 SAR intensity images acquired on 2021-05-19, 2021-05-25, and 2021-05-31, showing both the progressive crater collapse and the lava flow emplacement.

The Sentinel-1 SAR images allow observation of the lava lake drainage and progressive crater collapse, as evidenced by the increasing size of the crater size in the days following the eruption onset (Fig. 55 insets). On a larger spatial scale, the VH polarization of the SAR intensity images allow to capture the emplacement of the lava flow, which appears darker than the surroundings (Fig. 55).

The interferometric processing of two Sentinel-1 acquisitions allows the measurement of ground deformation occurring between these two dates. Fig. 56 is an interferogram generated from the differential interferometry (DInSAR) of two Sentinel-1 products, acquired on 2021-05-19 16:20 and 2021-05-31 16:20 UTC respectively (ascending orbit). The interferograms are displayed with a wrapped interferometric phase, whereby each fringe (full phase cycle ranging between 0 and 2π) corresponds to 2.8 cm in the radar line-of-sight (LOS). The large-scale deformation pattern displays two lobes with opposite displacements directions, typically interpreted as the result of a dike intrusion along the symmetry axis (Biggs and Pritchard, 2017), with a propagation path nearly North-South.

master = 2021-05-19, slave = 2021-05-31 (dt = 12 days)

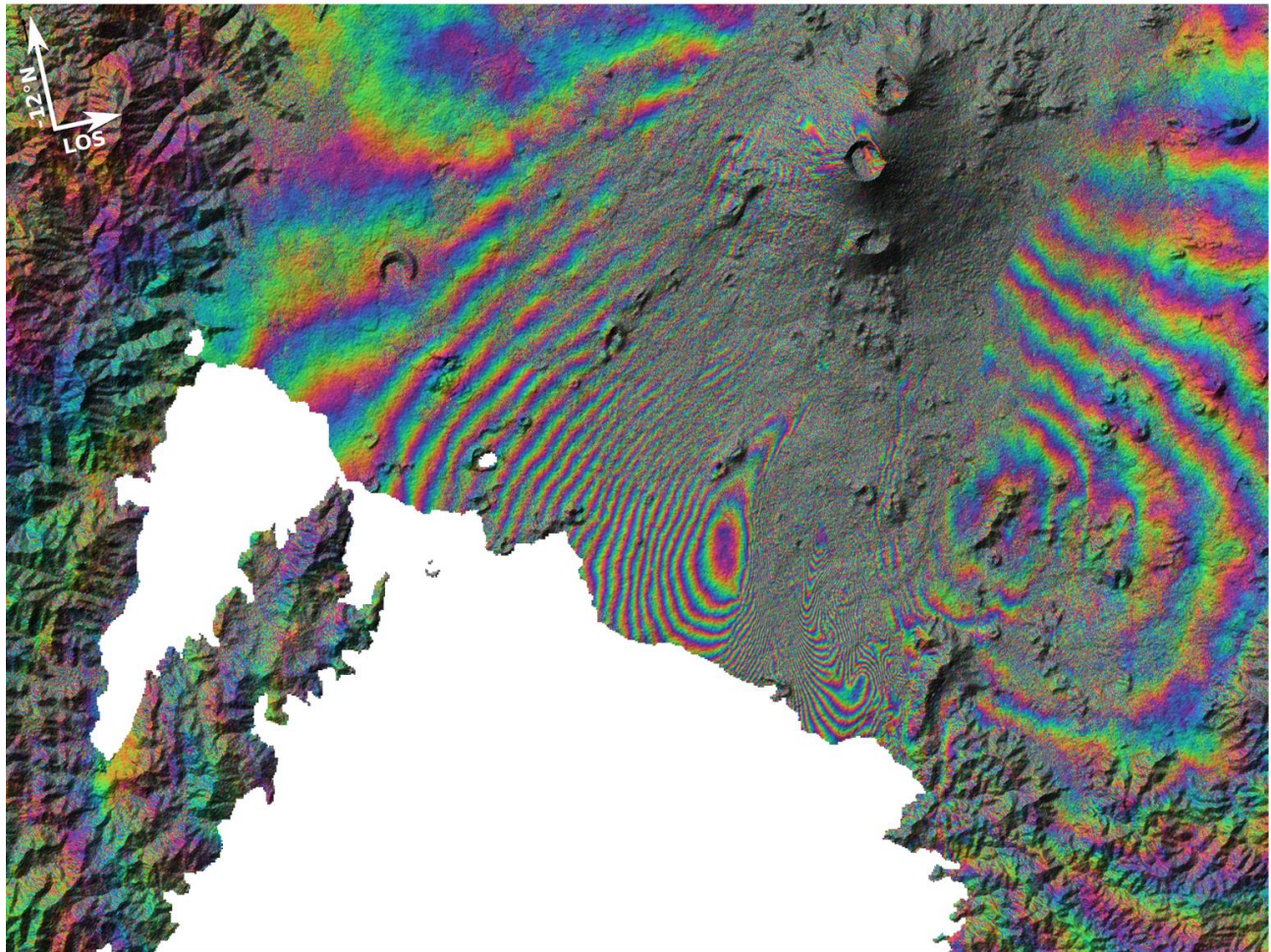


Fig. 56. Sentinel-1 interferogram generated from the images acquired on 2021-05-19 and 2021-05-31 (VV polarization), showing the deformation related to the dike propagation.

The analysis of Sentinel-5P TROPOMI products by MOUNTS allow the recovery of SO₂ mass (Theys et al. 2019, Valade et al. 2019). On the other hand, the analysis of the Sentinel-2 SWIR bands allows the recovery of thermal anomalies (Massimetti et al. 2020). The analysis of both shows that after the eruption onset, both the SO₂ emissions and the thermal anomalies decreased significantly (Fig. 57), as the lava lake was drained and the crater floor collapsed.

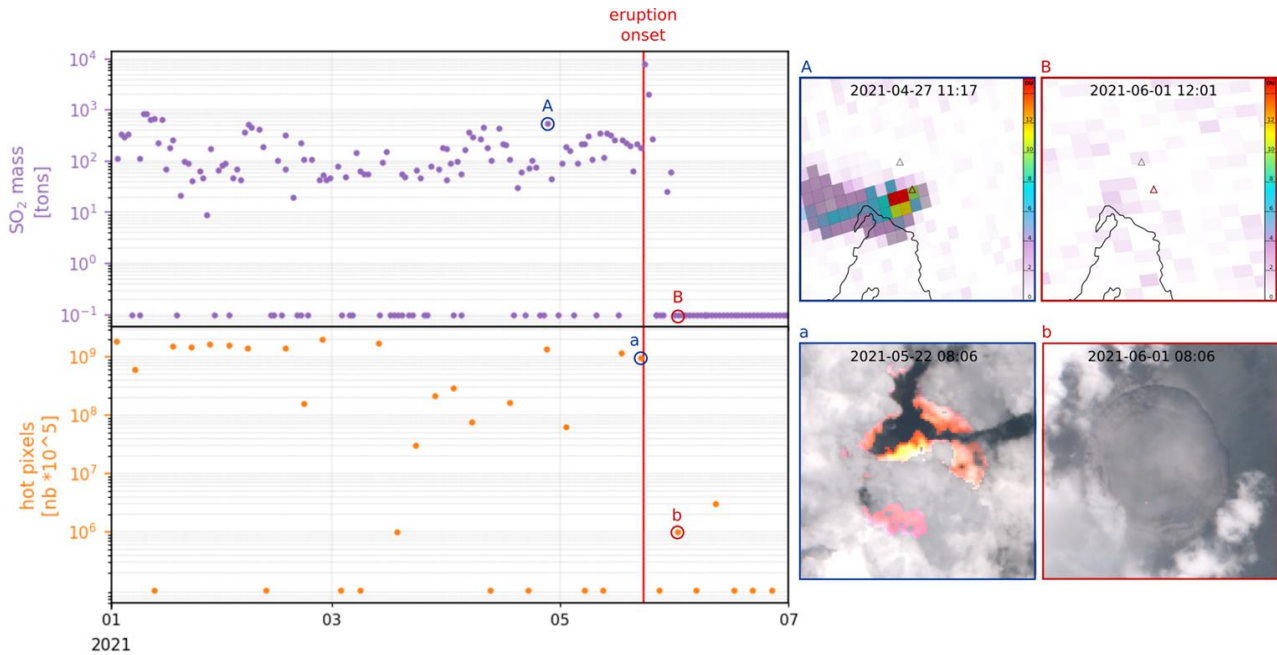


Fig. 57. SO₂ emissions and thermal anomalies recovered from Sentinel-5P and Sentinel-2 sensors, in the months preceding the eruption onset and in the following weeks.

c. Nyamulagira Volcano

Analysis of the Sentinel-1 SAR images allow recovery of the depths variations of both lava lakes and/or pit crater. This is done by measuring the length of the shadow casted by the pit crater walls in radar geometry, and multiplying it by the cosine of the radar incidence angle (Wadge et al., 2011). The method has been applied to track lava lake level variations at Nyiragongo (Barrière et al., 2018) and Erta Ale (Moore et al., 2019), and at Nyamulagira it has recently been applied by MOUNTS to provide variations of the pit-crater floor (Burgi et al. 2021).

Figure 4 is modified from from Burgi et al. (2021), and shows the variations of the pit crater floor at Nyamulagira during the period 2018-Jan to 2020-June. The time-series shows 3 phases, corresponding to the filling (Rise 1), emptying (Fall), and re-filling (Rise 2) of the pit-crater (red, blue and green respectively). This filling and emptying dynamics have been described and modeled in a recent study (Burgi et al. 2021).

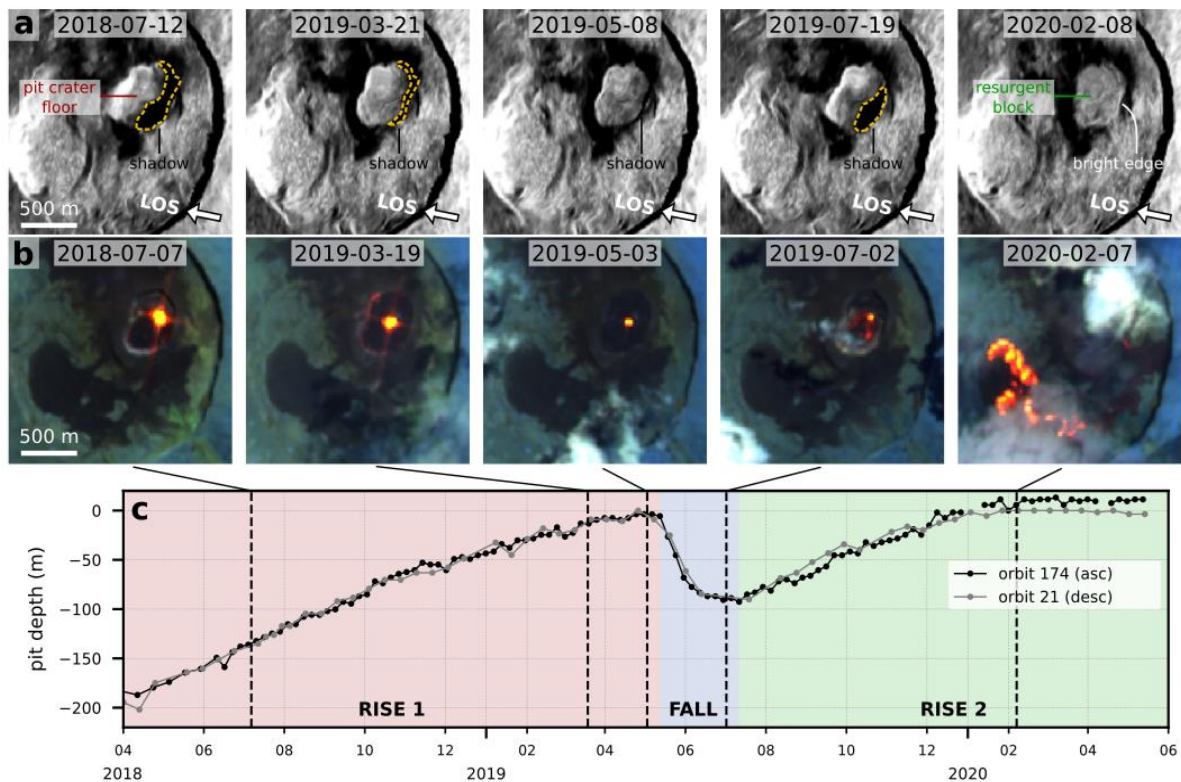


Fig. 58. Variations of the pit crater floor at Nyamulagira during the period 2018/01 to 2020/06, analyzed by MOUNTS from Sentinel-1 images. Figure modified from Burgi et al. (2021). (a) Sentinel-1 SAR images (descending orbit 21, LOS direction represented by white arrow), geocoded and speckle-filtered. (b) Sentinel-2 SWIR bands 12-11-8A. (c) Pit crater depth estimated from Sentinel-1 SAR images with ascending and descending orbits.

References:

- Barrière, J., d'Oreye, N., Oth, A., Geirsson, H., Mashagiro, N., Johnson, J.B., Smets, B., Samsonov, S., Kervyn, F., 2018. Single-station seismo-acoustic monitoring of Nyiragongo's lava lake activity (D.R. Congo). *Front. Earth Sci.* 6, 82
- Biggs, J.; Pritchard, M.E. Global volcano monitoring: What does it mean when volcanoes deform? *Elements* 2017, 13, 17–22.
- Burgi P.-Y., Valade, S., Coppola D., Boudoire G., Mavonga G., Rufino F., and Tedesco D., Unconventional filling dynamics of a pit crater, *EPSL*, 2021
- Massimetti, F., Coppola, D., Laiolo, M., Valade, S., Cigolini, C., Ripepe M., Volcanic Hot-Spot Detection Using SENTINEL-2: A Comparison with MODIS–MIROVA Thermal Data Series, *Remote Sens.*, 2020, 12(5), 820
- Moore, C., Wright, T., Hooper, A., Biggs, J., 2019. The 2017 eruption of Erta 'Ale volcano, Ethiopia: insights into the shallow axial plumbing system of an incipient mid-ocean ridge. *Geochem. Geophys. Geosyst.* 20, 5727–5743

- Theys, N.; Hedelt, P.; De Smedt, I.; Lerot, C.; Yu, H.; Vlietinck, J.; Pedernana, M.; Arellano, S.; Galle, B.; Fernandez, D.; et al. Global monitoring of volcanic SO₂ degassing with unprecedented resolution from TROPOMI onboard Sentinel-5 Precursor. *Sci. Rep.* 2019, 9, 1–10
- Valade, S., Ley, A., Massimetti, F., D’Hondt, O., Laiolo, M., Coppola, D., Loibl, D., Hellwich, O., Walter, T.R., *Towards Global Volcano Monitoring Using Multisensor Sentinel Missions and Artificial Intelligence: The MOUNTS Monitoring System*, *Remote Sens.*, 2019, 11, 1528
- Wadge, G., Cole, P., Stinton, A., Komorowski, J.-C., Stewart, R., Toombs, A.C., Legendre, Y., 2011. Rapid topographic change measured by high-resolution satellite radar at Soufriere Hills volcano, Montserrat, 2008–2010. *J. Volcanol. Geotherm. Res.* 199, 142–152

5.3. Thermal activity at Nyiragongo and Nyamulagira volcanoes (DR Congo) detected by the MIROVA system

In this short report I summarize the satellite thermal observations made by the MIROVA system (www.mirovaweb.it) on the Nyiragongo and Nyamulagira volcanoes during 2021.

a. Nyiragongo volcano:

During 2021, the MIROVA system, based on the analysis of MODIS data, detected 373 images with thermal anomalies with VRP (Volcanic Radiative Power) values between 0.2 and 2700 MW. The temporal analysis reveals that in the period between 1 January and 22 May 2021, thermal anomalies were frequently of high intensity, with VRPs exceeding 1000 MW (Fig. 59). This thermal activity is compatible with the presence of the convective lava lake that has grown inside the summit crater since 2002. On May 22, a lateral eruption drained the lava lake producing a lava flow that quickly reached the city of Goma. Unfortunately the event was not detected by MODIS due to significant cloud cover. However, it is possible to observe the sudden collapse of the thermal flow caused by the disappearance of the lava lake. Over the following months, small thermal anomalies began to resurface, indicating the renewed rise of magma within the Nyiragongo surface system (Fig. 59). In particular, this rise occurred impulsively in late September 2022, with VRP reaching values > 500 MW for the first time, and again starting from late November 2022 with VRP reaching VRP values > 1000 MW essentially compatible with the thermal flux recorded before the eruption of May 2021

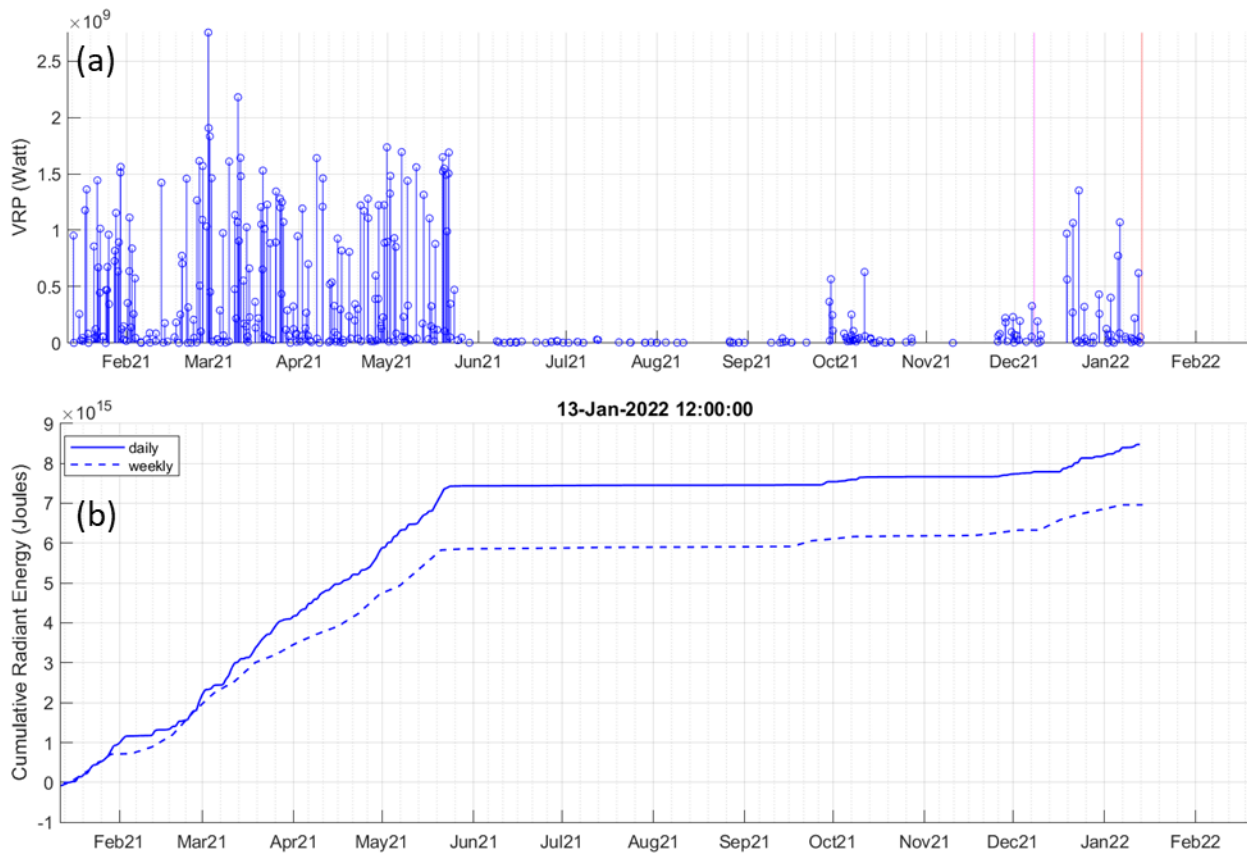


Fig. 59. (a) Volcanic Radiative Power (VRP) recorded at Nyiragongo volcano by the MIROVA system during 2021. (b) Cumulative Radiant Energy recorded in the same period.

b. Nyamulagira volcano

The thermal activity of Nyamulagira in 2021 is shown in Fig. 60. From the time series we can distinguish three different periods. The period between January and June 2022, characterized by moderate thermal anomalies (<100 MW). This period is followed by a phase of thermal activity characterized by frequent but discontinuous high thermal anomalies that have reached VRP values higher than 200 MW. This intermittent activity lasted until October 2021 and was followed again by a phase with low or moderate thermal anomalies that lasted until the end of 2021.

www.geo-gsnl.org

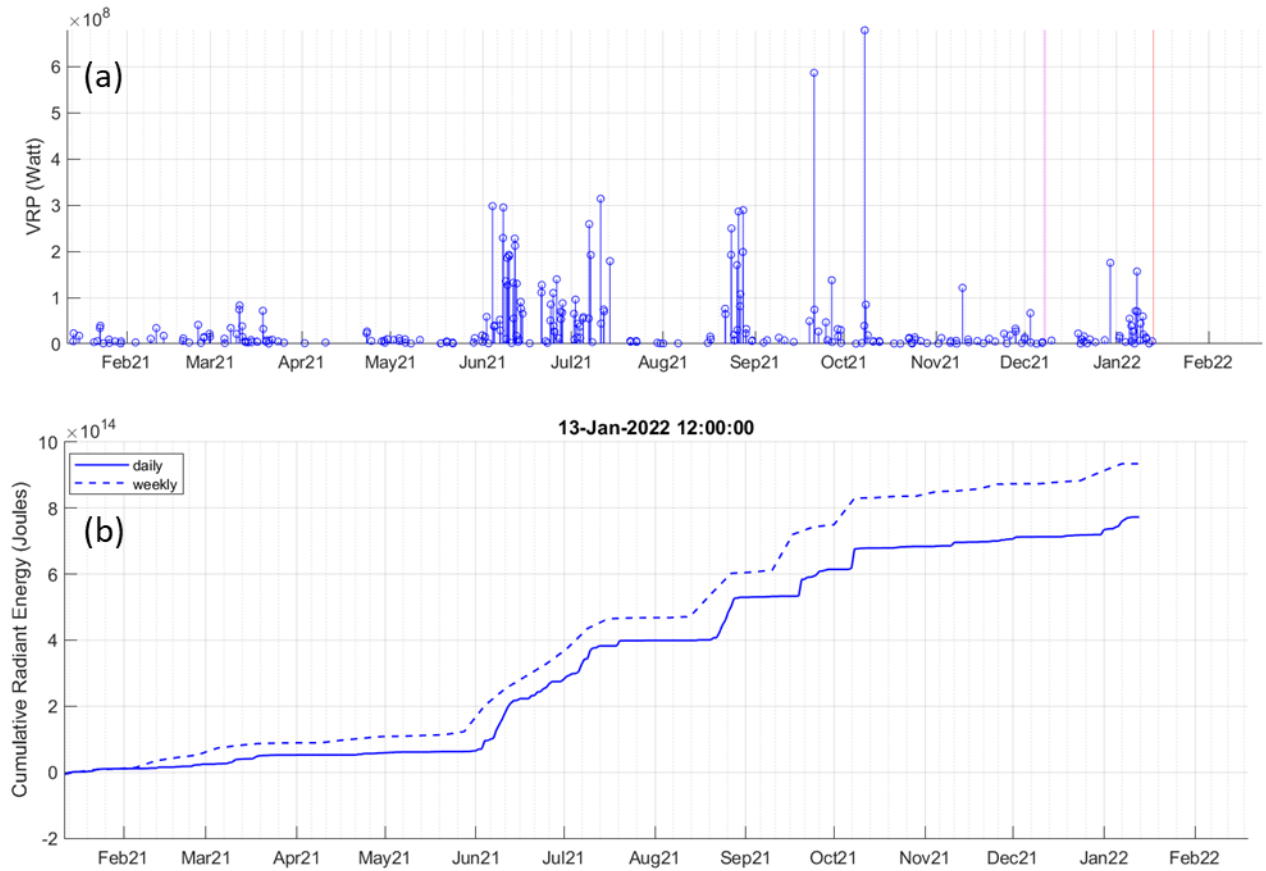


Fig. 60 – (a) Volcanic Radiative Power (VRP) recorded at Nyamuragira volcano by the MIROVA system during 2021. (b) Cumulative Radiant Energy recorded in the same period.

Publications

Peer reviewed journal articles

Lowenstern JB, Wallace K, Barsotti S, Sandri L, Stovall W, Bernard B, Privitera E, Komorowski J-C, Fournier N, Balagizi C, Garaebiti E., 2022. Guidelines for volcano-observatory operations during crises: recommendations from the 2019 volcano observatory best practices meeting. J Appl. Volcanol. 11, 3 (2022). <https://doi.org/10.1186/s13617-021-00112-9>

Plisnier P-D, Kayanda R, Obiero K, Vodacek A, Abegaz H, Achieng A, Akonkwa B, Albrecht C, Balagizi C et al., 2022. Need for a long-term multi-lake harmonized monitoring of African Great Lakes. Accepted for publication in the Journal of Great Lakes Research

Kasereka MM, Cuoco E, Zabene FZ, Balagizi C., 2021. Baseline for rainwater chemistry and quality as influenced by Nyiragongo volcano permanent plume, East Africa. Chemosphere. 2021 Nov; 283: 130859. <https://doi.org/10.1016/j.chemosphere.2021.130859>

Burgi P-Y, Valade S, Coppola D, Boudoire G, Mavonga G, Rufino F, Tedesco D, 2021. Unconventional filling dynamics of a pit crater, EPSL, 2021

Conference presentations/proceedings

Balagizi C., 2021. Virunga volcanoes monitoring infrastructure: Ground-based network and satellite remote sensing. Workshop on volcano monitoring infrastructure on the ground and in space. DOI: 10.13140/RG.2.2.14094.48961

Balagizi C., 2020. How global collaboration and open science can support hazard and risk assessment in low income countries: the case of the Goma Volcano Observatory experience, DR Congo. Understanding Risk Forum. DOI: 10.13140/RG.2.2.10854.24642/1

Trasatti E., Ganci G., Tolemei C., 2021. The 2021 Nyiragongo crisis: results from remote sensing monitoring. IAVCEI webinar on the 2021 Nyiragongo eruption: "The 2021 Nyiragongo eruption, sequence, and implications"

Research products

The main research products of the Virunga Supersite for the period from January 2020 to December 2021 are included in the present report. Thus, they will be accessible via the link to the report which will be available once the report has been approved; the report will also be available at the GEO GSNL website, Virunga Supersite section at <http://geo-gsnl.org/supersites/permanent-supersites/virunga-supersite/>. However, there is a plan to open a website for the Virunga Supersite which will help to share the research products.

Type of product	Product provider	How to access	Type of access
Updated Virunga lava flows map (1938 to present): Nyiragongo 2021 lava flows have been added	Balagizi C (GVO), Griswold J (VDAP-USGS), Ganci G & Trasatti E (INGV)	<i>Supersite coordinator or scientists who produced the map</i>	<i>Public</i>
Seismic map of the earthquakes that followed the Nyiragongo May 2021 eruption	Mavonga C, Kyambikwa A & Sadiki (OVG)	<i>Supersite coordinator or scientists who produced the map</i>	<i>Limited to GSNL scientists</i>
Map of fractures created by the Nyiragongo 2021	Ciraba H, Iragi K, Kavuke J., NZamu S, Balagizi C (GVO)	<i>Supersite coordinator or scientists who produced the</i>	<i>Limited to GSNL scientists, and</i>

<i>eruption and the seismicity that followed the eruption</i>	<i>and Habiyakare T & Niyitegeka T (RMB)</i>	<i>map</i>	<i>later on to the Public after publication in scientific journal</i>
<i>Gas composition of the Nyiragongo 2021 eruptive vent (CO₂, SO₂ and H₂S)</i>	<i>Balagizi C, Kasereka M & Mashagiro N (GVO), and Lowenstern J & Peter</i>	<i>Supersite coordinator or scientists who produced the map</i>	<i>Limited to GSNL scientists</i>
<i>Data related to air quality in Goma and Lake Kivu</i>	<i>Balagizi C, Kasereka M & Mashagiro N (GVO), and Lowenstern J & Peter</i>	<i>Supersite coordinator or scientists who produced the map</i>	<i>Limited to GSNL scientists</i>
<i>Data of Lake Kivu Physico-chemical composition during Nyiragongo 2021 eruption</i>	<i>Balagizi C, Kasereka M & Safari F (GVO)</i>	<i>Supersite coordinator or scientists who produced the map</i>	<i>Limited to GSNL scientists and later on to the Public after publication in scientific journal</i>
<i>Rainwater chemistry in the Virunga</i>	<i>Kasereka M & Balagizi C (GVO)</i>	<i>Supersite coordinator or scientists who produced the map</i>	<i>Public</i>
<i>Maps of InSAR analysis of surface deformations between January 2020 and December 2021</i>	<i>Trasatti E and INGV team, Valade S (UNAM), Balagizi C (GVO)</i>	<i>Supersite coordinator or scientists who produced the map</i>	<i>Limited to GSNL scientists and later on to the Public after publication in scientific journal</i>
<i>Scheme of the Nyiragongo area with the feeding dyke (dyke modelling) during the Nyiragongo 2021 eruption</i>	<i>Trasatti E and associated INGV team, Balagizi C (GVO)</i>	<i>Supersite coordinator or scientists who produced the map</i>	<i>Limited to GSNL scientists and later on to the Public after publication in scientific journal</i>
<i>DSM in the area of Nyiragongo volcanic field derived from Pléiades images acquired after Nyiragongo 2021 eruption</i>	<i>Ganci G and associated INGV team, Balagizi C (GVO)</i>	<i>Supersite coordinator or scientists who produced the map</i>	<i>Limited to GSNL scientists and later on to the Public after publication in scientific journal</i>

Research product issues

All the research products are not open to the public; some are still under embargo to allow the scientific team to publish their results. However, the results are fully open for hazards assessment and crisis managements, and were already sent to institutions locally involved in crisis management in both DRC and Rwanda. The results are also available on request to GSNL scientists, particularly the member of the Virunga Supersite scientific team, as the goal is to publish a unique scientific paper that include the results from the teams.

6. Dissemination and outreach

All the scientific products were already sent to local institutions that are involved in hazards assessment, particularly the GVO that monitors the Nyiragongo and Nyamulagira active volcanoes. The products were used during the response to the May 2021 eruption of Nyiragongo during which a scientific task was formed to support the response to the crisis, and which Virunga scientific team was involved and data collected through the Virunga Supersite umbrella were used to guide local authorities manage the crisis.

Due to the COVID 19 pandemic we were not available to travel to attend conferences; this was the case for the Cities on Volcanoes 11 in Heraklion, Crete (Greece) which has been postponed to June 12-17, 2022. The Understanding Risk Forum which was initially programmed to take place in Singapore was fortunately moved virtual and we had the chance to present the Virunga Supersite. The Virunga Supersite was also present at two other virtual meetings, namely at the Workshop on volcano monitoring infrastructure on the ground and in space (organized by the Global Volcano Monitoring Infrastructure Database GVMID, in collaboration with the World Organization of Volcano Observatories, WOVO), as well as at the IAVCEI's webinar on the 2021 Nyiragongo eruption.

Furthermore, it is worth to mention the following:

a. The Virunga Supersite attracted new members at local, regional and international level; and include:

#	Names	Department Institution	Country
1	Alain Rhubango Ruhembe	Department of geology, University of Goma	Democratic Republic of the Congo
2	Titus Habiyakare	Rwanda Mines, Petroleum and Gas Board(RMB), Seismology Section	Rwanda
3	Tite Niyitegeka	Rwanda Mines, Petroleum and Gas Board(RMB), Seismology Section	Rwanda
4	Adriano Nobile	KAUST – King Abdullah University of Science and Technology Earth Science and Engineering - Crustal Deformation and InSAR group	Saudi Arabia
5	Sébastien Valade	Universidad Nacional Autónoma de México, Instituto de Geofísica	Mexico
6	Diego Coppola	University of Turin	Italy

b. Virunga Supersite became an UNAVCO Associate member:

The Virunga Supersite as became an UNAVCO Associate member after our application to join the UNAVCO Inc. consortium was approved for Associate Membership by the UNAVCO Board of Directors. This association expands the Virunga Supersite scientific community, which we expect will help improve the volcano monitoring infrastructure to collect and process EO and ground-based data, their processing and interpretation and hence reduce the related risks.

c. Training of local scientists :

- 1°) Two workers of the Goma Volcano Observatory have benefited from the funding of the Volcano Active Foundation (<https://volcanofoundation.org/>) to take a 2 years Licence level (equivalent to masters). Niche Mashagiro, a GVO technician has that finished his two years licence networking, and Patient Shamavu (GVO junior researcher) who specialized in hydrobiology with emphasis on Lake Kivu and rivers of the Virunga Volcanic Province.
- 2°) Albert Kyambikwa is a GVO Junior researcher working in the department of semiology, and who has gained a scholarship to attend two years masters in volcanology at the University at Buffalo and is working with Dr. Stephan Kolzenburg of the Department of Geology at the University at Buffalo. They are working on the Reconstruction and modeling of lava rheology at Nyiragongo Volcano, their work is summarized below:

The volcano's recent effusive eruption in May 2021 caused catastrophic destruction to the neighboring communities, highlighting the need for a detailed understanding of lava flow propagation improved hazard maps that will ensure the safety of those living in these surrounding communities by informing reasonable urban planning projects and effective evacuation plans. This goal is even more relevant now as the populations density in affected communities continues to grow and urban sprawl and development remains high.

To create more accurate models, and thus, more accurate hazard maps, the focus of this research is to improve the understanding of the rheological characteristics of Nyiragongo lavas. This will help to optimize lava flow models by including customized rheological parameters relevant to this volcano and its eruptive dynamics. The goal is to develop an approach that is able to assess eruptive scenarios in near real time as well as to evaluate potential future scenarios.

This approach will use data collect during mapping and sampling of the May 2021 lava flow from Nyiragongo volcano for textural analysis and viscosity measurements. Quantifying the

lava's rheology and characterization of the lava's textural evolution during emplacement will enable the implementation and optimization of a lava propagation simulation model.

3°) Arsène Tumaini Sadiki : one year training in volcano seismology at Istituto Nazionale di Geofisica e Vulcanologia (INGV), Osservatorio Etneo - Sezione di Catania; Italy

Arsène Tumaini Sadiki is a junior researcher working in the department of seismology of the Goma volcano Observatory, and has been awarded a one year ICTP TRIL Fellowship through the partnership between ICTP and INGV. He will be working with Eugenio Privitera and Mariangela Scotto of Osservatorio Etneo at INGV/Catania, and will focus his work at the systematic analysis and classification of seismic signal sequences associated with eruptive crises by using the autoregressive techniques: application to Nyiragongo and Nyamulagira volcanoes, DR Congo.

4°) Olivier Munguiko Munyamahoro has been accepted for a short-term scientific training at the 2022 CSAV International Training Course in Volcano Hazards Monitoring. The courses will be held from June 4 to July 29, 2022 at Hilo campus – University of Hawaii in partnership with the Hawaiian Volcano Observatory, and second part in Vancouver, Washington at the USGS Cascades Volcano Observatory. This training is fully funded by the USGS's Volcano Disaster Assistance Program (VDAP-USAID).

d. The USGS's Volcano Disaster Assistance Program (VDAP-USAID) has donated to the Goma Volcano Observatory a server and computers to help in real time processing of seismic data. The VDAP also supported the GVO with the internet that allowed real time seismic data transmission which played a key role in responding to the Nyiragongo May 2021 eruption crisis. The volcanic gas team has received materials to maintain the MultiGAS equipment, and include sensors for replacement, calibration gases as well as masks for protection.

e. The Linda Project initiative (<https://LindaProject.org>)

The Linda Project is a community-based solution providing a sustainable safety net for the Goma Volcano Observatory (GVO, OVG in French) to accomplish its core mission: monitoring the Nyiragongo, Nyamuragira, and Lake Kivu. The Linda Project is powered by the Congolese diaspora and the academic, scientific, tech, and business communities; GVO senior researchers included. The Linda Project is based on the idea that solutions rooted in the targeted community are the most resilient. The Linda Project is also a strong advocate for OPEN DATA science in studying the Virunga volcanoes.

Working closely with the department of Seismology of the GVO, we supported the cost of data communication for five seismic stations of GVO that are not part of the Airtel network from July 2021 to 2021. In 2021, we were instrumental in providing financial and administrative support to a GVO researcher (visa fees and payment of local flights, field works support,...) to start a master's program in the USA. We will continue such support in 2022 to ensure that GVO researchers can get the best training possible.

In October 2021, we acquired an M2M gateway that will allow real time data transmission from equipment located in the field around Nyiragongo and Nyamulagira volcanoes (e.g. seismic stations) to servers located at Goma Volcano Observatory office where data has to be processed. We are fundraising to buy our first seismic stations that will produce seismic OPEN DATA in the study of the Nyiragongo volcano. This would be the first of a network of seismic stations sponsored by the LindaProject.

In March 2022, we will also start an open data citizen seismic network in Goma and across the Democratic Republic of the Congo using Raspberry Shake sensors. In the North Kivu Province, the goal of this citizen network is to collect open data on the Nyiragongo and Nyamulagira volcanoes. We will work closely with schools and local universities to use this network to educate the local community living near the volcanoes, and those in the area with high seismic hazards level.

7. Funding

The Virunga Supersite has no funding; all the activities were realized by scientists working on a voluntary basis.

8. Stakeholders interaction and societal benefits

The Goma Volcano Observatory (GVO) remains the main and direct beneficiary of the Virunga Supersite services and products. Hence, the GVO has a full access to the raw and processed data and products that were obtained under the Virunga Supersite umbrella. The EO data and products played a key role in the response to the Nyiragongo volcano May 2021 crisis, as raw data were made available to scientists to support the crisis management. The products that include, among others; the map of fractures created by the Nyiragongo 2021 eruption, the air quality during the eruption, the monitoring of lake Kivu stability during the volcanic crisis, the maps of InSAR analysis of surface deformations, the scheme of the Nyiragongo area with the feeding dyke, the DSM in the area of Nyiragongo volcanic field derived from Pléiades images were used by decisions makers during the volcanic crisis, along with the others that were previously produced by the Virunga Supersite.

The products were used by both by governmental and non-governmental agencies that were involved in responding and managing the Nyiragongo 2021 eruption crisis at both national and regional levels. During the Nyiragongo volcanic crisis, the strong seismic activity and ground deformation that followed the eruption, Virunga Supersite products were used in the production of daily volcanic activity updates and alerts, and others means to communicate to the public.

9. Conclusive remarks and suggestions for improvement

The Virunga Supersite is presently well established and operating group. During the first 2 years of existence (i.e. November 2017 to November 2019), the Supersite successfully generated research results associated to with pre-crisis assessment of hazards in the Virunga region, supported volcano monitoring activities, disaster and crisis preparedness and management. In the course of 2020 and the first trimester of 2021, some of these activities continued (e.g. supporting volcano monitoring and hazards assessment).

The two major goals for the period from November 2019 to November 2021 were (1) the training of local researchers and (2) the support to the development of local infrastructures. Despite the constraints due to the COVID19 pandemic, we have succeeded to create opportunities for the training of some local scientists in close collaboration with Virunga international scientists. Further, the USGS-VDAP has donated some equipment to support ground data collection and processing. We will continue working on these two goals which are, by the way, long term objectives. Few months ago the Virunga Supersite scientific team wrote a project to get funds that aim at helping solve the issues of situ data collection by acquiring the necessary equipment, infrastructures development for both ground-based and EO data processing, and for the capacity building of local scientists. The proposal has been submitted to some funders, but still no positive feedback has been received.

We are still in need of more Pleiades images in the Virunga region as initially requested; because of the issue of clouds affecting the quality of the images which was already mentioned, but also to better constrain the last eruption of Nyiragongo volcano. We therefore suggest, once again, that second redundancy acquisitions should be planned to obtain the complete coverage which are free of clouds. We therefore request that these second redundancy acquisitions to not be included in the yearly quota of the images to be delivered to the Supersite by the CNES. We have planned to take images using a specialized drone, but the luck of funds deed not allow to performing this work.

Similarly, more to the south of the Virunga Supersite AOI there have been intense landslide and flooding that caused the loss of several lives and destruction of infrastructures, houses included, in the city of Uvira (DRC) and the north shore of Lake Tanganyika. Pleiades images are also need to study and assess this hazards, and suggest to the government a solution.

10. Dissemination material for CEOS (discretionary)

Below are summarized the Dissemination materials for the COES, please refer to section 5 for further details.

1	Updated Virunga lava flows map (1938 to present): Nyiragongo 2021 lava flows have been added
2	Seismic map of the earthquakes that followed the Nyiragongo May 2021 eruption
3	Map of fractures created by the Nyiragongo 2021 eruption and the seismicity that followed the eruption
4	Gas composition of the Nyiragongo 2021 eruptive vent (CO ₂ , SO ₂ and H ₂ S)
5	Data related to air quality in Goma and Lake Kivu
6	Data of Lake Kivu Physico-chemical composition during Nyiragongo 2021 eruption
7	Rainwater chemistry in the Virunga
8	Maps of InSAR analysis of surface deformations between January 2020 and December 2021
9	Scheme of the Nyiragongo area with the feeding dyke (dyke modelling) during the Nyiragongo 2021 eruption
10	DSM in the area of Nyiragongo volcanic field derived from Pléiades images acquired after Nyiragongo 2021 eruption